LABYRINTH SEAL LEAKAGE ANALYSIS

A Thesis

by

ORCUN INAM

Submitted to the Office of Graduate Studies of
Texas A&M University
in partial fulfillment of the requirements for the degree of

MASTER OF SCIENCE

August 2011

Major Subject: Mechanical Engineering

LABYRINTH SEAL LEAKAGE ANALYSIS

A Thesis

by

ORCUN INAM

Submitted to the Office of Graduate Studies of
Texas A&M University
in partial fulfillment of the requirements for the degree of

MASTER OF SCIENCE

Approved by:

Chair of Committee,	Gerald Morrison
Committee Members,	Michael Pate
	Ding Zhu
Head of Department,	Jerald A. Caton

August 2011

Major Subject: Mechanical Engineering

ABSTRACT

Labyrinth Seal Leakage Analysis.

(August 2011)

Orcun Inam, B.En., Gazi University, Turkey

Chair of Advisory Committee: Dr. Gerald L. Morrison

Annular seals are devices used in turbomachinery to avoid flow losses which reduce efficiency. The dynamic stability of the machine is also improved by the seal. Thus, it is an important subject to understand the flow behavior through the seal.

Straight through triangular labyrinth seals are one of the most commonly used types of non-contacting annular seals. The energy dissipation through these seals is achieved by a series of teeth and cavities. As the flow passes above each tooth, a portion of its pressure energy is converted into kinetic energy. A portion of this kinetic energy is dissipated through turbulence-viscosity interaction in the cavity that follows. Moreover, some portion of the pressure energy is also lost through viscosity of the fluid. This research aims to understand the effects of flow parameters and seal geometry on these losses. This will make it possible to estimate the mass flow leakage through the seal.

ANSYS Fluent is used to simulate the flow through the seal. The effect of seal geometry is studied by varying clearance, pitch, tooth height, tooth width and upstream side angle. It was found that, amongst other geometrical parameters, tooth clearance and pitch has a strong influence on carryover coefficient. Smaller values of c/s have better

kinetic energy dissipation in the cavity. Carryover coefficient is also found to be a function of the Reynolds number and shaft speed.

Discharge coefficient of the seal presents the overall efficiency while carryover coefficient only shows the cavity performance. Discharge coefficient is also found to be a strong function of tooth clearance, pitch, Reynolds number and shaft speed. Remaining parameters have smaller effects. It was observed that the discharge coefficient of first tooth is always lower than those of intermediate teeth. The compressibility effects are presented by using an expansion factor which is the ratio of compressible flow discharge coefficient to incompressible flow discharge coefficient. It was found that the expansion factor is fairly independent of geometrical parameters but a strong function of flow parameters.

Considering the effects of seal geometry and flow parameters on carryover coefficient, discharge coefficient and expansion factor, the seal geometry is optimized to increase the kinetic energy dissipation and pressure head loss which in turn will reduce the mass flow leakage.

DEDICATION

Dedicated to my mother, Nurdan Koyluoglu

ACKNOWLEDGEMENTS

First of all, I would like to express my special thanks to my committee chair, Dr. Gerald L. Morrison, for providing me with the opportunity to work under his supervision. Dr. Morrison has been a constant source of extensive knowledge and motivation. He has been of great help throughout this thesis.

I am thankful to Dr. Michael Pate and Dr. Ding Zhu for being on my thesis committee and their support. I am also grateful to all faculty members of the Mechanical Engineering Department for providing me with important knowledge throughout my education at Texas A&M University.

I would also like to express my thanks to Texas A&M University as a whole for providing me with such a good educational environment.

NOMENCLATURE

A -	Clearance area, πDc
c -	Radial clearance, m
C_d -	Discharge coefficient for intermediate tooth
C_d^{1tooth} -	Discharge coefficient for first tooth
D –	Shaft diameter, m
h –	Tooth height, m
L -	Axial length of the seal, m
$\dot{m}$ -	Mass flow rate of leakage flow (kg/s)
P_i –	Tooth inlet pressure, Pa
P_e -	Tooth exit pressure, Pa
Pr –	Absolute pressure ratio, p_e/p_i
Re –	Clearance Reynolds number, $\frac{\dot{m}}{\pi D\mu}$
s -	Tooth pitch
w -	Tooth width
x -	Axial distance along seal, m
α -	Flow coefficient
β –	Divergence angle of jet, radians
γ -	Kinetic energy carryover coefficient
ε –	Dissipation of turbulent kinetic energy

κ –	Turbulent kinetic energy
μ–	Dynamic viscosity, Pa/s
ρ_i –	Fluid density at seal inlet, kg/m^3
ρ –	Fluid density at tooth inlet, kg/m^3
χ-	Percentage of kinetic energy carried over
ψ -	Expansion factor

TABLE OF CONTENTS

Page

Page

LIST OF FIGURES

Page

Page

Page

Page

Page

Page

LIST OF TABLES

Page

1. INTRODUCTION

High pressure turbines, which play a vital role in today's increasing energy needs, extract mechanical energy from fluid flow. Therefore, it is important to increase the efficiency of these machines. It has been a crucial subject to increase the efficiency by reducing the flow losses. A seal is a component that is used in order to meet this purpose. Seals can be divided into two main categories. The first one is contact seals which fully constricts the fluid flow. They effectively reduce the flow leakage and increase the efficiency. However, their disadvantages are that the moving parts degrade because of friction and excess of heat may be generated due to friction. Thus, they are not suitable for high speed moving parts which are common for turbomachinery applications. By utilizing a tortuous flow path, non-contact seals create extensive turbulence, decreasing the pressure of the fluid, in order to constrict the fluid flow. Therefore, non-contact seals effectively reduce the fluid leakage without causing degradation in the moving parts as contact seals do. Non-contact seals have many different kinds including labyrinth and honeycomb seals which are the most commonly used ones.

Labyrinth seals, innovated by C.A.Parsons [1], can mainly be divided into 3 categories; stepped, straight and staggered seals. Moreover, the tooth has two common profiles; rectangular and triangular teeth. Among them, straight-through triangular

---

This thesis follows the style of Journal of Turbomachinery.

profiles are one of the most common ones in steam turbines due to their high sealing capacity and ease of manufacture. These seals have triangular teeth over the rotor or stator part with cavities in between them. The illustrative geometry of a tooth-on-rotor straight labyrinth seal with triangular teeth is shown in Figure 1.1.

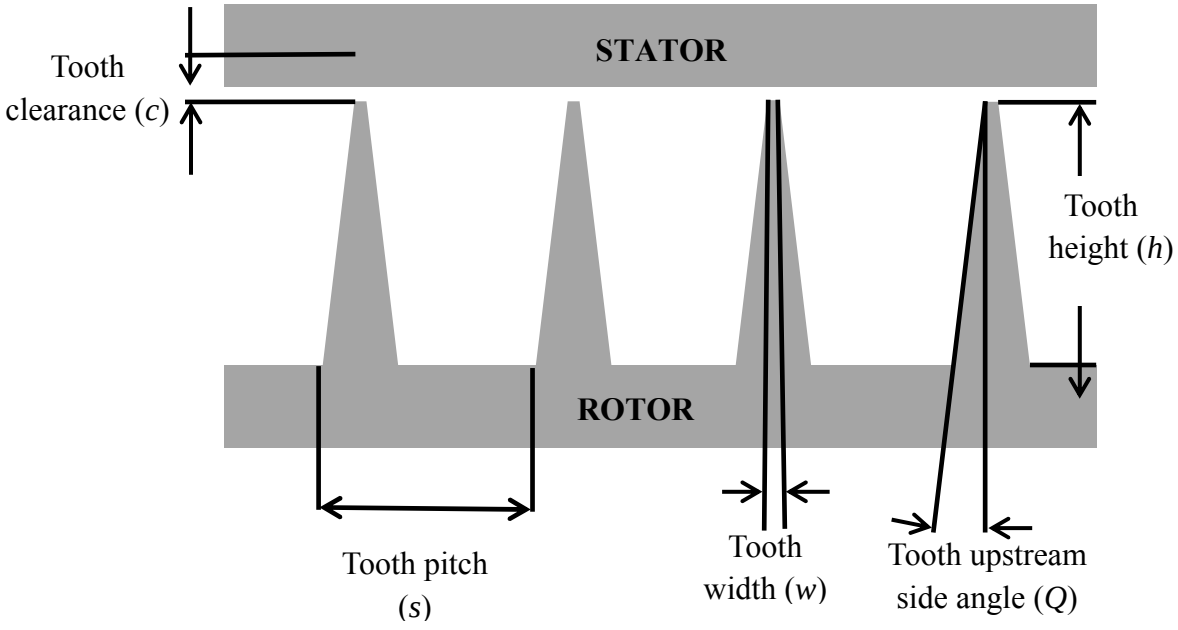

Figure 1.1 Labyrinth seal nomenclature

The smaller clearance, combined with the vena-contracta effect, causes an increase in the amount of pressure energy converted to kinetic energy. This kinetic energy is dissipated through the 3D turbulence in the cavity that follows as shown in Figure 1.2.

The streamlines in Figure 1.2 clearly shows the pattern of the vortex where the kinetic energy is dissipated. It is apparent that some portion of the flow is directly

carried over to the next tooth without being dissipated in the cavity. This portion is defined by the carry over coefficient. The main parameter to define carryover coefficient is the angle β as shown in Figure 1.2. As β angle decreases, a larger portion of the upstream flow is carried over to the next cavity without involving in dissipation process and as a result the amount of kinetic energy dissipated in the cavity decreases reducing the effectiveness of the seal.

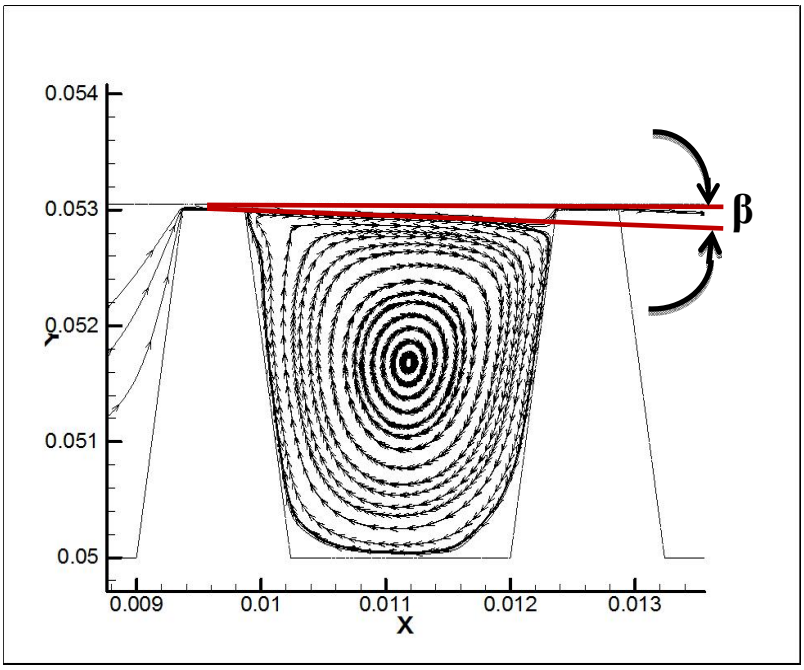

Figure 1.2 Flow pattern in the cavity

The relationship between the angle β and carryover coefficient is further defined by Hodkinson [2] based upon the single vortex seal cavity as shown in figure 1.2. The carryover coefficient γ is given by the following equation;

$$\gamma^2 = \frac{1}{1-\chi} \quad \text{(1.1)}$$

where the parameter χ is the percentage of the kinetic energy carried over into the next cavity and it is related to the angle β as in the following equation;

$$\tan(\beta) = c\frac{1-\chi}{\chi S} \quad \text{(1.2)}$$

The relationship between the kinetic energy carried over into the next cavity, χ, and the carryover coefficient, γ, is illustrated in Figure 1.3. When γ is 1, the kinetic energy carried over to the next cavity is 0 which means that all kinetic energy is dissipated in the cavity, which is the ideal case. On the other hand, higher carryover coefficient means that a larger portion of the kinetic energy is carried to the next cavity instead of being dissipated and the effectiveness of the seal is less.

Another parameter that is commonly used in labyrinth seals to understand the effectiveness is discharge coefficient. Discharge coefficient defines the overall efficiency of the sealing while the carryover coefficient tells about the dissipation only in the cavity. It basically defines the flow losses in each tooth. It is given by the following equation;

$$C_d = \frac{\dot{m}}{A\sqrt{2\,\rho\,(P_i - P_e)}} \quad \text{(1.3)}$$

where P_i is the pressure of the upstream cavity, P_e is the pressure of the downstream cavity, and ρ is the density of the fluid at where P_i is obtained.

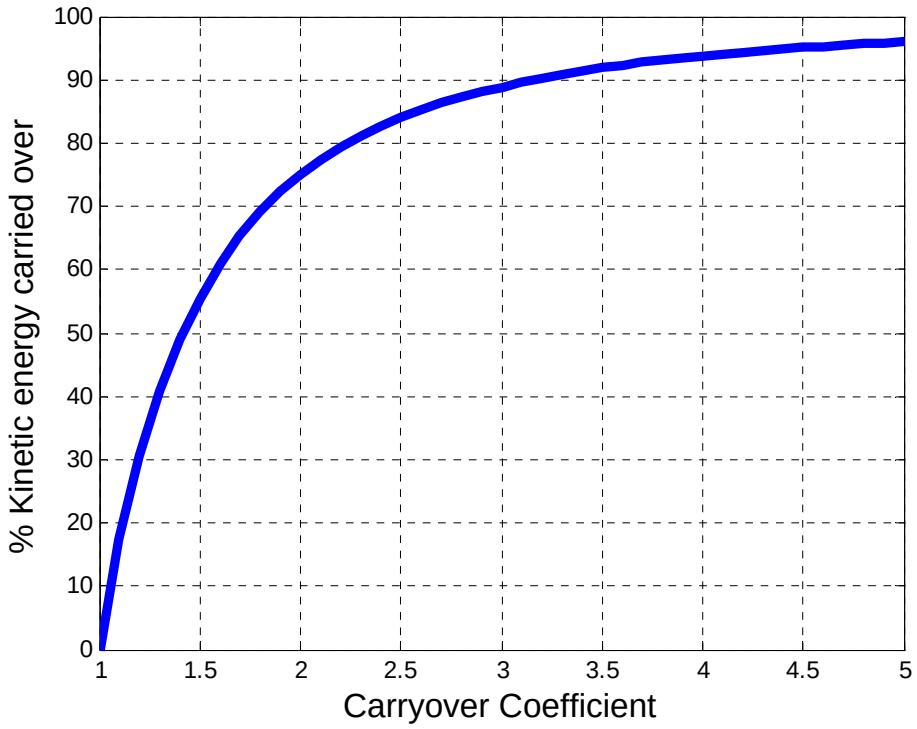

Figure 1.3 Relationship between γ and χ

It is apparent from equation 3 that the higher pressure across a tooth will result in lesser discharge coefficient for a constant mass flow rate. Since higher pressure difference is desired, it can be concluded that lesser discharge coefficient represents higher effectiveness of the sealing. Better understanding the effects of seal geometry, Reynolds number and rotation on these coefficients will result in the design of better performance seals.

2. REVIEW OF EXISTING LEAKAGE MODELS

The labyrinth seal was innovated by C.A.Parsons [1] in conjunction with his development of steam turbines. The first technical paper attempting to describe the fluid flow through the labyrinth seals was introduced by Becker [3]. He modeled the flow through the labyrinth seal as Poiseuille flow and tried to find a coefficient of friction.

After Becker published his paper, Martin [4] published a paper that gained universal interest and became the classical method to define the fluid flow through labyrinth seals. Martin considered the fluid flow through labyrinth seals to be similar to the flow in a series of orifices. He assumed that the kinetic energy was totally destroyed and the flow to be isothermal, which are not accurate for compressible flow. He created the leakage flow equation given in equation 2.1. Most subsequent studies were concerned with relaxing his restricting assumptions. Stodola [5] applied Bernoulli's equation to each tooth and then integrated over the entire seal using the continuity equation to obtain an equation similar to Martin's flow leakage rate for subcritical flow.

$$\dot{m} = \frac{A\,P_i}{\sqrt{RT_i}} \sqrt{\frac{1-\left(\frac{P_e}{P_i}\right)^2}{n-\ln\left(\frac{P_e}{P_i}\right)}} \quad \text{..... (2.1)}$$

Gercke [6] was the first one who recognized the importance of the kinetic energy carry-over between throttlings. He assumed the flow to be adiabatic and tried to account for the kinetic energy recovery between throttlings which Martin assumed to be complete. Egli [7] examined the effect of changing the number of sharp-edged teeth and recommended that Martin's formula be used only when there were four or more teeth in

series. For fewer teeth numbers, he used the Saint Venant-Wantzel orifice equation for each of the teeth. He observed for compressible flow that the pressure drop across each tooth increased and the last tooth was the first to reach the critical pressure ratio. He modified Martin's equation by using an empirically obtained coefficient as given in equation 2.2.He also conducted experiments for staggered labyrinth seals which showed that flow is greatly affected by the clearance and the thickness of the tooth.

$$\dot{m} = \gamma_{emperical} \frac{A\,P_i}{\sqrt{RT_i}} \sqrt{\frac{1-\left(\frac{P_e}{P_i}\right)^2}{n-\ln\left(\frac{P_e}{P_i}\right)}} \quad \text{.. (2.2)}$$

Dollin and Brown [8] revised Martin's equation assuming a polytropic thermodynamic path-function. As a result, they achieved a more general equation than that of Martin's. They also concluded that Martin's equation underestimates the fluid leakage because of his isothermal flow assumption. Hodkinson [2] modeled the flow leaving a tooth as a jet, a portion of which is carried over to the next cavity. The importance of his study is that it was the first attempt to analytically estimate the kinetic energy carry-over coefficient. He developed the following relation for leakage through the seal.

$$\dot{m} = A\,\alpha\,\psi\,\gamma\,\sqrt{\rho_i\,P_i} \quad \text{.. (2.3)}$$

where α is an experimentally determined coefficient.

The expansion coefficient is given as

$$\psi = \sqrt{\frac{1-\left(\frac{P_e}{P_i}\right)^2}{n-\ln\left(\frac{P_e}{P_i}\right)}} \quad \text{... (2.4)}$$

and the kinetic energy carry over coefficient is given as

$$\gamma = \sqrt{\frac{1}{1-\frac{n-1}{n}\frac{\frac{c}{s}}{\frac{c}{s}+0.02}}} \quad \text{(2.5)}$$

Jeri [9] conducted tests on labyrinth seals with no more than 9 teeth. He concluded that when the tooth width to clearance ratio is greater than 2, the restrictor behaves like a rounded nozzle rather than a sharp-edged orifice. He concluded that an optimum tooth-depth to tooth-spacing ratio should be slightly less than unity and two closely spaced restrictors can yield higher leakage ratio than a single one.

Kearton and Keth [10] investigated a staggered labyrinth seal and derived a theoretical leakage formula similar to Stodola's and Martin's. Bell and Bergelin [11] modeled labyrinth seal flow as flow through annular orifices. They attempted to explain the effect of Reynolds number. They observed that at low Reynolds numbers, the mechanism of energy loss is mainly viscous shear in the fluid and kinetic effect is only significant at the entrance of the orifice. On the other hand, at higher Reynolds numbers, kinetic effects become predominant in forms of fluid acceleration, contraction, expansion and turbulent friction. They also stated that at higher Reynolds numbers, the increasing tooth width increases frictional losses but also increases pressure recovery. For lower Reynolds numbers, pressure recovery does not exist and the frictional losses increase as the tooth width increases.

Zabriskie and Sternlicht [12] simplified the methods of Trutnovsky and Becker. They treated the labyrinth seal as a very tortuous flow path that requires the estimation of a friction factor and flow coefficient. They used Kearton's values for flow coefficient

and estimated friction factors which are given as a function of Reynolds number. However, the scarcity of their friction factor data limits the usefulness of their method. The paper by Vermes [13] on labyrinth seals represents one of the most important studies. He basically adjusted Martin's formula for nonisothermal flow. He used the flow coefficients from Bell and Bergelin and treated the geometric complications of nonstraight-through seals from Gercke's methods. A correction factor for kinetic energy carry-over is derived and incorporated into Martin's formula.

Zimmerman and Wolf [14] examined the labyrinth seals and presented a calculation method for leakage. They stated that since the carry-over effect is not present in the first tooth, it should be more effective at reducing the flow than at least some of the downstream teeth. They also observed that the pressure in the second cavity can sometimes be higher than that of the first cavity, which seemingly is a contradiction. They explained this anomalous pattern as a result of the vena-contracta, the narrowest point of the carry-over jet, which can occur in the downstream cavity raising its pressure. Wittig et al. [15] used prediction codes to estimate the discharge coefficients in labyrinth seals and compared his results with experimental data. They observed that the effect of rotation on leakage is only significant when the Reynolds number is low and Taylor number is high. The authors stated that the discharge coefficient significantly depends on the clearance but this dependence decreases with increasing number of teeth. Discharge coefficients were found to increase with increasing clearance, meaning that pressure difference between consecutive cavities reduces, but this pattern becomes less predominant when the number of teeth is greatly reduced. Saikishan [16] studied the

effects of tooth geometry on fluid flow characteristics. He considered the tooth on stator case and calculated the kinetic carry over and discharge coefficients for different geometries. He compared his results with experimental data.

3. RESEARCH OBJECTIVES

The objective of the study is to understand the effects of geometry, dimension and Reynolds number on labyrinth seal leakage and create an empirical equation to estimate the leakage. As a result, the designers will be able to quickly estimate the flow leakage which will make it possible to consider more design options without doing experimental or CFD analysis. These objectives will be met through the following steps;

1- Gambit® will be used to create geometry and mesh of the labyrinth seal with 4 teeth on rotor. The flow through the seal is axisymmetric and thus it can be analyzed as 2D flow in order to save computing time.

2- FLUENT® will be used to do the simulations under different flow and geometry conditions as described in the following steps.

3- To understand the effect of geometry, different geometries will be created and simulated.

4- Some of the seal geometries will be simulated with rotational speed and the results will be compared to the non-rotating rotor simulations in order to understand the effects of rotation.

5- Reynolds number will be increased until the flow is choked for all of the seal geometries.

6- TecPlot® will be used to do the post processing. Carryover coefficient, discharge coefficient and expansion factor will be calculated for all of the simulations.

7- The expansion factor will be evaluated by comparing the discharge coefficients for compressible and incompressible flow.

8- An empirical equation for the seal leakage will be obtained.

9- Results will be compared to earlier experimental results and existing leakage equations.

4. COMPUTATIONAL METHOD

Computational methods offer faster solutions with significantly less cost compared to experimental methods. For this study, computational methods are chosen to investigate the flow behavior through the labyrinth seal. GAMBIT 2.4.6 is used to draw the geometry and generate the mesh. Commercial code FLUENT 12.0.16 is used to perform CFD simulations.

FLUENT 12.0.16 uses a finite volume discretization method to solve the Navier-Stokes equations. Based on the comparisons to experiments conducted by Morrison and Al-Ghasem [17], it is known that the standard k- ε model is accurate for simulating the flow through the labyrinth seal. The descriptions of the standard k- ε turbulence model and the finite volume discretization are given in Appendix A.

In order to save computational time, the flow domain is reduced to 2D. Considering that the flow is axisymmetric in 3D domain, this assumption will give results within acceptable accuracy. All of the simulations have 4 teeth on rotor. An example of the mesh structure of a cavity is given in Figure 4.1. It can be seen that the mesh, which completely consists of rectangular cells, is finer near the walls and the clearance region. The reason is that the Y^+ should remain below 5 in order to solve the laminar sub layer as mentioned by Morrison and Al-Ghasem [17]. Further refinement near the wall region is done to meet this requirement and as a result the final mesh is finer near the walls and clearance region.

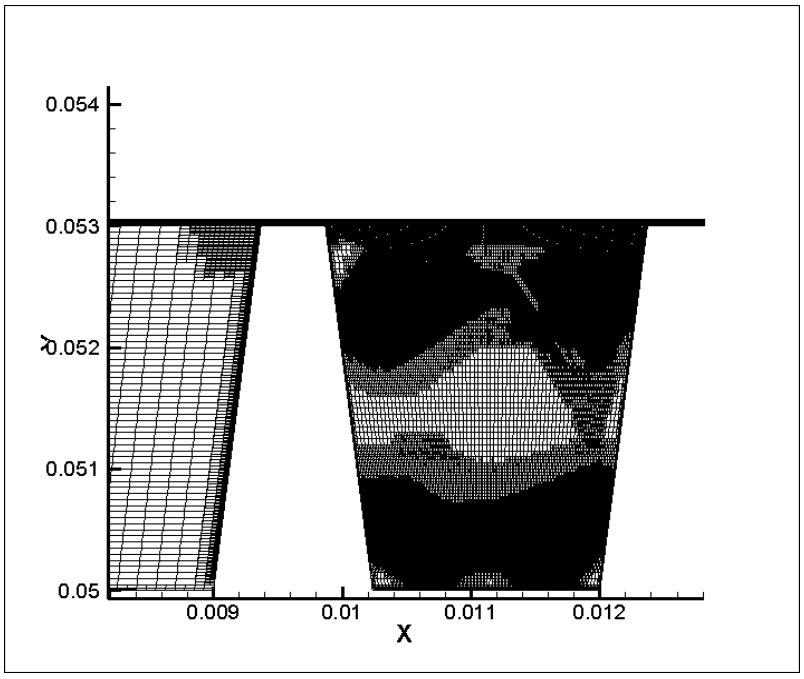

Figure 4.1 Mesh structure of the seal geometry

The standard wall function does not accurately solve the flow in the viscous sub layer in the near-wall region. In order to model the flow in this region, Morrison and Al-Ghasem [17] suggested the use of the enhanced wall treatment used in conjunction with the standard k-ε turbulence model. Enhancened wall treatment model allows the Y^+ values up to 5 and effectively solves the boundary layer with pressure gradient effects.

The accuracy of a CFD simulation mainly depends on the grid structure. Compared to the coarse mesh, the finer mesh gives more accurate result but takes longer to solve the flow and needs more computational resources. When the grid cell number reaches an optimum value, the solution does not change even if the number of nodes increases. In order to determine this point, a grid independency study must be conducted.

This study, grid independency study is based on Y^+ and pressure gradient adaptation. The solution has been performed by successively reducing the maximum allowed pressure gradient value until the solution is independent of further refinement. It is observed that incompressible flow requires lesser pressure gradient in order to reach a grid independent solution compared to compressible flow. Moreover, the Y^+ value is also continuously checked to make sure that it is below 5. The graph in Figure 4.2 illustrates an example for grid independency study. It is shown that the solution does not change with further refinement after a total number of nodes reaches 85000.

.

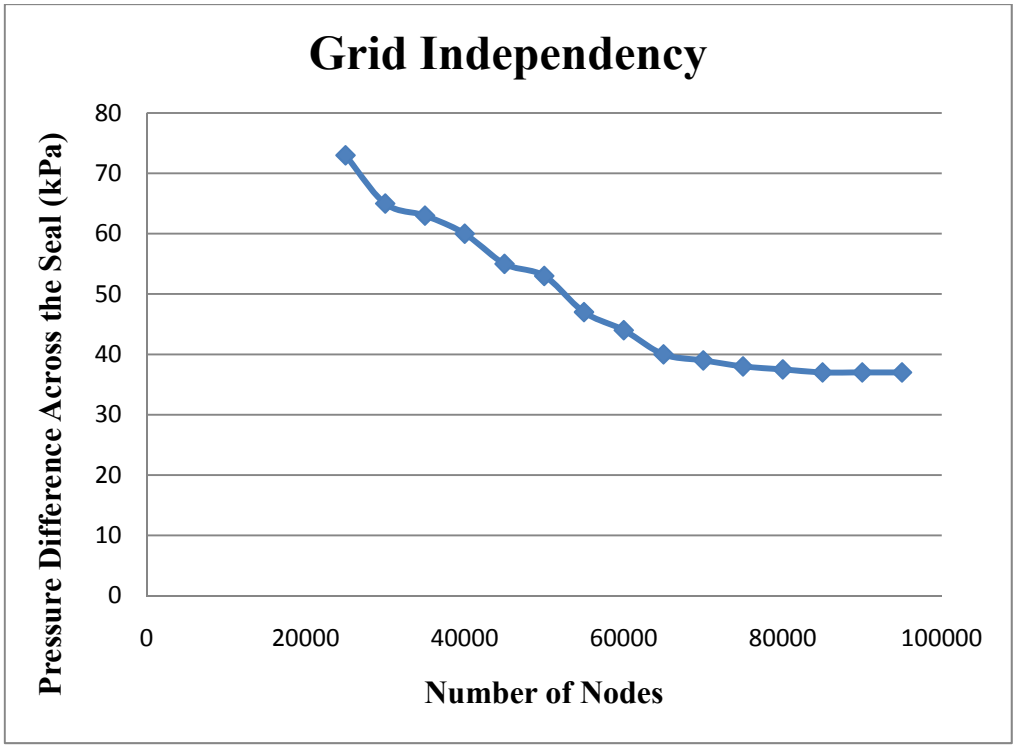

Figure 4.2 Grid independency study

5. LABYRINTH SEAL GEOMETRIES

In order to meet the research objectives as mentioned in section 3, the seal geometry is varied by changing tooth height, clearance, pitch, tooth upstream side angle and tooth width. All seal geometries have been analyzed by increasing mass flow rate until a maximum pressure difference is attained or the flow is choked. For compressible flow, the flow is choked when the Mach number at the last clearance region is above 1. For incompressible flow, the maximum overall pressure difference through the seal considered is 200 atm. The main reason to stop increasing mass flow rate when the flow is choked is that in a real situation, no more flow can go through the clearance region if the flow is choked.

It is known that the performance of the labyrinth seal is also affected by the rotational speed of the shaft. In order to understand the effect of rotation on seal performance, some of the geometries have been studied under rotational shaft condition. Table 5.1 summarizes all of the geometries that have been simulated in this study. Labyrinth seal geometries namely G1, G4 and G21 have been studied under rotational shaft condition and varying mass flow rate. The remaining geometries have been simulated under the no shaft rotation condition and varying mass flow rate. All seals considered in this study are tooth on rotor, four teeth (there cavities), and a shaft radius of 50 mm. The dimension of the lengths in table 5.1 is mm.

Table 5.1 Labyrinth seal geometries

Seal Code	Clearance	Pitch	Tooth width	Tooth height	Upstream side angle	c/s	w/s	h/s
G1	0.05	3	0.5	3	7	0.0167	0.1667	1.0000
G2	0.2	3	0.5	3	7	0.0667	0.1667	1.0000
G3	0.2	12	0.5	12	7	0.0167	0.0417	1.0000
G4	0.2	12	0.5	3	7	0.0167	0.0417	0.2500
G5	0.8	3	0.5	3	7	0.2667	0.1667	1.0000
G6	0.8	12	0.5	12	7	0.0667	0.0417	1.0000
G7	0.2	9	0.5	3	7	0.0222	0.0556	0.3333
G8	0.2	3	0.5	3	0	0.0667	0.1667	1.0000
G9	0.2	12	0.5	3	0	0.0167	0.0417	0.2500
G10	0.05	3	0.5	3	0	0.0167	0.1667	1.0000
G11	0.8	12	0.5	3	0	0.0667	0.0417	0.2500
G12	0.8	3	0.5	3	0	0.2667	0.1667	1.0000
G13	0.2	12	0.5	12	0	0.0167	0.0417	1.0000
G14	0.2	12	2	12	7	0.0167	0.1667	1.0000
G15	0.1	3	0.5	3	7	0.0333	0.1667	1.0000
G16	0.075	3	0.5	3	7	0.0250	0.1667	1.0000
G17	0.06	3	0.5	3	7	0.0200	0.1667	1.0000
G18	0.05	3	0.2	3	7	0.0167	0.0667	1.0000
G19	0.05	3	0.1	3	7	0.0167	0.0333	1.0000
G20	0.05	3	0.75	3	7	0.0167	0.2500	1.0000
G21	0.05	3	1	3	7	0.0167	0.3333	1.0000
G22	0.05	3	0.05	3	7	0.0167	0.0167	1.0000
G23	0.05	3	0	3	7	0.0167	0.0000	1.0000
G24	0.05	3	0.5	1	7	0.0167	0.1667	0.3333
G25	0.05	3	0.5	2	7	0.0167	0.1667	0.6667
G26	0.05	3	0.5	4	7	0.0167	0.1667	1.3333
G27	0.05	3	0.5	5	7	0.0167	0.1667	1.6667

6. CARRYOVER COEFFICIENT

6.1 Calculation of Carryover Coefficient

The carryover coefficient shows the energy dissipation by vortices in the cavity. The ideal value for the carryover coefficient is 1 which means that all of the kinetic energy of the fluid is dissipated in the cavity by the vortices. Larger values of the carryover coefficient indicate a larger portion of the kinetic energy is carried over to the next cavity instead of being dissipated. The definition by Hodkinson [2] is used in this study. This definition assumes only one large vortex in the cavity as shown in figure 6.1. The following equations are used to calculate the percentage of the kinetic energy carried over and the carryover coefficient.

$$\gamma^2 = \frac{1}{1-\chi} \quad \text{(6.1)}$$

where χ is the percentage of kinetic energy carried over into the next cavity which is related to the angle β as defined in the following equation;

$$\tan(\beta) = c\frac{1-\chi}{\chi\, s} \quad \text{(6.2)}$$

The divergence angle β in equation 6.2 is calculated by investigating the main streamline which separates the portion of the flow involving in circulation from the rest of the flow directly moving to the next cavity. The illustration is shown in figure 6.1. The higher the divergence angle, the lower will be the carryover coefficient which converges to the ideal case.

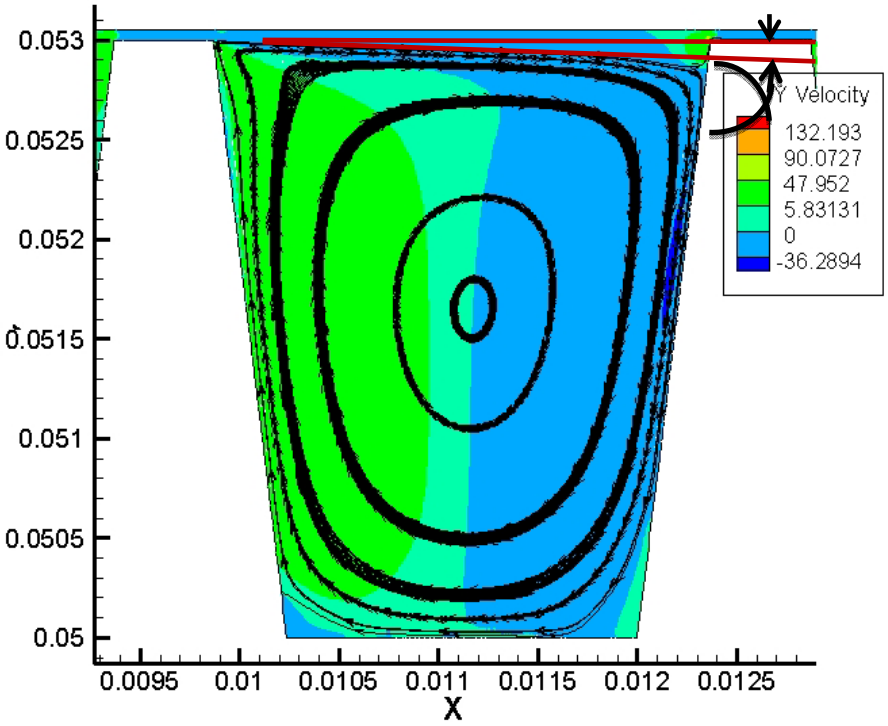

Figure 6.1 Streamlines in the cavity without rotation
(G1, c/s=0.0167, s=3, h/s=1, w/s=0.167, Re=4000, incompressible flow, W_{sh}=0)

The contours show the distribution of the y component of the velocity with values as shown in the legend. The point where the main streamline hits the next tooth wall has zero velocity. When the rotational speed is zero or small (i.e. 50 m/s or a little higher depending on the geometry), this kind of streamline distribution is expected. However, when the rotational speed is higher, the flow is dominated by the centrifugal effects and the distribution of the streamlines is significantly affected. Figure 6.2 shows the streamlines and y component of velocity contours for the same geometry as in figure 6.1. However, the rotational speed is 350 m/s while it is zero for figure 6.1.

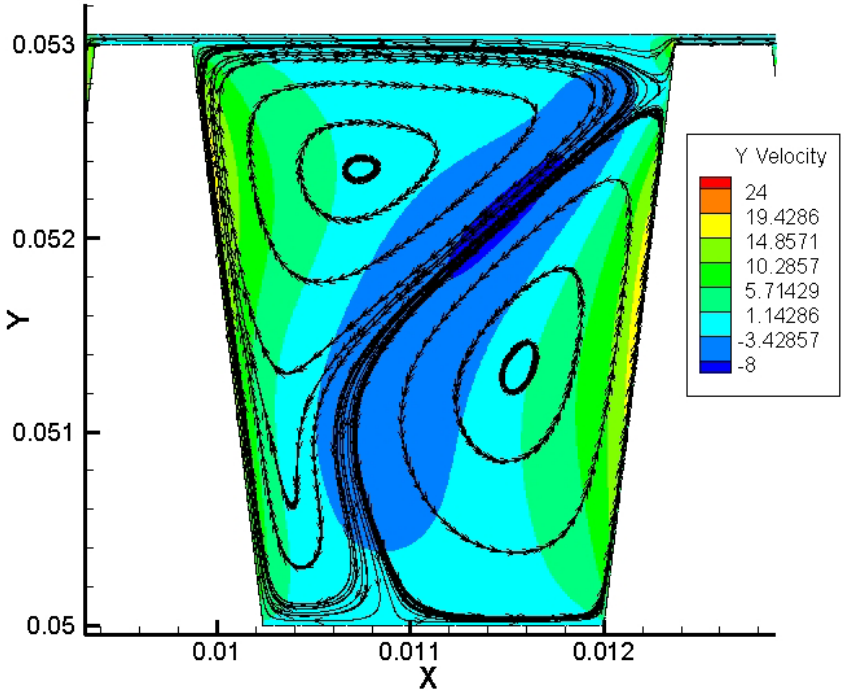

Figure 6.2 Streamlines in the cavity with rotation
(G1, c/s=0.0167, s=3, h/s=1, w/s=0.167, Re=4000, incompressible flow, W_{sh}=350)

It is apparent that the main streamline separating the through flow and the circulation from the rest of the flow moving to the next cavity does not hit the next wall but wraps around the smaller vortex then moves to the next cavity. In this case, the carryover coefficient definition of Hodkinson [2] is not applicable and it is assumed that carryover coefficient is 1.

6.2 Effect of Reynolds Number

In this section, the effect of Reynolds number will be investigated while varying the clearance and pitch for zero shaft speed. The results presented here are for incompressible flow. The effects of compressibility will be discussed in section 8.

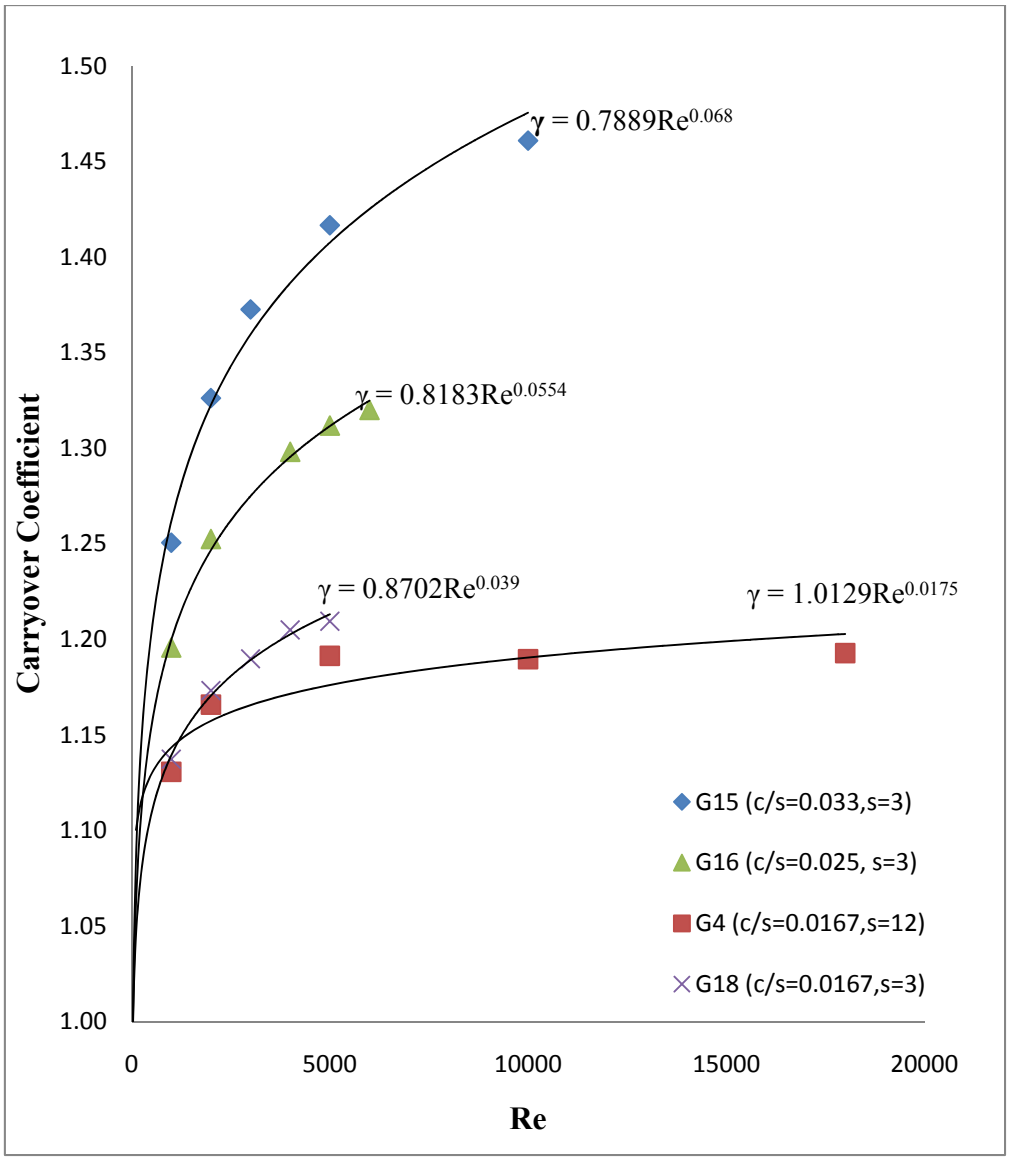

Figure 6.3 Effect of Reynolds number on γ (incompressible flow, W_{sh}=0)

Figure 6.3 shows the results from G15 and G16 which are the same seals where only the clearance is changed. It can be seen that carryover coefficient increases with increasing clearance for a fixed value of pitch. Hence, the energy dissipated in the cavity decreases with increasing clearance. G18 is modified from G15 and G16 where the clearance is further decreased and also the tooth width is also decreased. This resulted in an even smaller carryover coefficient which means that a larger portion of the kinetic energy is dissipated in the cavity.G4 is created by increasing the clearance and pitch value of G18 by a factor of 4 so the clearance to pitch ratio is same as G18. Moreover, the tooth width is also same with G15 and G16. The carryover coefficient value of this seal (G4) is close to that for G18 even though they have different tooth widths. However, it is significantly lower than those of G15 and G16 where the clearance to pitch ratio is higher but the tooth width is same. Therefore, the carryover coefficient is primarily dependent upon the c/s ratio and Reynolds number, which was neglected by Hodkinson [2]. The relationship between the carryover coefficient and Reynolds number is best represented with power functions as shown in figure 6.3. The tooth width and cavity depth are also factors but the carryover coefficient is much less dependent upon these factors.

The reason why the carryover coefficient increases as Reynolds number is increased can be attributed to the relationship between the axial velocity of the fluid particle and the Reynolds number. When the Reynolds number is high, the axial velocity of the fluid particle is also high but the radial velocity is similar compared to a low Reynolds number case assuming that the rotational shaft speed is same. As a result, the

fluid particle with higher axial velocity moves to the next cavity faster than fluid particle with lower axial velocity. Therefore, it does not have as much time to diverge as the fluid particle with lower axial velocity. Thus, the divergence angle for the fluid particle with lower axial velocity (figure 6.4) is higher compared to that of a fluid particle with higher axial velocity (figure 6.5). When the divergence angle is lower, a larger portion of the fluid moves to the next cavity without involving in dissipation. As a result, the carryover coefficient increases. The same pattern is also observed by Saikishan [16] even though he simulated the tooth-on-stator case.

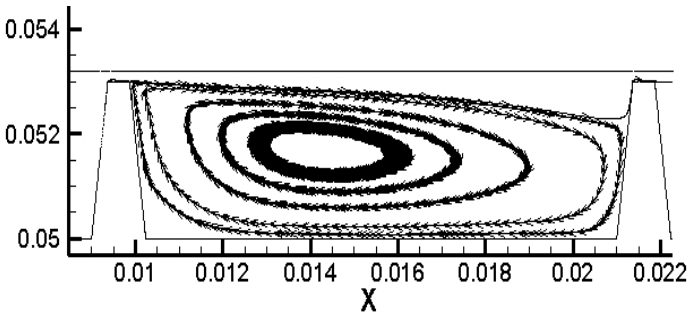

Figure 6.4 Streamlines in the first cavity of G4 (Re=1000, incompressible flow, W_{sh}=0)

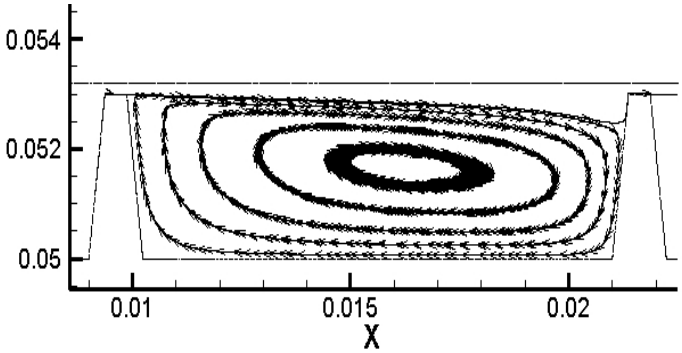

Figure 6.5 Streamlines in the first cavity of G4 (Re=18000, incompressible flow, W_{sh}=0)

Moreover, it should be noted that this pattern loses its effect with further increment in Reynolds number. As can be seen from figure 6.3, the carryover coefficient is slightly increasing when the Reynolds number is varying between 10000 and 18000. When the flow is about to reach maximum pressure difference, the carryover coefficient is almost constant even though the Reynolds number increases. Knowing that this condition exists for G4 when the Reynolds number is 18000, this can be observed comparing the carryover coefficients when Reynolds number is 15000 and 18000 from figure 6.3.

6.3 Effect of Clearance

Hodkinson [2] found that clearance is one of the major parameters that affects the carryover coefficient. He used a non-dimensional parameter, clearance to pitch ratio, to understand the dependence of carryover coefficient on clearance. He found that an increase in tooth clearance will result in an increase in carryover coefficient given that the rest of the parameters are kept the same. This is also confirmed by Saikishan's research that presents the tooth-on-stator case [16].

From a basic point of view, one can expect that more fluid can flow over the tooth without being effected (or less effected) by the tooth when c/s ratio increases, keeping s constant. In other words, a larger portion of the fluid directly flows to the next cavity without dissipating its kinetic energy. Thus, the percentage of the kinetic energy carried over to the next cavity increases and accordingly carryover coefficient increases as plotted in figure 1.3. This pattern is illustrated in figure 6.6. This figure is exaggerated

in order to better visualize the situation. The dimensions and streamlines are also only illustrative and does not exactly represent the real situation but the pattern is similar to that of real situation. Knowing that higher clearance causes the carryover coefficient to increase, which means that the effectiveness of the seal cavity reduces, it can be concluded that the clearance should be kept as small as possible. However, the clearance should still be higher than a certain value because the labyrinth seal surfaces could touch each other and wear away if an imbalance occurs or some dirt gets caught in the flow domain. In this study, the minimum clearance is chosen as 0.05 mm.

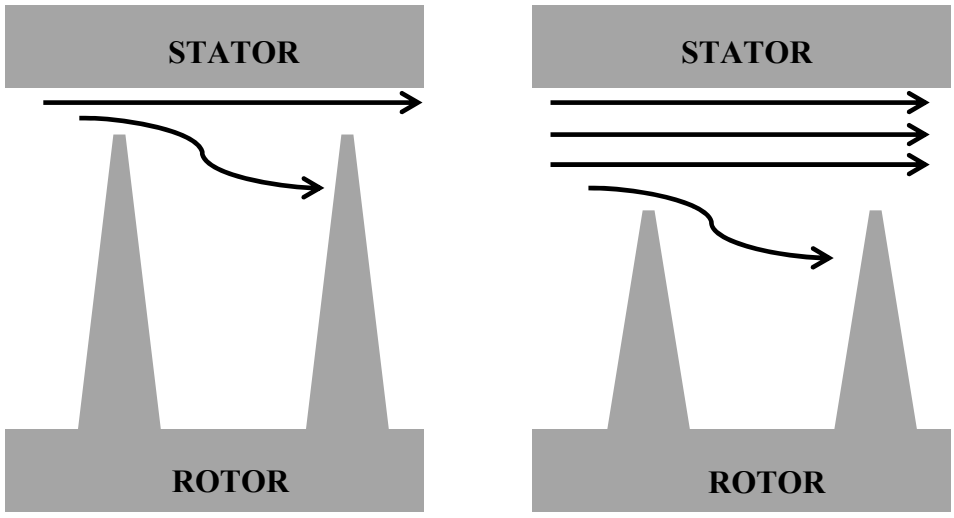

Figure 6.6 Illustrative streamlines for low (left) and high (right) clearance

In order to better understand the effect of clearance, several seal geometries have been simulated. Tooth width, pitch and height is kept constant while the clearance is varying in order to understand the sole effect of clearance. G1, G2, G15 and G16, as

given in table 5.1, are chosen to present the clearance effects. Figure 6.7 illustrates the carryover coefficient distribution for the first cavity of G1, G2, G15 and G16. For the second and third cavities, the pattern is very similar but carryover coefficient slightly increases. This increment in carryover coefficient is only %1-3, thus it is decided to present the results of only the first cavity.

As can be seen from figure 6.7, the carryover coefficient increases as the clearance is increased. It should be noted that higher clearance allows a larger mass flow rate to pass through the clearance region before the pressure drop is over 200 atm. This can be seen by comparing the c/s ratios and Reynolds numbers of the geometries in figure 6.7. As tooth clearance is increased (keeping the tooth pitch same), the maximum Reynolds number also increases. Comparing G1 and G16, increasing clearance by a factor of 1.5 causes carryover coefficient to increase by a factor of 1.1. The amount of increment in carryover coefficient slightly increases as Reynolds number increases. Comparing G15 and G2, increasing the clearance by a factor of 2 causes the carryover coefficient to increase by a factor of 1.2 for low Reynolds numbers and up to 1.35 for higher Reynolds numbers where the flow in G15 is about to choke.

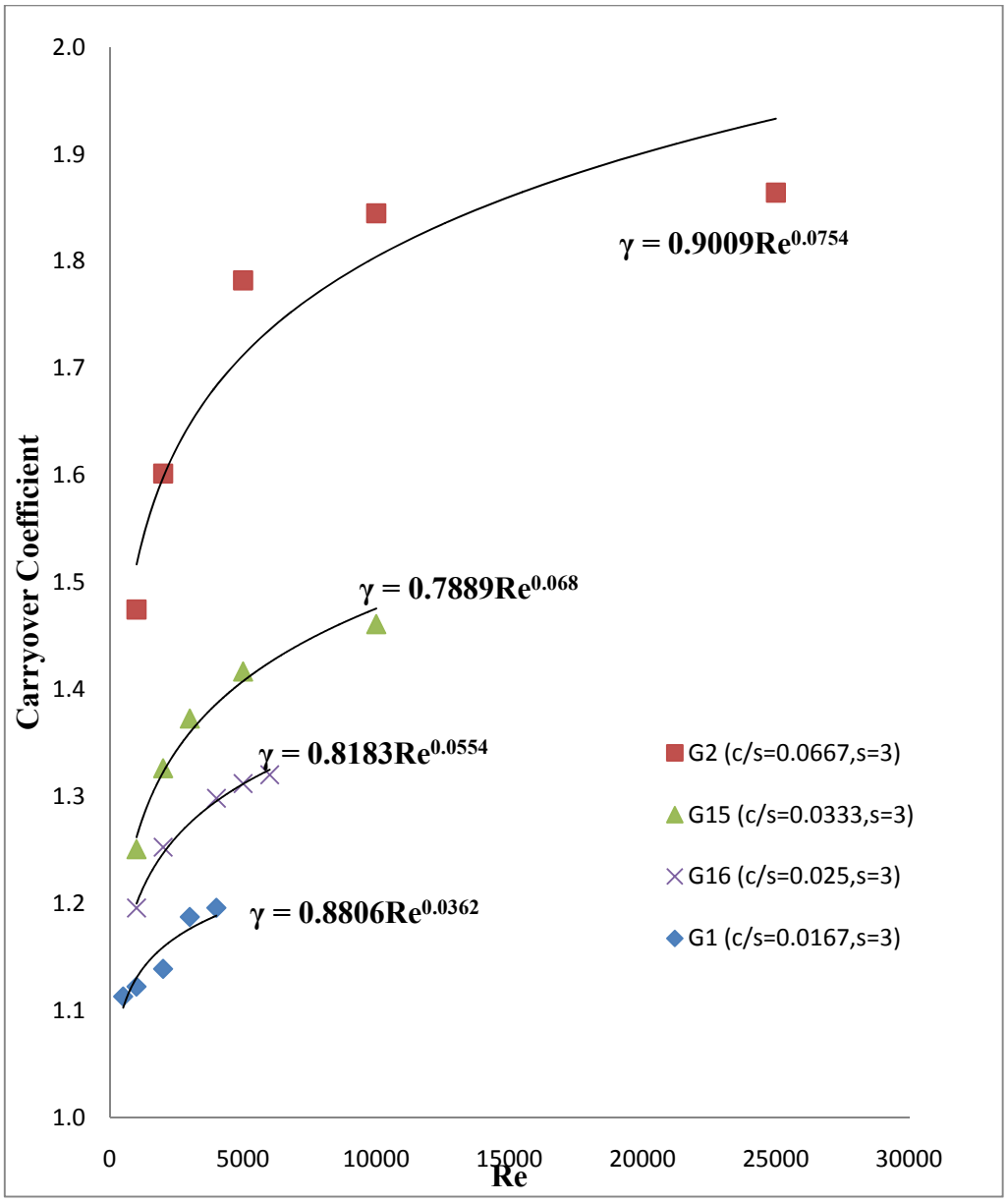

Figure 6.7 Effect of clearance on γ (Incompressible flow, W_{sh}=0)

In order to better understand how carryover coefficient increases as the clearance is increased, the streamlines should be investigated. As an example, G1 and G2 are chosen at the same Reynolds numbers to present streamlines. They have the maximum

clearance difference and they will better visualize the situation. Figure 6.8 and 6.9 shows the streamlines in the first cavity of G1 and G2 respectively.

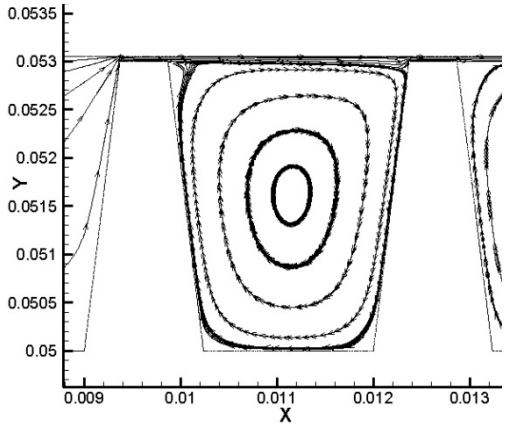

Figure 6.8 Streamlines in the first cavity of G1 (c/s=0.0167, s=3, Re=5000, incompressible flow, W_{sh}=0)

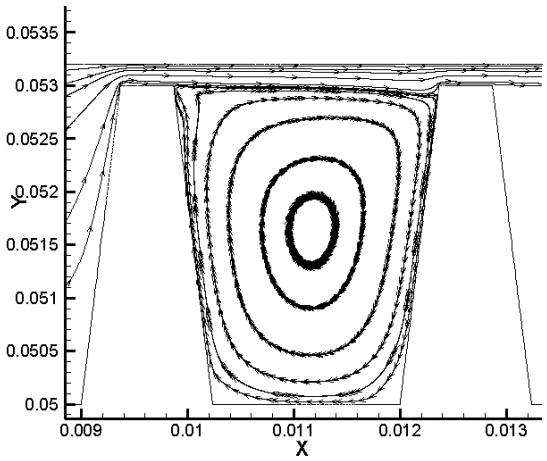

Figure 6.9 Streamlines in the first cavity of G2 (c/s=0.0667, s=3, Re=5000, incompressible flow, W_{sh}=0)

Figure 6.8 and 6.9 show similar streamline distributions. The divergence angles for these simulations are 1.547^{o} and 1.754^{o} respectively. The main reason is that

although they have the same mass flow rate, the clearance region of G2 is larger and accordingly the axial velocity through this region is lower. As a result, the fluid particles in G2 have more time to move in the radial direction compared to that of G1. Consequently, it impinges to a lower point of the downstream tooth wall compared to that of G1 and the divergence angle is higher. We know from section 6.2 that higher divergence angle will result in lower carryover coefficient given that other parameters are kept same. However, in this case, even though the divergence angle of G2 is higher compared to that of G1, the carryover coefficient is significantly higher. The reason is that the clearance of G2 is 4 times higher than that of G1 while the divergence angle is only 1.15 times higher than that of G1. Thus, the effect of clearance dominates the effect of divergence angle as can be seen from equation 6.2. This phenomenon was illustrated in figure 6.6.

Consequently, it is clear that higher clearance results in higher carryover coefficient. It should be kept in mind that higher carryover coefficient means that a larger portion of the kinetic energy is carried over to the next cavity without being dissipated in the vortex. Therefore, it reduces the effectiveness of the sealing. Thus, clearance should be kept as small as possible for better sealing performance.

6.4 Effect of Tooth Width

The complex flow pattern inside the cavity is also affected by tooth width. This section aims to present the effects of tooth width on carryover coefficient. This will be done by keeping the other parameters constant while the tooth width and Reynolds

number are varying. G19, G20, G21 and G23, as given in table 5.1, are chosen to do the analysis. The results are plotted in figure 6.10. Tooth height, pitch and clearance are same for all of the simulations in figure 6.10.

Considering G19, G20 and G21, it can be seen from figure 6.10 that the effect of tooth width is negligible for low Reynolds numbers (up to 2000). However, when Reynolds number is further increased, the smaller tooth width gives lower carryover coefficient. This pattern is more obvious when the Reynolds number is highest. Comparing G19 and G21, the carryover coefficient increases by a factor of 1.05 at the maximum Reynolds number when the tooth width is increased by a factor of 10. Since the pitch was kept same, larger tooth width leaves smaller distance from one tooth to another. As a result, compared to that of small tooth width case, the fluid particle impinges on a higher point of the downstream tooth wall reducing the amount of flow being circulated in the vortex. Therefore, a larger portion of the flow moves to the next cavity and carryover coefficient increases.

It should be noted that the sharp tooth profile (G23) shows a different pattern compared to other profiles. Even though the w/s ratio is smallest for G23, it gives the highest carryover coefficient provided that Reynolds number is smaller than 3000. For the maximum Reynolds number, the carryover coefficient of G23 is 1.22 which is between G19 and G20.

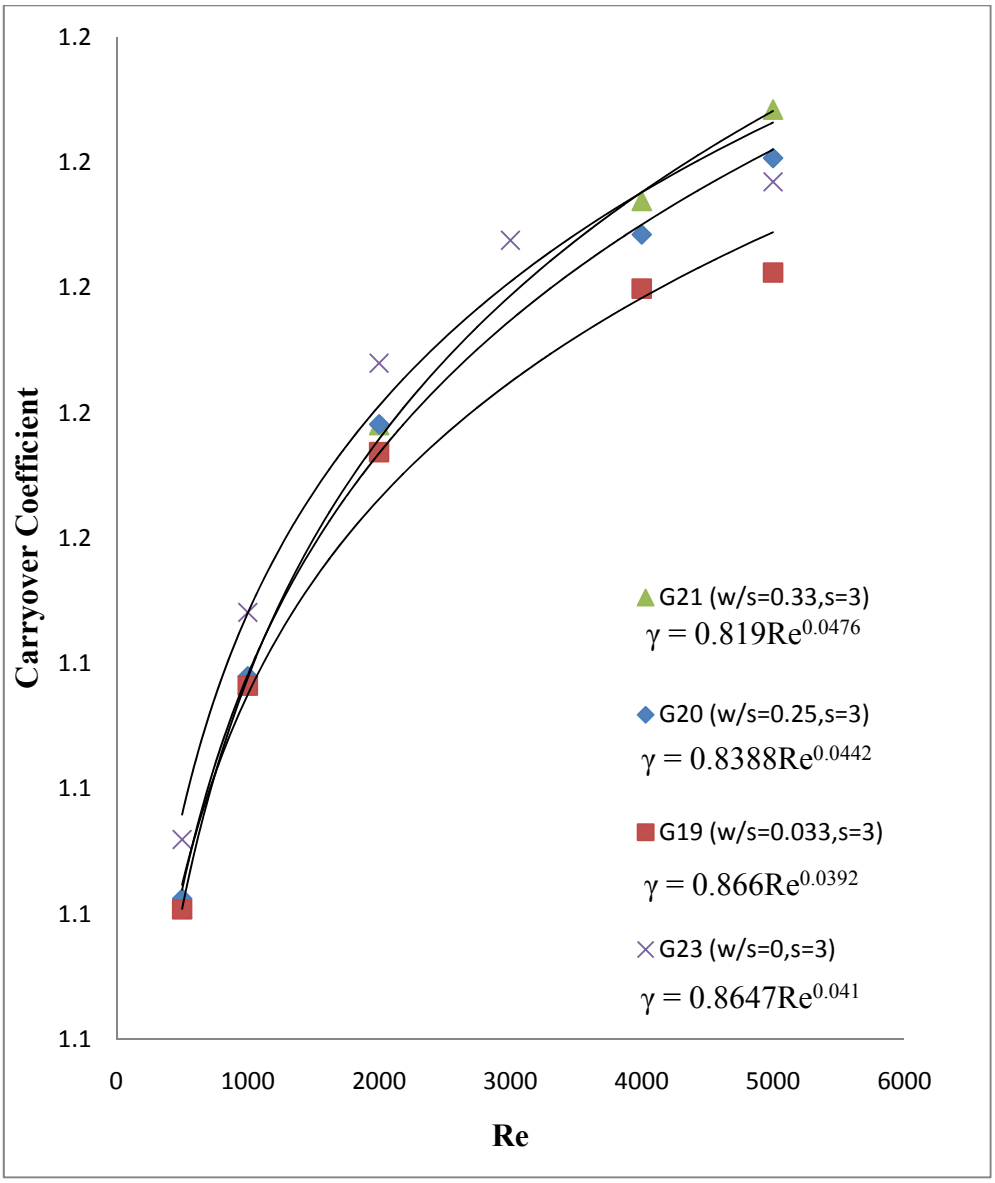

Figure 6.10 Effect of tooth width on γ (incompressible flow, W_{sh}=0)

Figure 6.11 and 6.12 shows the streamlines along with radial velocity contours of G20 and G19 respectively. The wider tooth (G20) causes the streamlines to converge even after the inlet of the tooth, which is called vena-contracta effect. However, streamlines diverge again and moves along the tooth surface until the exit as shown in

figure 6.11. The same effect is also present for narrower tooth (G19). However, since this profile has a narrow tooth width, the streamlines diverge without moving along the tooth surface as shown in figure 6.12. As a result, the divergence angle is bigger and the corresponding carryover coefficient is lower. This effect is more prominent when the Reynolds number is high.

Consequently, considering the sole effect of tooth width, the lower tooth width produces lower carryover coefficient compared to larger tooth width expect from sharp tooth case for high Reynolds numbers. For lower Reynolds numbers, the effect of tooth width is negligible.

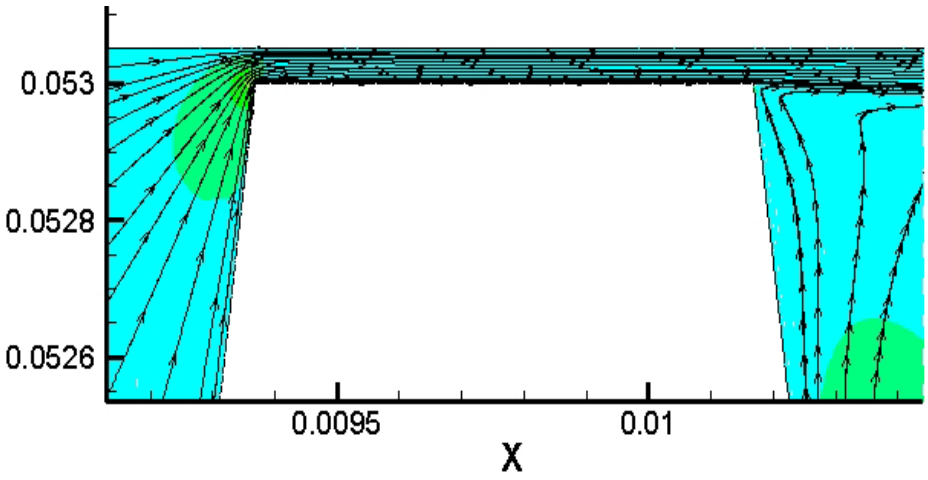

Figure 6.11 Streamlines and radial velocity contours of G20 (c/s=0.0167, w/s=0.25, s=3, Re=5000, incompressible flow, W_{sh}=0)

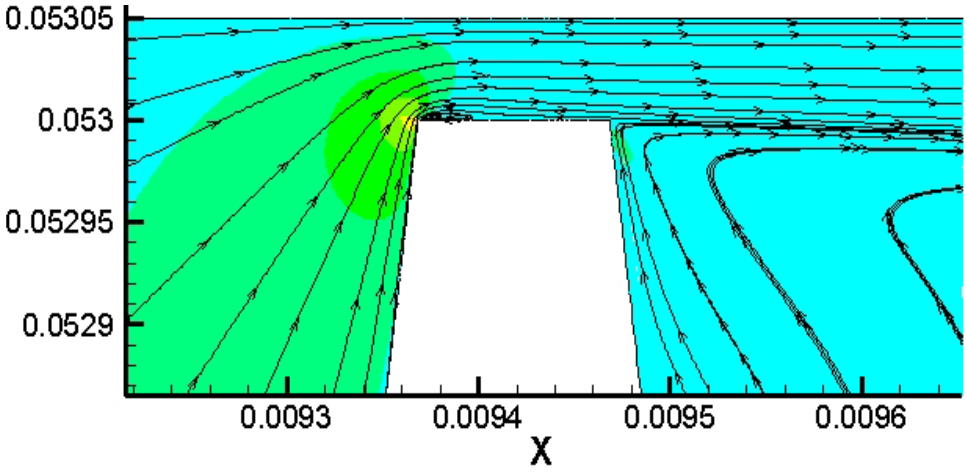

Figure 6.12 Streamlines and radial velocity contours of G19 (c/s=0.0167, w/s=0.033, s=3, Re=5000, incompressible flow, W_{sh}=0)

6.5 Effect of Tooth Pitch

It was shown that clearance to pitch ratio is a major parameter that affects the flow behavior through the labyrinth seal. As discussed in section 6.3, the carryover coefficient increases as this ratio is increased. This can either be done by increasing the clearance or decreasing the pitch. If the tooth pitch is decreased rather than increasing the clearance, the axial distance that fluid particle moves will also decrease so the portion of the flow directly moving to the next cavity without involving in circulation will increase, reducing the effectiveness of the seal. In order to present the effect of pitch on carryover coefficient, G2 and G4 are chosen. As can be seen from table 5.1, they have similar dimensions apart from tooth pitch which is four times larger for G4 compared to that of G2. Since the c/s ratio is decreased for G4, lower carryover coefficient is obtained. As can be seen from figure 6.13, G4 has significantly lower

carryover coefficient compared to that of G2. This effect is more prominent for higher Reynolds numbers. This result agrees with the findings of section 6.3. The same pattern is also observed by Saikishan [16].

It is apparent from figure 6.13 that the dependence of G4 on Reynolds number is significantly lower than that of G2. As Reynolds number changes from 1000 to 2000, the carryover coefficient of G4 slightly increases while a significant increment is observed for that of G2.

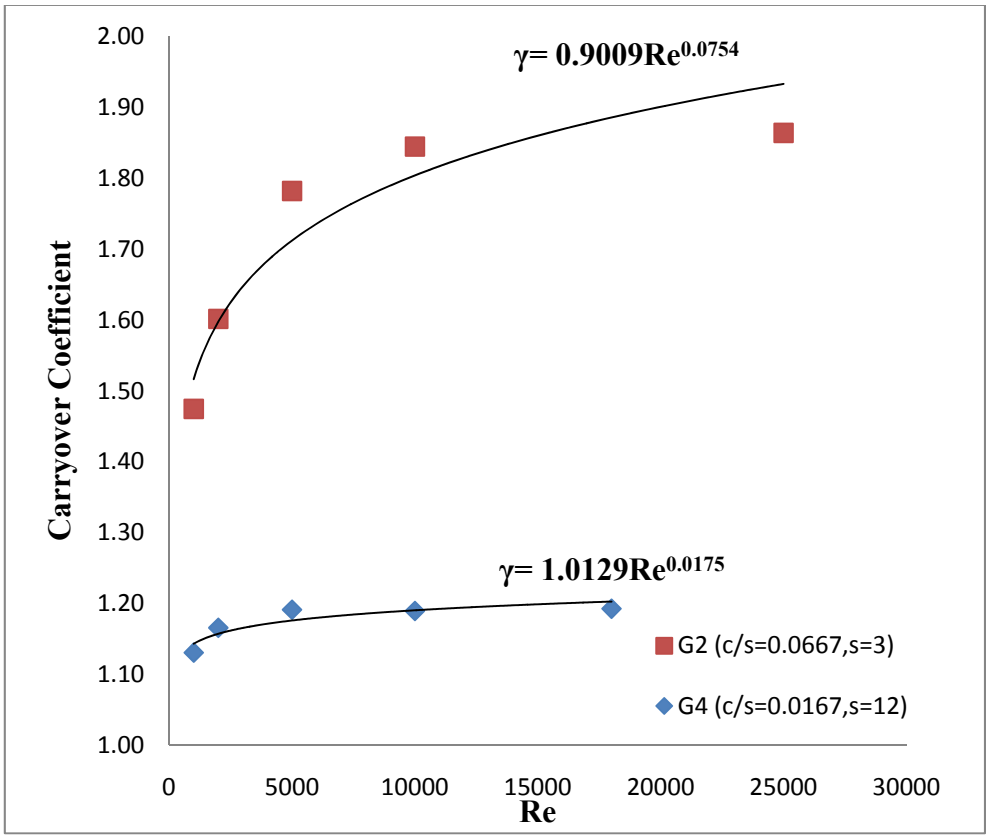

Figure 6.13 Effect of tooth pitch on γ (incompressible flow, W_{sh}=0)

The physics behind the effect of pitch on carryover coefficient can be illustrated by streamlines and velocity contours. Figure 6.14 shows the axial velocity contours and streamlines for G2 and figure 6.5.3 shows those of for G4. Comparing the axial velocities of G2 and G4 from figures 6.14 and 6.15 respectively, it is apparent that larger tooth pitch (G4) causes a significant reduction in the axial velocity inside the seal cavity while the smaller pitch does not allow this because the flow quickly enters the next tooth clearance. As a result, the axial velocity of G4 is significantly lower immediately before the inlet of downstream tooth compared to that of G2, even though they are similar at the exit of upstream tooth. Lower axial velocity allows fluid particle to move towards the rotor due to its radial velocity. Therefore, the fluid particle impinges on a lower part of the downstream tooth wall, increasing the divergence angle. As a result, the carryover coefficient decreases indicating that a larger portion of the kinetic energy is dissipated in the cavity.

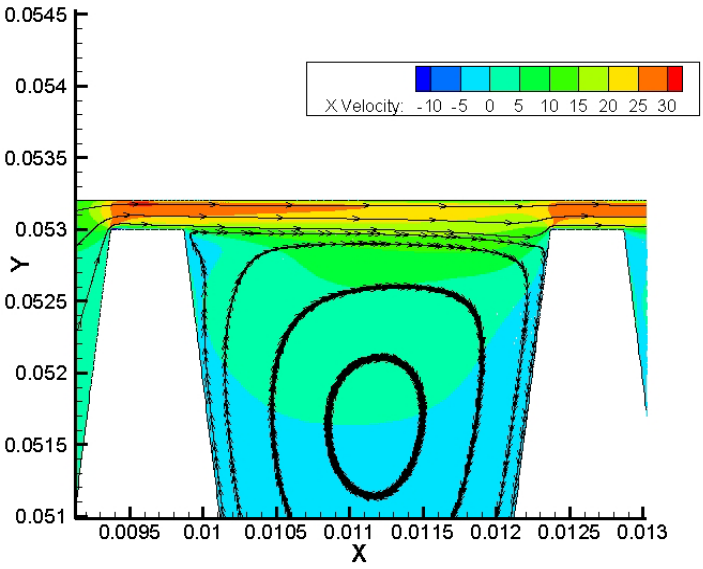

Figure 6.14 Streamlines in the first cavity of G2
(c/s=0.0667, w/s=0.167, s=3, Re=5000, incompressible flow, W_{sh}=0)

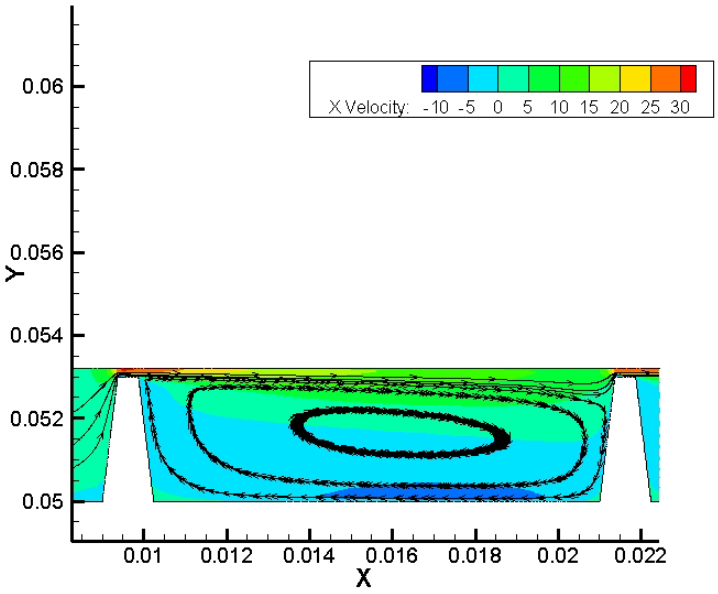

Figure 6.15 Streamlines in the first cavity of G4
(c/s=0.0667, w/s=0.0416, s=12, Re=5000, incompressible flow, W_{sh}=0)

In sections 6.3 and 6.4, clearance to pitch ratio was used as the dimensionless reference parameter. The effect of this ratio is again investigated here with a different comparison. G6 has four times higher tooth clearance, height and pitch ratio compared to G2 but the tooth widths are same. As a result, the c/s ratios are same for both cases. For the same c/s ratios, similar carryover coefficients are expected. As can be seen from figure 6.16, the carryover coefficient is almost the same for G2 and G6. G6 has negligibly higher carryover coefficients for Reynolds number 2000 and 5000. This may be due to w/s being smaller.

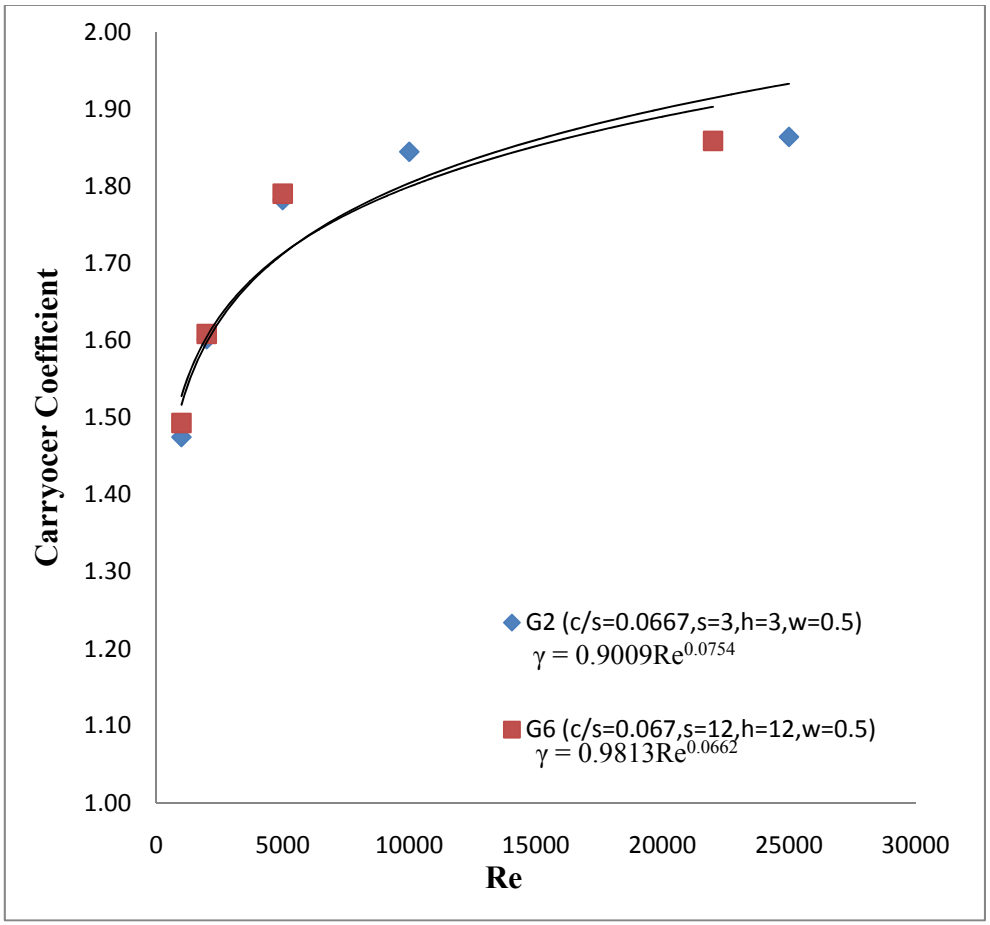

Figure 6.16 Comparison of same c/s ratios (incompressible flow, W_{sh}=0)

6.6 Effect of Tooth Height

The aspect ratio of the cavity (h/s) could have some effect on carryover coefficient. G24, G25 and G27 are chosen in order to present this effect. They all have the same tooth clearance, width and pitch. The height is varied and the dependence on Reynolds number is plotted in figure 6.17.

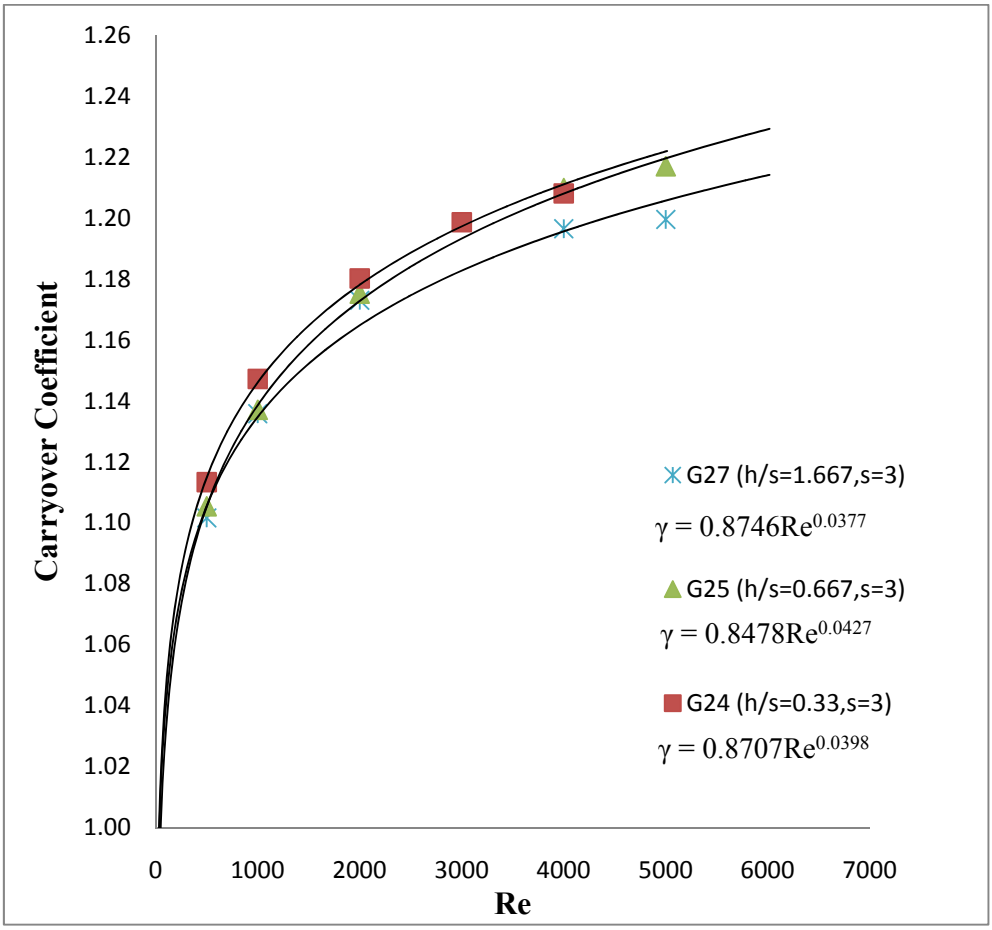

Figure 6.17 Effect of tooth height on γ (Incompressible flow, W_{sh}=0)

According to figure 6.17, the deeper cavity produces slightly lower carryover coefficient. This can be attributed to the secondary circulation zone which occurs when the tooth height is increased. Figures 6.18 and 6.19 show the streamlines for G25 and G27 respectively. As can be seen from figure 6.19, as the tooth height is increased, a secondary vortex occurs under the main large vortex. This vortex can be the reason for the enhanced divergence of the main streamline. However, it should be noted that the dependence of carryover coefficient on tooth height is such that an increase in tooth height by a factor of 5 reduces carryover coefficient by only 2%. This is even less when the Reynolds number is lower (i.e. 500 and 1000).

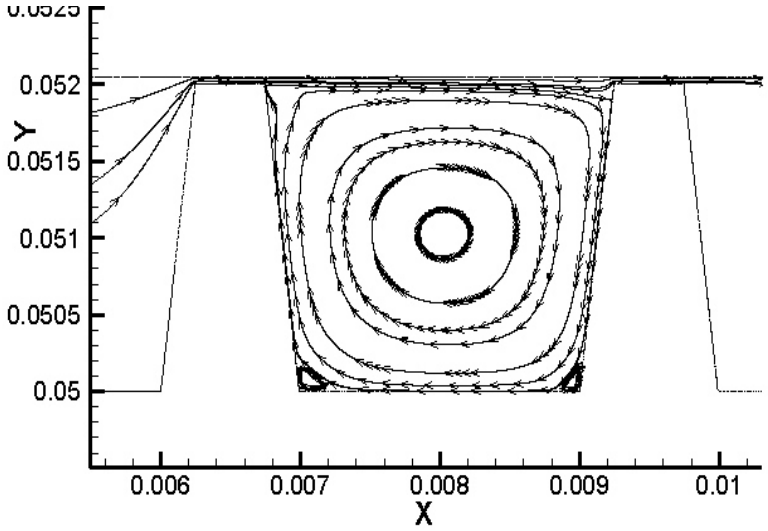

Figure 6.18 Streamlines in shallow cavity
(G25, c/s=0.01667, h/s=0.667, s=3, Re=5000, incompressible flow, W_{sh}=0)

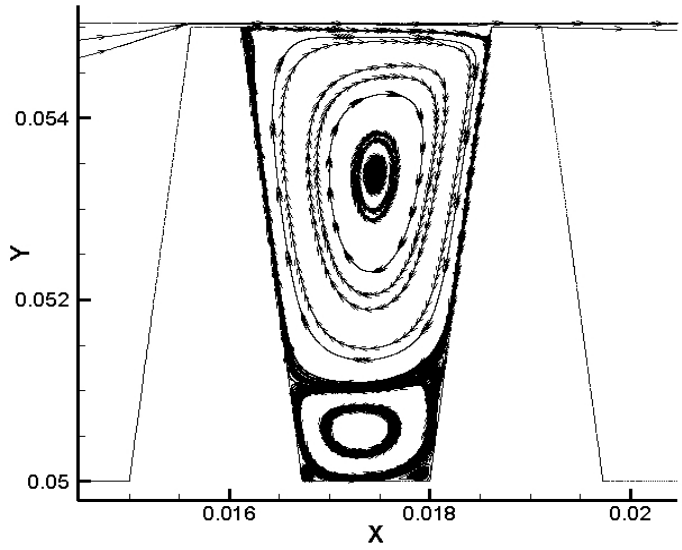

Figure 6.19 Streamlines in deep cavity
(G27, c/s=0.01667, h/s=1.667, s=3, Re=5000, incompressible flow, W_{sh}=0)

6.7 Effect of Upstream Side Angle

As shown in the labyrinth seal nomenclature (figure 1.1), the tooth profile has an angle on both upstream and downstream sides. The angle at the upstream side, *Q*, is investigated in this study. G3 and G13 have the same dimensions other than *Q* which is 7^o and 0^o respectively for G3 and G13. Similarly, G4 and G9 have the same dimensions other than *Q* which is 7^o and 0^o respectively for G4 and G9. Thus, the sole effect of *Q* can be obtained by examining these geometries.

It can be seen from figure 6.20 that *Q* of 0^o produces a higher carryover coefficient for both comparisons. This difference is more prominent for high Reynolds numbers. Changing *Q* from 7^o to 0^o causes the carryover coefficient to increase approximately 4% for both G3 and G4. It is attributed to the radial component of the

momentum of the main jet. For Q=0^o case, the radial component of the momentum of the jet before the cavity moving along the tooth is higher than that of Q=7^o case. As a result, it pushes the main jet even further to the stator wall decreasing its divergence. As a result, the carryover coefficient increases for this case.

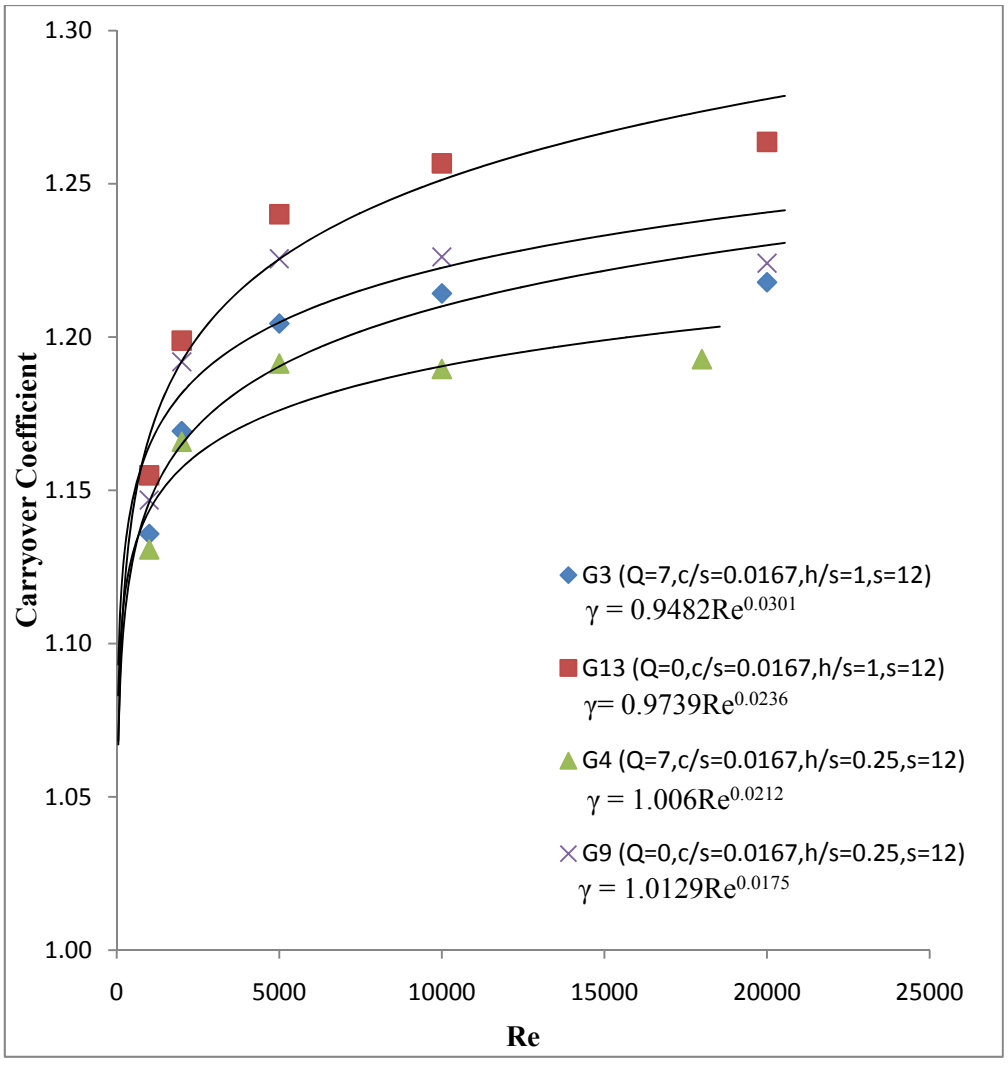

Figure 6.20 Effect of upstream side angle on γ (incompressible flow, W_{sh}=0)

Figures 6.21 and 6.22 show the streamlines of G3 and G13 respectively when the Reynolds number is 1000.As mentioned above, the divergence of the main streamline of G13 is less compared to that of G3. As a result, the carryover coefficient is higher.

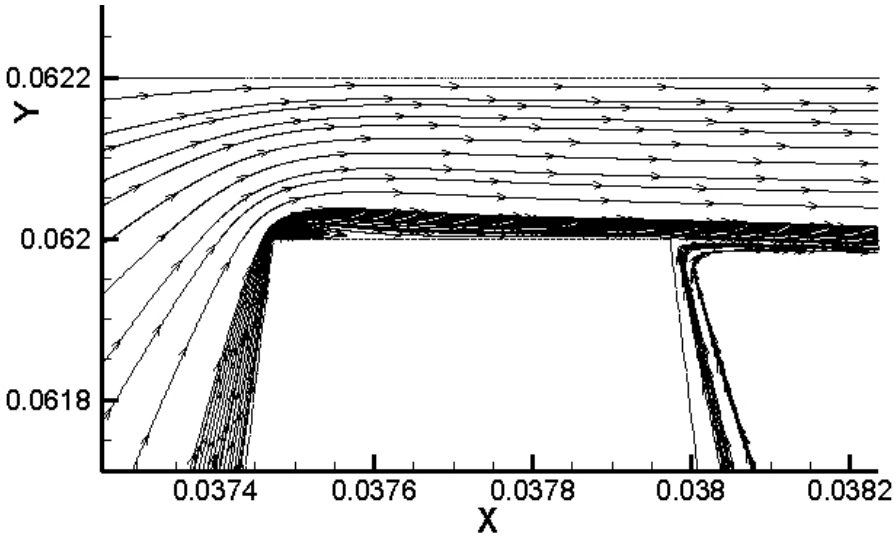

Figure 6.21 Streamlines above first tooth of G3
(Q=7, c/s=0.0167, s=12, Re=10000, incompressible flow)

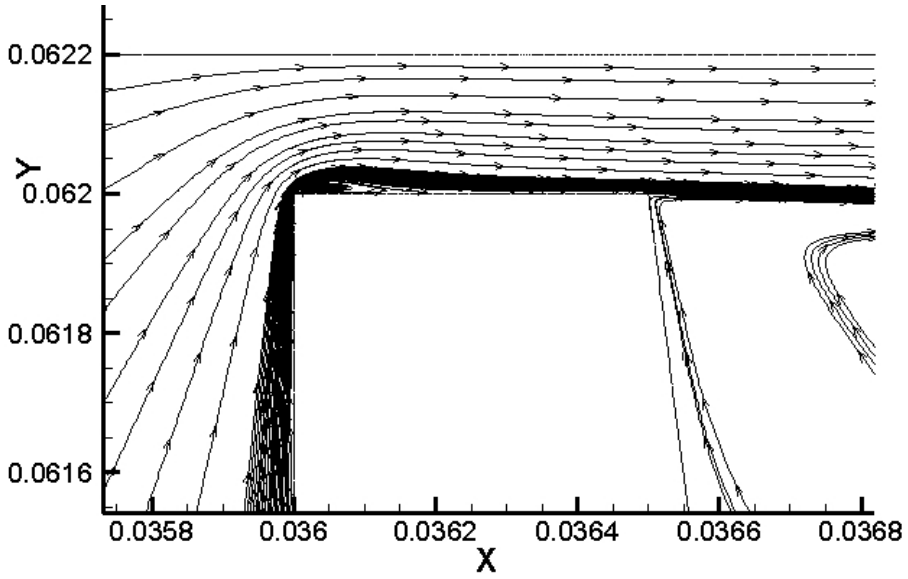

Figure 6.22 Streamlines above first tooth of G13
(Q=0, c/s=0.01667, s=12, Re=10000, incompressible flow)

The effects of geometrical parameters and Reynolds number are discussed so far without considering the effect of shaft rotation. It was observed that each geometrical parameter has an effect on carryover coefficient. These effects are summarized in the table 6.1.

Table 6.1 Effects of geometrical parameters and Re on γ

Increasing	γ
c	increases
s	decreases
w	increases
h	decreases
Q	decreases
Re	increases

Table 6.1 presents the response of carryover coefficient to an increase in the variables on the left hand side. Among these variables, c, s and Re are considered primary variables which have significant effect on carryover coefficient. On the other hand, w, h and Q are considered secondary parameters which have small effect on carryover coefficient. Amongst them, tooth height has the smallest effect. The effect of secondary variables almost vanishes when the Reynolds number is small.

6.8 Effect of Shaft Speed

The sections so far considered only the stationary rotor case. However, in real applications, the rotor is rotating introducing a swirl velocity to the flow. The effect of swirl velocity is usually defined by the Taylor number. This section aims to present the relationship between shaft speed and carryover coefficient for a given seal geometry.

Since shaft speed is a dimensional parameter, it is not convenient to use it directly to present its effects on carryover coefficient. The Taylor number will be used as the non-dimensional parameter to show the shaft speed effects on carryover coefficient. The Taylor number introduces the ratio of centrifugal forces to viscous forces. Taylor number has various expressions which are not essentially equivalent. In this study, the following definition is used.

$$Ta = \frac{W_{sh}\, c}{v}\left(\frac{c}{r_{sh}}\right)^{1/2} \quad (6.3)$$

One of the most important effects of shaft rotation is that it causes secondary vortices. This is especially apparent when the Reynolds number is low and the Taylor

number is high. This relationship between the secondary vortex presence and the Re/Ta ratio is further discussed in Demko's [18] study. This secondary vortex prevents the mainstream jet from impinging on the downstream tooth wall. As a result, the definition of carryover coefficient by Hodkinson [2] is not applicable as discussed in section 6.1 and the carryover coefficient for that kind of flow is assumed to be 1. Figure 6.23 shows the streamline and pressure distribution in the cavity without rotation and figure 6.24 shows those with rotation, keeping all other parameters the same. One single streamline is chosen in order to better present the flow path of the fluid particle. If the rest of the streamlines are to be plotted, the vortices similar to that of figure 6.1 and 6.2 will be seen. As can be seen from figure 6.23, the main streamline directly impinges on the downstream tooth wall when the shaft is not rotating. However, as can be seen from figure 6.24, when the shaft speed is considered, the main streamline can move downwards without impinging on the wall until it reaches the rotor and moves back to the clearance region along the wall of the downstream tooth, creating a secondary vortex for larger Taylor numbers.

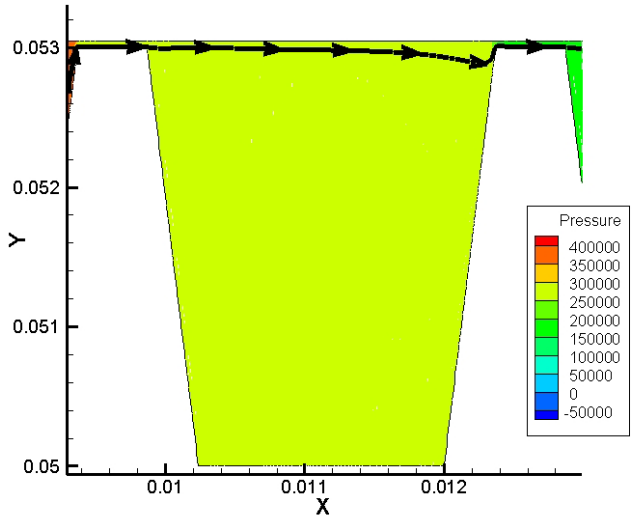

Figure 6.23 Main streamline impinging on the wall
(G1, c/s=0.0167, s=3, h/s=1, w/s=0.167, Re=4000, incompressible flow, W_{sh}=0)

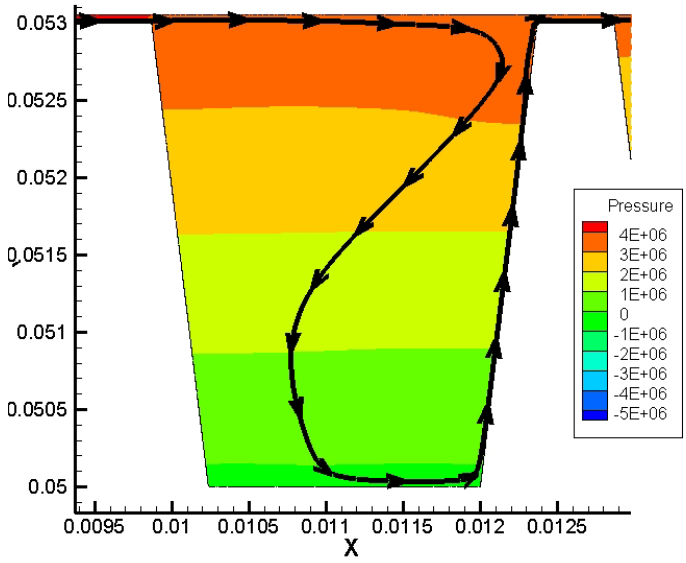

Figure 6.24 Main streamline creating secondary vortex
(G1, c/s=0.0167, s=3, h/s=1, w/s=0.167, Re=4000, incompressible flow, W_{sh}=350)

Shaft rotation also has a significance effect on pressure distribution. As can be seen from figure 6.23, the static pressure distribution in the cavity is uniform both in radial and axial direction when the shaft is stationary. However, the pressure is significantly increasing in the radial outwards direction when the shaft is rotating as in figure 6.24. This is caused by the centrifugal force due to the swirl velocity imparted to the fluid by the shaft. As a result, the static pressure is maximum near the stator wall region and minimum near the rotor wall region. Moreover, increasing shaft speed also increases the shear stress at the wall.

Figure 6.25 shows the variation of carryover coefficient of the first cavity of G1 when the shaft speed is gradually increased from 0 to 350 m/s, corresponding Taylor numbers are presented in the x axis. It is observed that the shaft speed has a strong effect on carryover coefficient. This effect is not linear and fluctuating as the shaft speed varies. For G1 as shown in figure 6.25, the effect of shaft speed decreases the carryover coefficient for low Reynolds number (i.e. 1000 and 2000).

When Reynolds number is 1000, the carryover coefficient significantly decreases until Taylor number is 200. For higher Taylor numbers, shaft speed causes a secondary vortex and the carryover coefficient is set to 1. When the Reynolds number is 2000, a 5% overall decrease in carryover coefficient is observed. When Reynolds number is 3000 and 4000, this secondary vortex is not observed and the carryover coefficients are evaluated as given in figure 6.25. When the Reynolds number is 3000, the carryover coefficient gradually increases as the shaft speed is increased. The overall increase for this Reynolds number is 8%. For Re=4000, the carryover coefficient initially increases and then decreases with an overall increase around 3%. It is apparent that the effect of shaft speed in flow behavior and accordingly the carryover coefficient is very complex and does not follow a certain pattern.

Figure 6.26 shows the variation of streamlines in the first cavity of G1 for all set of Reynolds numbers as shaft speed increases. The secondary vortices can be observed for low Reynolds numbers at low shaft speeds while they can only be observed at high shaft speeds for high Reynolds numbers.

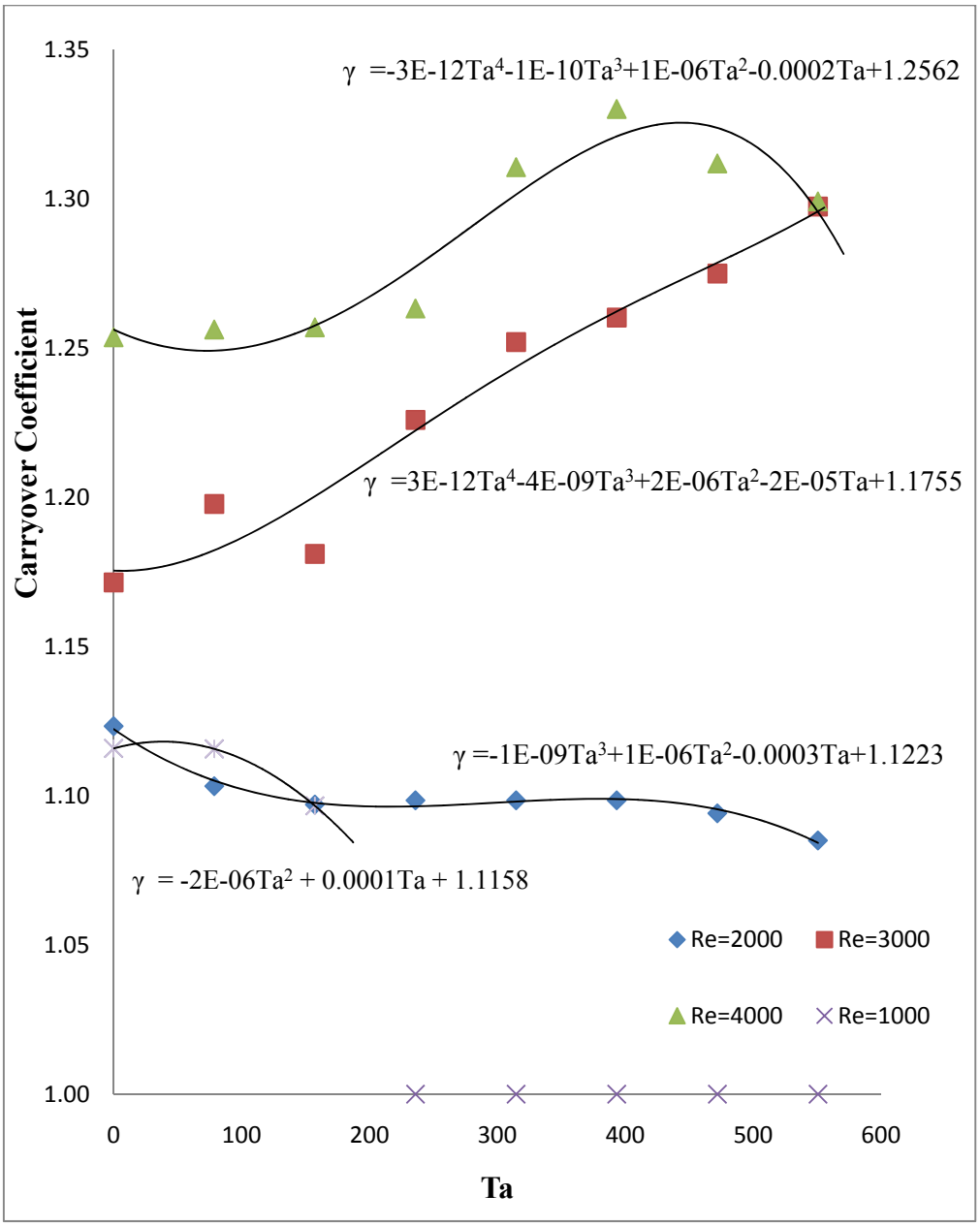

Figure 6.25 Effect of shaft speed on first cavity γ
(G1, c/s=0.0167, s=3, h/s=1, w/s=0.167, incompressible flow)

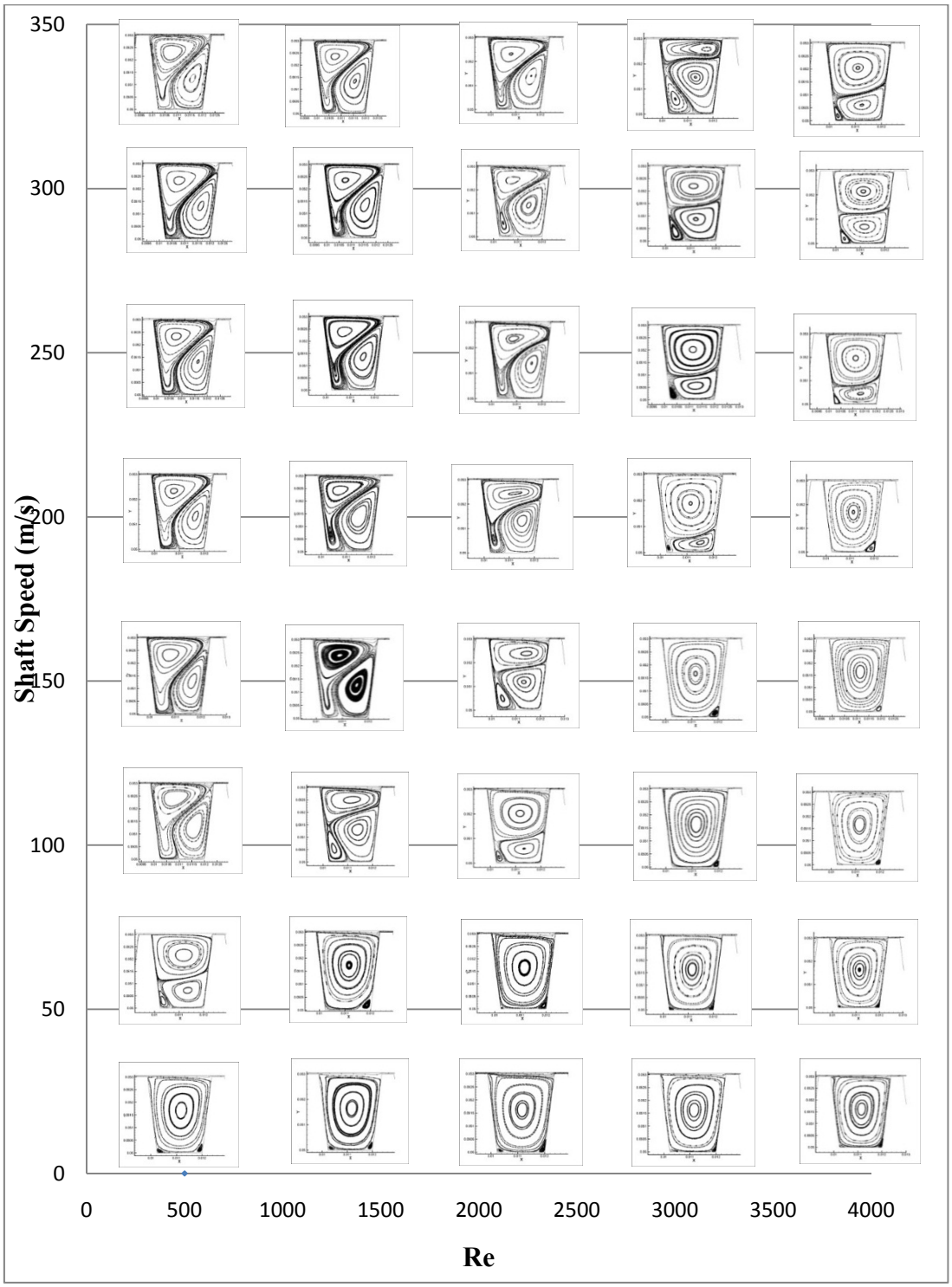

Figure 6.26 Variation of streamlines with respect to Re and shaft speed (G1, c/s=0.0167, s=3, h/s=1, w/s=0.167, incompressible flow)

Figure 6.27 shows the carryover coefficient of the first cavity for different Reynolds numbers for G4. It is seen that the effect of shaft speed on carryover coefficient of G4 somewhat follows a pattern. As shaft speed increases, the carryover coefficient decreases. It is observed that the secondary vortex has occurred in G4 possibly due to the shallow and long cavity profile. For Reynolds numbers of 1000 and 2000, secondary vortex immediately occurs when the shaft speed is more than 50 m/s. When the Reynolds number is 5000, the carryover coefficient drastically decreases as Taylor number increases until the presence of secondary vortex. Similar pattern with relatively less decrement in carryover coefficient is observed at Reynolds number 10000. When the Reynolds number is 18000, the carryover coefficient gradually decreases until the shaft speed is 350 m/s, which is the maximum speed simulated. Thus, it can be stated that it is harder for secondary vortex to be present for higher Reynolds numbers. The variation of streamlines in the cavity with respect to Reynolds number and shaft speed is presented in figure 6.28. As Demko [18] stated in his study, there seems to be a critical ratio of Taylor number to Reynolds number at which the secondary vortex occurs. This will be discussed at the end of this section.

The c/s ratio of G4 is same with that of G1 but the pitch and clearance are increased by a factor of 4. As discussed earlier, c/s is a major dimensionless parameter upon which the carryover coefficient is dependent. However, it seems that when the rotational effect is present, the dependence upon the c/s ratio reduces. Thus, it is clear that the combined effects of flow and geometrical properties should be investigated, which will be done in the next section.

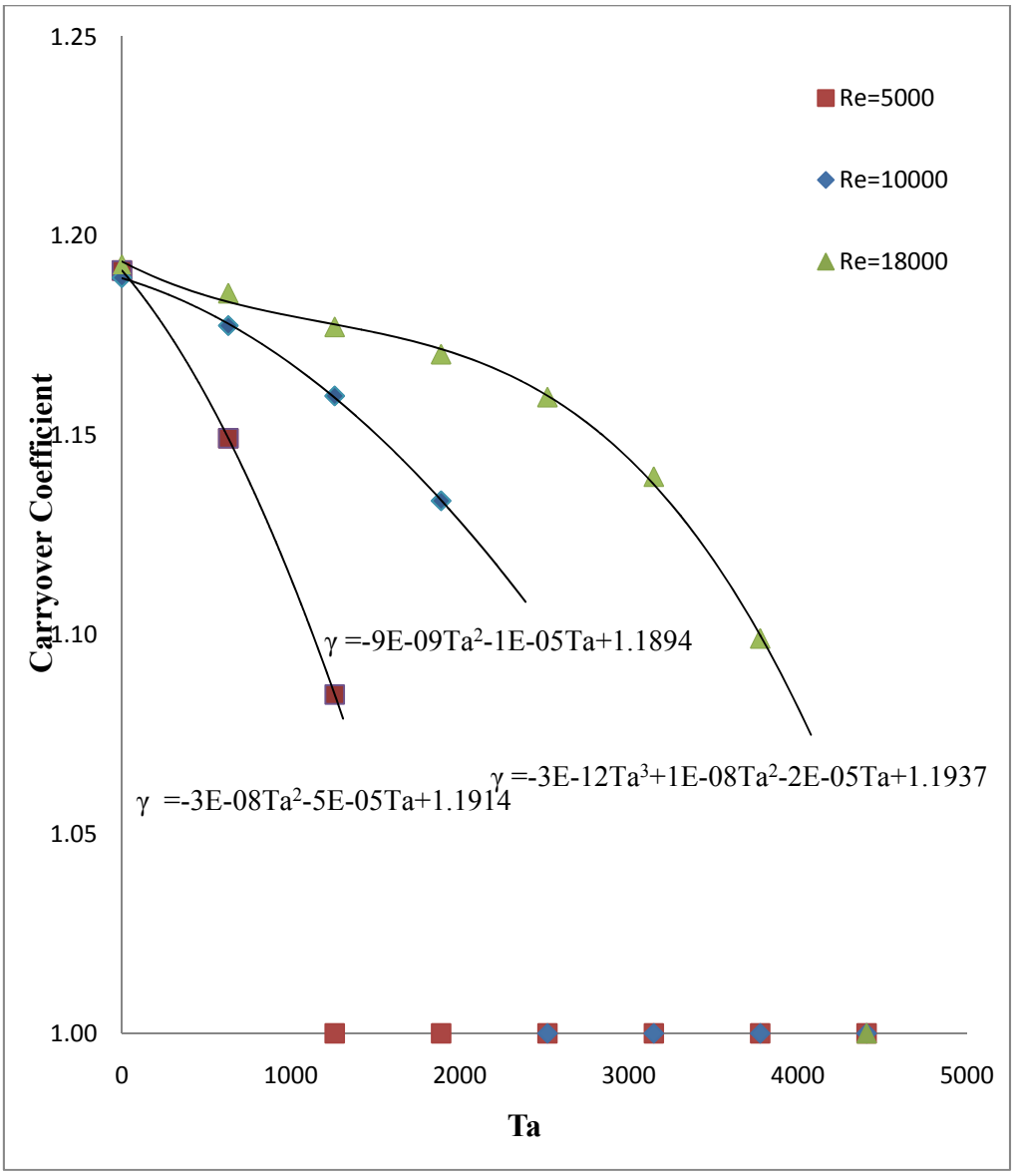

Figure 6.27 Effect of shaft speed on first cavity γ
(G4, c/s=0.0167, s=12, h/s=0.25, w/s=0.04167, incompressible flow)

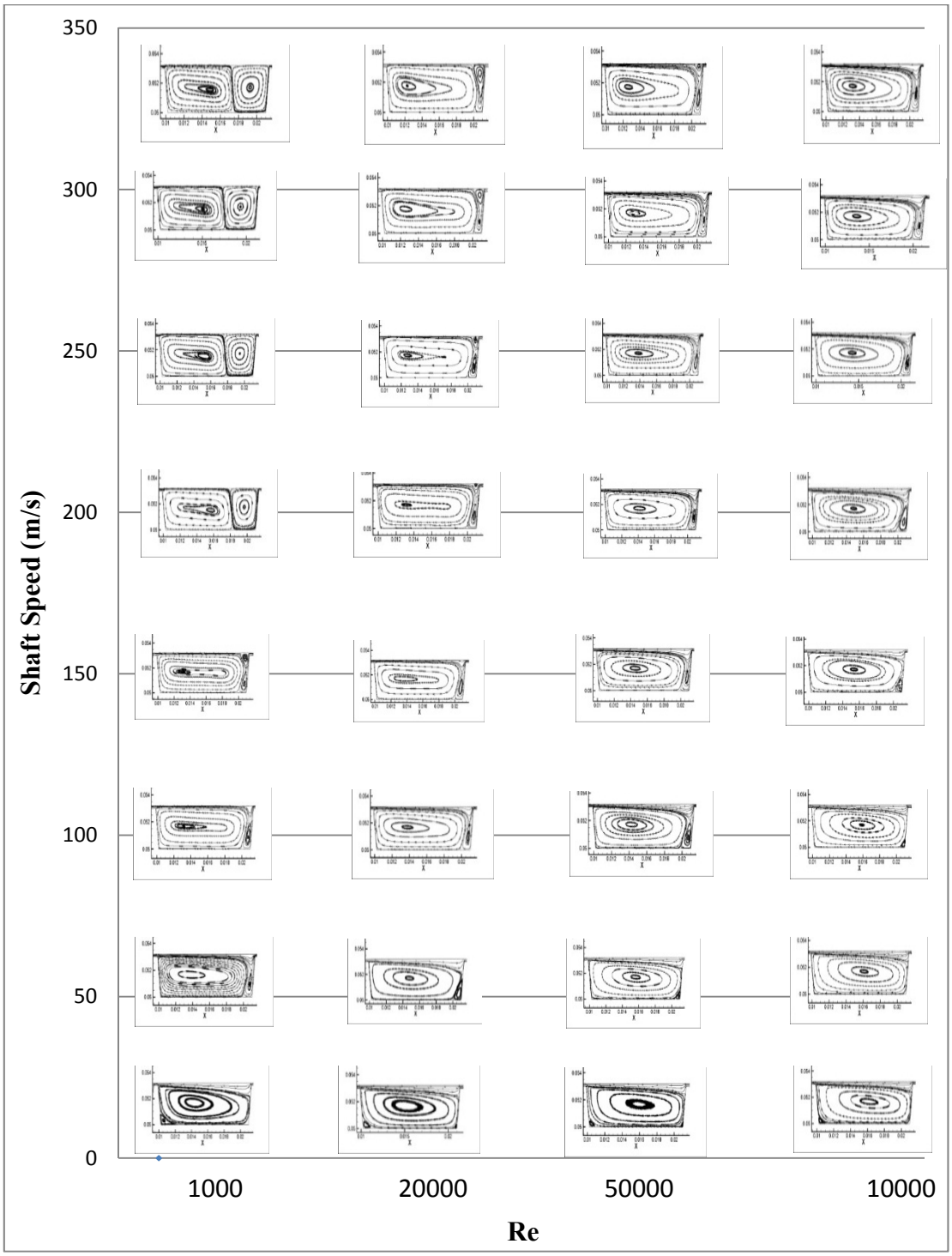

Figure 6.28 Variation of streamlines with respect to Re and shaft speed (G4, c/s=0.0167, s=12, h/s=0.25, w/s=0.04167, incompressible flow)

Figure 6.29 presents the carryover coefficients of the first cavity of G21 for different Reynolds numbers. G21 has twice width length compared to G1 and other parameters are similar to G1. However, the effect of shaft speed on this case is significantly different than that of G1. All Reynolds numbers show a decrease in carryover coefficient as shaft speed increases. This pattern is more prominent when the Reynolds number is lower. The secondary vortex is observed at a Taylor number of 220 when Reynolds number is 1000. The overall decrement in carryover coefficients are 10%, 6.6% and 5.6% respectively for Reynolds numbers of 2000, 4000 and 5000.

Figure 6.30 shows the distribution of streamlines in the first cavity of G21 as shaft speed and Reynolds number vary. As discussed earlier, the presence of secondary vortex at high Reynolds numbers requires higher shaft speed. As the vortex structure is considered from left to right for a given shaft speed, it can be observed that the secondary vortex gradually decreases. This pattern can be better observed for high shaft speeds (i.e. more than 200). The secondary vortex separates the large vortex in to two vortices. Then it wraps around the small vortex at the bottom of the cavity. For high Reynolds numbers and low shaft speeds (less than 200), these two vortices totally vanish leaving one single large vortex. However, when shaft speed is higher than 200 at high Reynolds numbers, two vortices are observed.

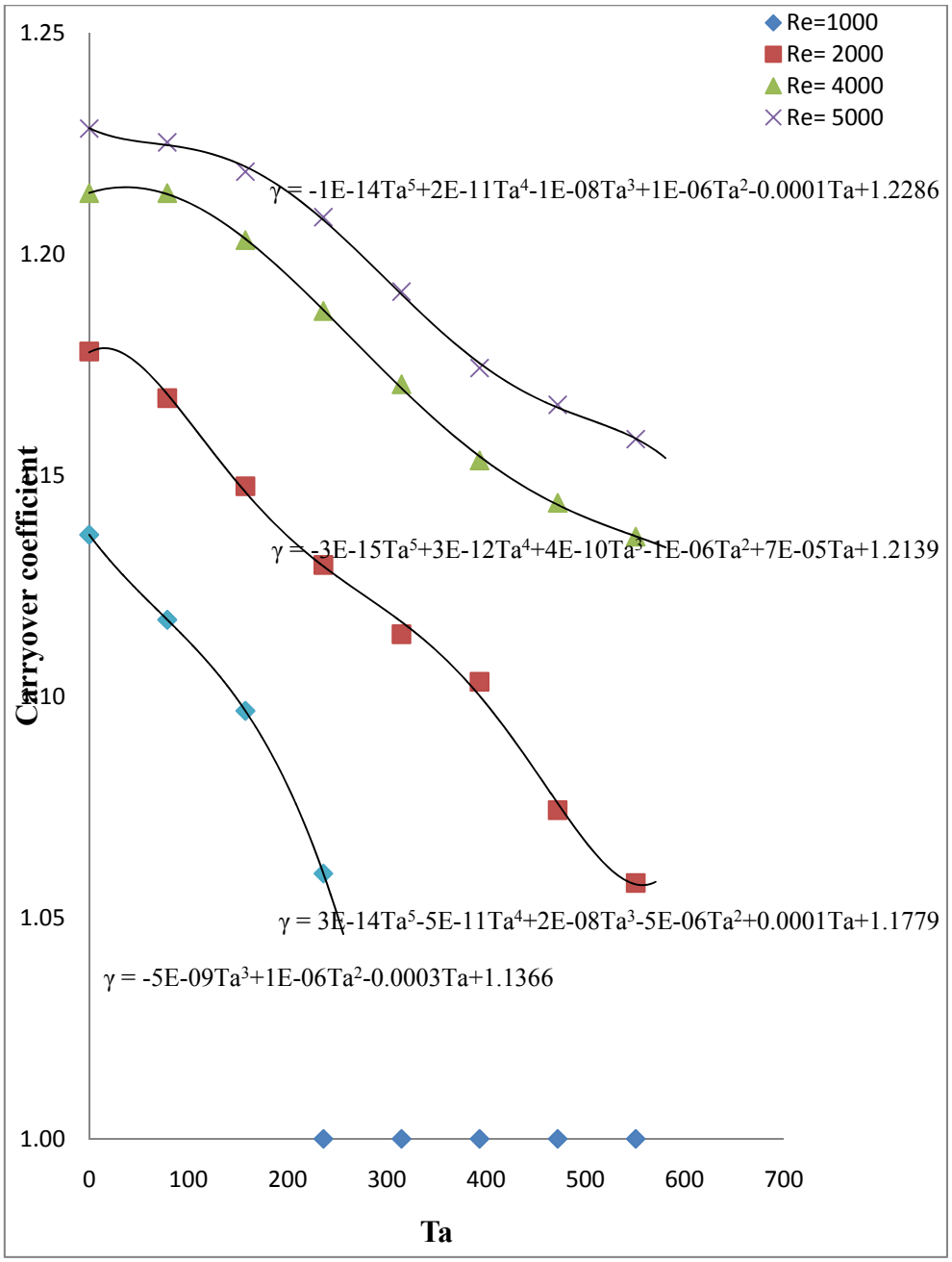

Figure 6.29 Effect of shaft speed on first cavity γ
(G21, c/s=0.0167, s=3, h/s=1, w/s=0.333, incompressible flow)

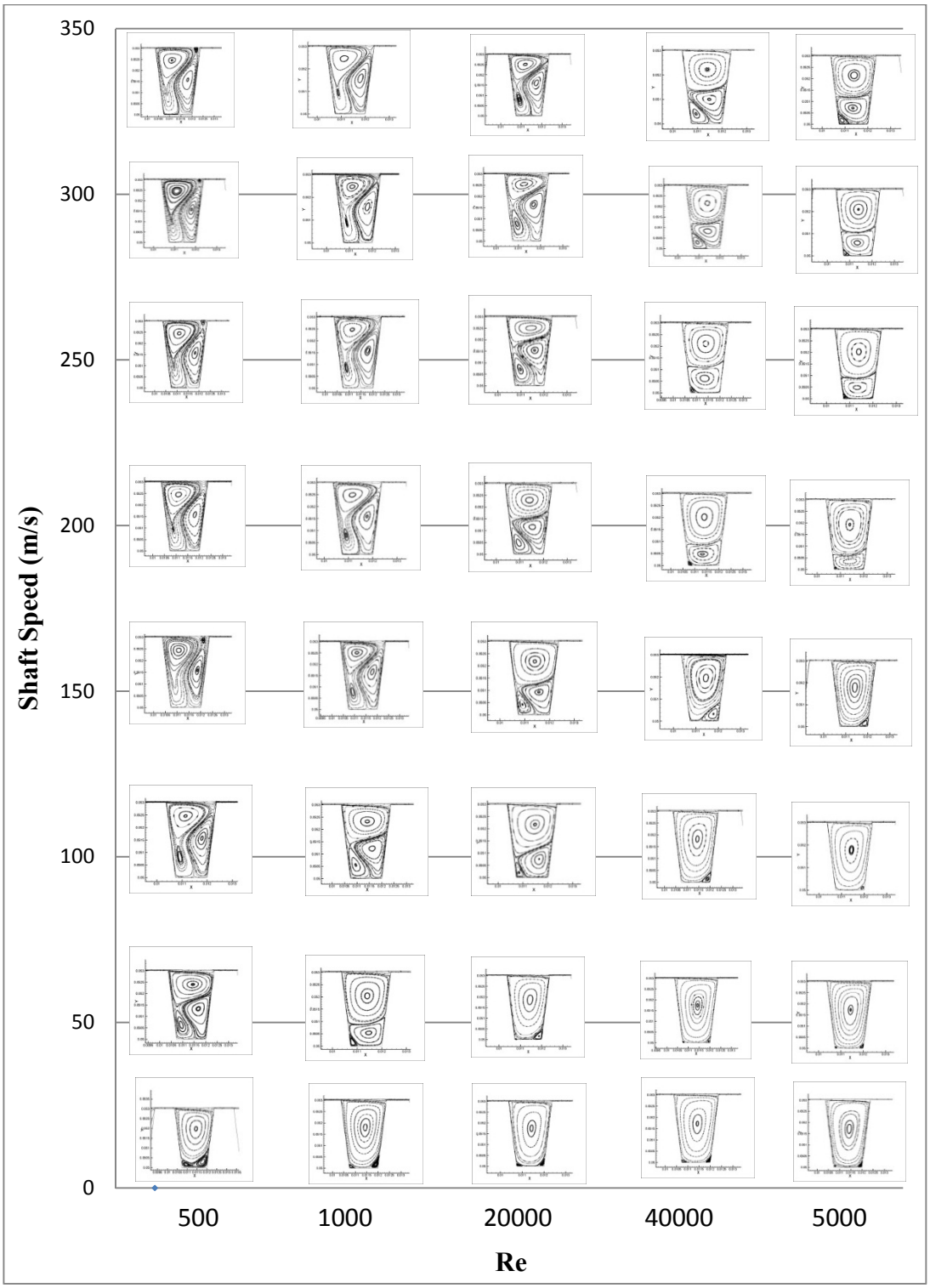

Figure 6.30 Variation of streamlines with respect to Re and shaft speed (G21, c/s=0.0167, s=3, h/s=1, w/s=0.333, incompressible flow)

From figures 6.25, 6.27 and 6.29, it can be observed that low Reynolds number flows can easily create a secondary vortex as the Taylor number increases. For G1, this is observed when Ta/Re ratio is 0.31 and 0.24 respectively for Reynolds numbers of 500 and 1000. For G4, this is observed when Ta/Re ratio is 0.31, 0.25, 0.20 and 0.24 respectively for Reynolds numbers of 2000, 5000, 10000 and 18000. Similarly, for G21, this is observed when Ta/Re ratio is 0.2 and 0.24 respectively for Reynolds numbers of 500 and 1000.

Considering all of the Ta/Re ratios together, it is observed that the secondary vortex occurs when Ta/Re ratio is between 0.2 and 0.31. However, it should be noted that these ratios are evaluated approximately. For example, considering G4 when the Reynolds number is 2000, assume that the flow does not have a secondary vortex at a certain Taylor number of 630. Then, the secondary vortex is observed and it is fully developed at a Taylor number of 1260. In this case, the critical ratio is evaluated by using the value at which secondary vortex is observed (1260). However, in order to obtain the exact critical point, many different Taylor numbers between the point at which secondary vortex is not observed and the point at which secondary vortex is observed should be investigated. By this way, more accurate results can be achieved. Therefore, these results show that the critical Ta/Re point lies approximately between 0.2 and 0.31. Using these results, the following graph is generated.

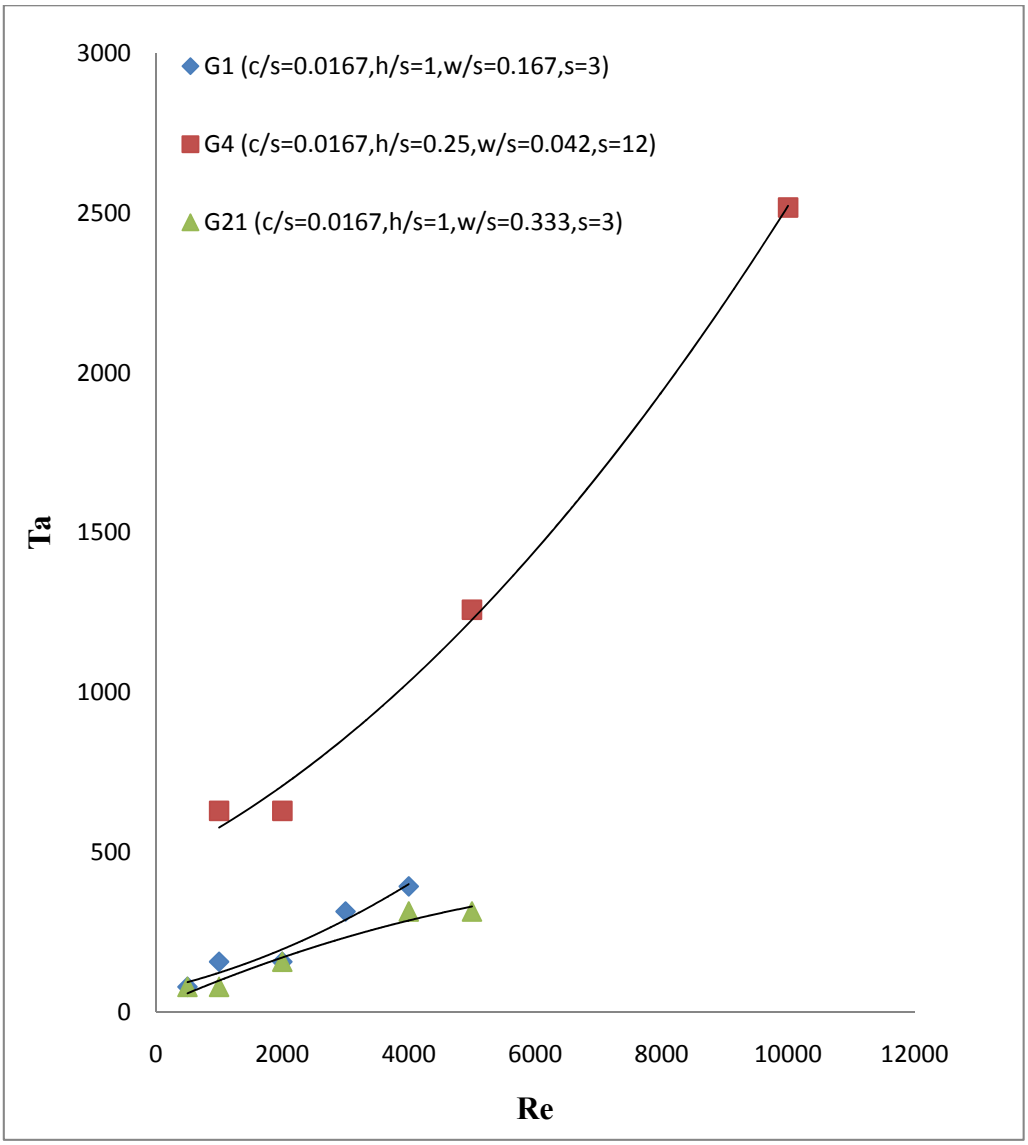

Figure 6.31 Flow map indicating region where secondary recirculation forms

Figure 6.31 shows at which Reynolds and Taylor number secondary recirculation zone forms for G1, G4 and G21. The region above the trend lines of each seal has secondary recirculation zone while the region below only has one large circulation zone. It is clear that Reynolds number strongly effects the secondary recirculation. As

Reynolds number increases, higher shaft speed is required for secondary recirculation to form.

Comparing G1 and G4, it is apparent that the h/s ratio has a significant effect on secondary flow formation. The w/s ratios of these geometries are also different due to higher toot pitch of G4 even though the width values are the same. However, comparing G1 and G21, it can be concluded that tooth width has negligible effect on secondary flow formation. Thus, h/s ratio is also a major parameter that affects secondary circulation as well as Reynolds number.

It is shown that the shaft speed can decrease the carryover coefficient up to 10%. In some cases, it can also increase it up to 8%. In general, it can be concluded that the shaft speed usually reduces the carryover coefficient. However, its effect seems to depend on geometrical features. For example, the effect of shaft speed on carryover coefficient is very different for cases G1 and G21 possibly due to tooth width and the axial distance between the consecutive teeth. Moreover, for G1 and G4, the shaft speed effect is different even though the c/s ratio is same but the dimensions are different. As a result, it is clear that the combined effects of the shaft speed and geometrical features should be studied. This will be done in the following section

.

6.9 Combined Effects

From sections 6.2 to 6.8, it was shown that the carryover coefficient is a function of both geometrical and flow properties. Amongst geometrical properties, tooth clearance and pitch have a stronger effect on carryover coefficient compared to tooth height, width and upstream side angle. Amongst flow properties, Reynolds number usually has a stronger effect compared to Taylor number. Moreover, when combined effects are considered, the prominences of the effects of those parameters are affected by other parameters. Hence, this section aims to understand the combined effects of parameters on carryover coefficient. This will be done by introducing 3D surface graphs, along with 2D plots, in which the effects of many parameters can be seen at the same time.

Figure 6.32 shows the first cavity carryover coefficients of G1 and G21. Apart from tooth width, all other parameters are same. It was shown that increasing tooth width by 30% causes a 2% increase in carryover coefficient at high Reynolds numbers. Moreover, it was discussed that the shaft speed causes the carryover coefficient to decrease. Thus, one would expect the lowest carryover coefficient at the point where the shaft speed is highest and the tooth width is smallest at high Reynolds numbers. However, the combined effect of shaft speed and tooth width can cause a resultant effect which is different from individual effects.

As can be seen from figure 6.32, the carryover coefficient of G1 is slightly lower than that of G21 for the shaft speeds up to 150 m/s with a corresponding Taylor number of 200. Moreover, increasing shaft speed also slightly reduces the carryover coefficient.

These patterns are slightly more prominent when the Reynolds number is more than 2000. So far, these observations agree with the results of section 6.4 and 6.7. However, when the Taylor number is more than 200, the opposite effect is observed. The carryover coefficient of the smaller tooth width (G1) increases by 8.5% while that of wider tooth width (G21) decreases by 5% as the Taylor number and Reynolds number reach the highest value before the overall pressure difference across the seal is 200 atm. For low Reynolds numbers (up to 2000), the secondary recirculation zone is observed. However, when Reynolds number is more than 2000, neither the secondary recirculation zone nor its incipience is observed. Thus, this unexpected pattern cannot be attributed to the secondary recirculation. Moreover, at low Taylor numbers (up to 200) for all Reynolds numbers, the smaller width gives lower carryover coefficient. Thus, it can be concluded that a sharper tooth produces a better carryover coefficient at low Taylor numbers, regardless of Reynolds number, while wider tooth produces a better carryover coefficient at higher Reynolds and Taylor numbers. Similar to all observations that were stated so far, this pattern is more prominent at high Reynolds numbers.

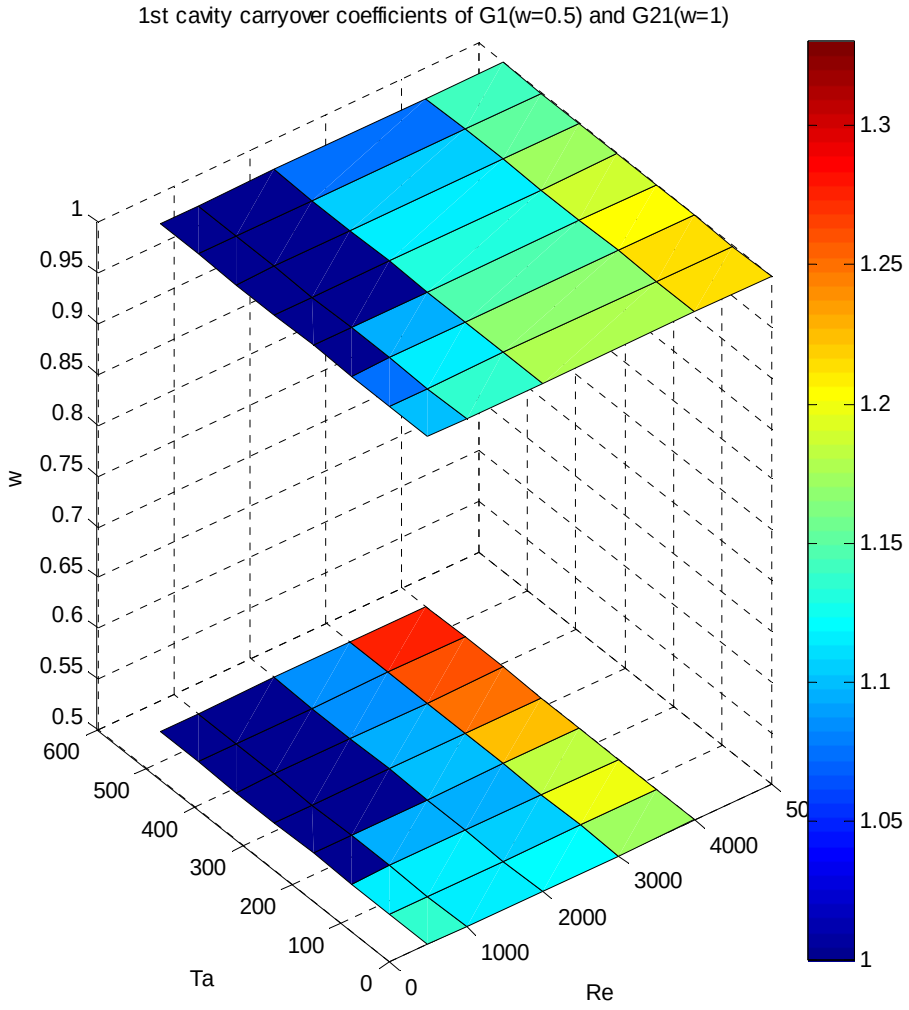

Figure 6.32 First cavity γ comparison of G1(c/s=0.0167, s=3, h/s=1, w/s=0.167, incompressible flow) and G21(c/s=0.0167, s=3, h/s=1, w/s=0.333, incompressible flow)

Figure 6.33 shows the carryover coefficients for the 2nd and 3rd cavities of G1 and G21. It should be noted that the distribution is very similar to that of first cavity. However, as can be seen from the contours, the carryover coefficient slightly decreases (1-3%).

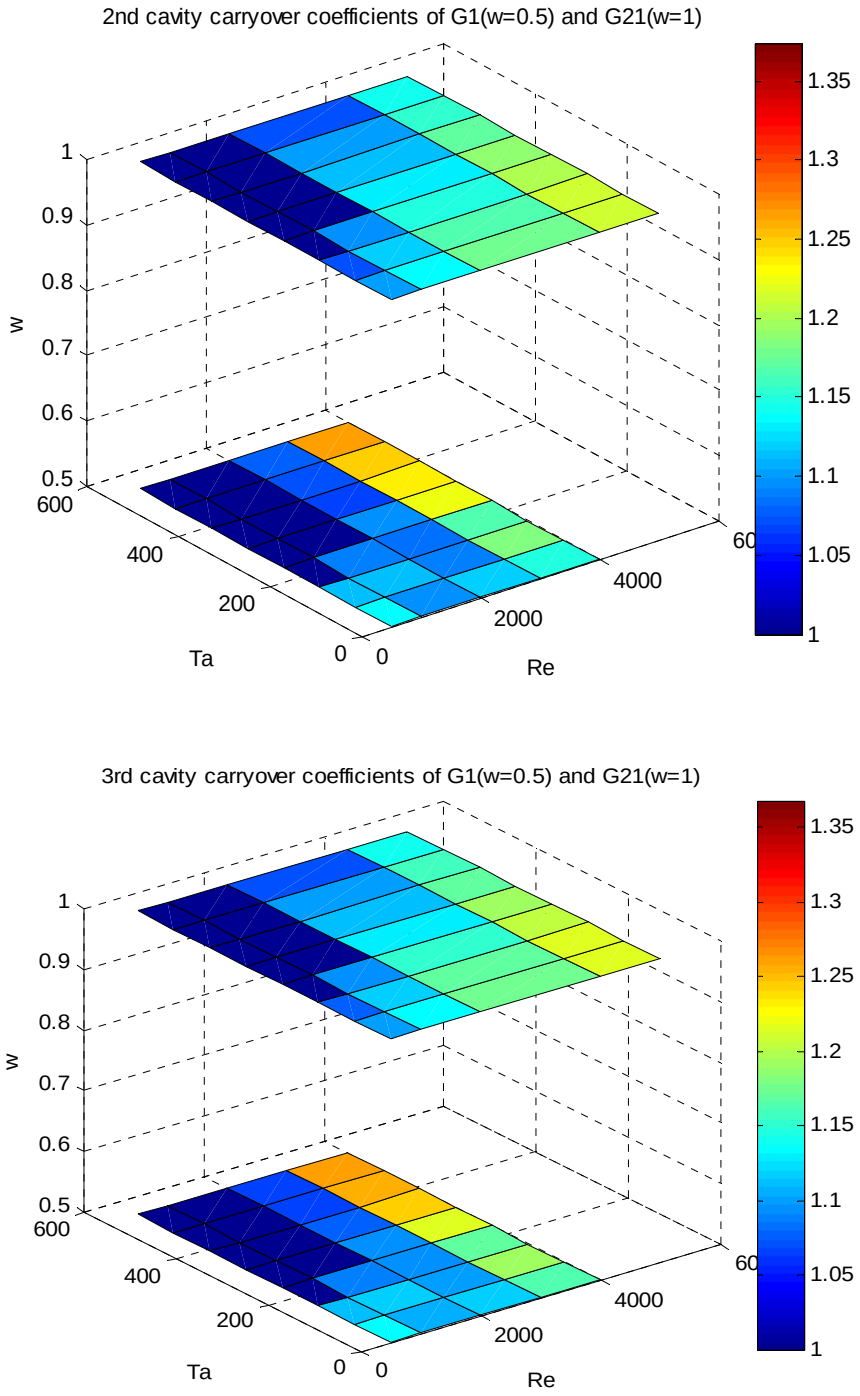

Figure 6.33 Carryover coefficients of 2nd (top) and 3rd (bottom) cavities of G1(c/s=0.0167, s=3, h/s=1, w/s=0.167, incompressible flow) and G21(c/s=0.0167, s=3, h/s=1, w/s=0.333, incompressible flow)

The combined effects of clearance, pitch and shaft speed can be studied by comparing cases G1 and G4. They have the same c/s ratio but both clearance and pitch of G4 are four times higher than those of G1. Since the clearance of G4 is much higher than that of G1, an overall pressure difference of 200 atm occurs around a Reynolds number of 18000 while for G1 it is around 4000. Moreover, the wide pitch of G4 makes it easier for the secondary vortex to occur. As a result, the secondary vortex occurs when the shaft speed is more than 100 m/s (Ta=1250). Therefore, the carryover coefficient cannot be evaluated for this range and it is not included in the graph. Figure 6.34 shows first cavity carryover coefficient of these cases. Second and third cavity carryover coefficients are not presented because their values are same as first cavity as validated for G1 and G21 in figures 6.32 and 6.33.

As stated earlier, the carryover coefficient increases as Reynolds number increases. Both G1 and G4 show agreement with this pattern. However, the effect of shaft speed is more complicated and does not always follow a certain pattern, possibly due to the presence or incipience of the secondary vortex. The most observed effect of the shaft speed is to reduce the carryover coefficient which is agreed by G4 in figure 6.27. G1 also follows this pattern except at the maximum Reynolds number. The most important result that can be obtained from figure 6.34 is that even though the c/s ratio, which is the major non-dimensional parameter for comparison, is kept constant, carryover coefficient can slightly increase for higher clearance and pitch values. It should also be noted that this increment is only 2.4% for this case.

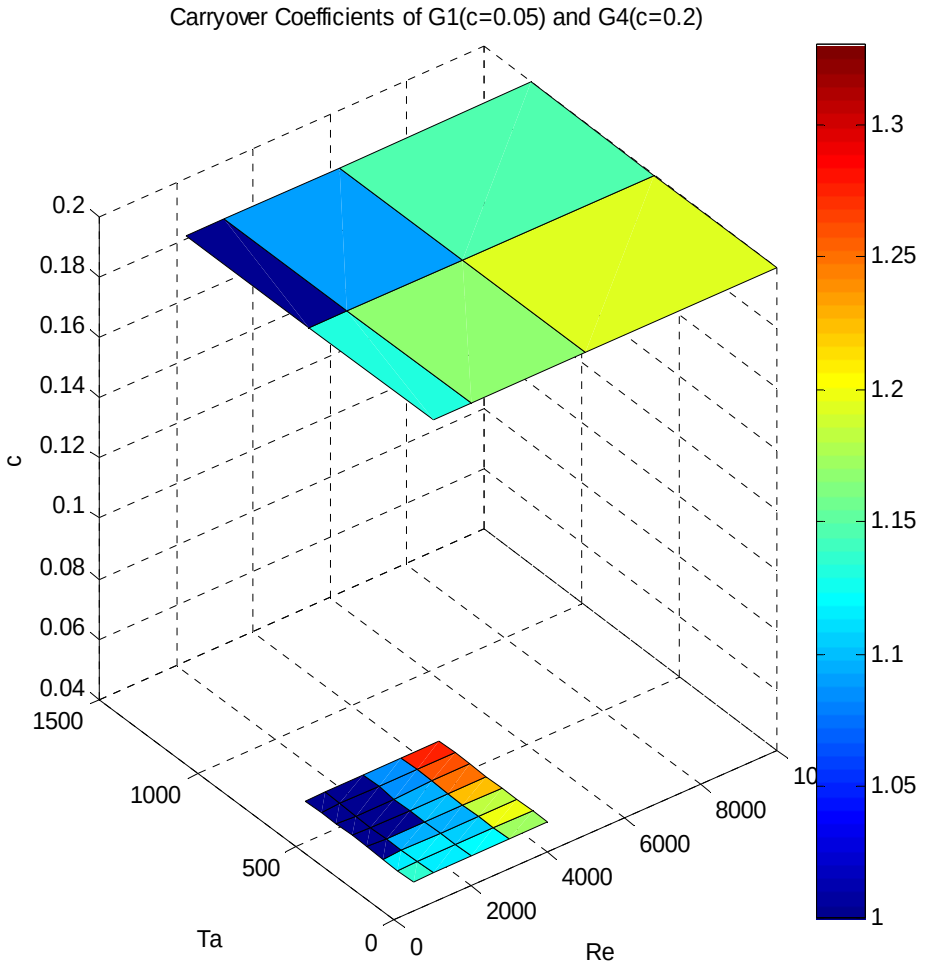

Figure 6.34 First cavity γ of G1 (c/s=0.0167, s=3, h/s=1, w/s=0.167, incompressible flow) and G4 (c/s=0.0167, s=12, h/s=0.25, w/s=0.04167, incompressible flow)

7. DISCHARGE COEFFICIENT

7.1 Calculation of Discharge Coefficient

Discharge coefficient is a non-dimensional parameter that is used for defining the total losses that occur as fluid flows through one pitch length which consists of one tooth and one cavity. As discussed in section 6, carryover coefficient measures the amount of kinetic energy dissipation only in the cavity. However, the throttling process also causes some pressure loss. Thus, discharge coefficient should be studied in order to better understand the overall effectiveness of the seal. The discharge coefficient in this study is calculated from equation 7.1.

$$C_d = \frac{\dot{m}}{A\sqrt{2\,\rho\,(p_i - p_e)}} \quad \text{..... (7.1)}$$

A is the clearance area of the tooth, ρ is the density of the compressible fluid at the upstream cavity, $\dot{m}$ is the mass flow rate and P_i and P_e represent inlet and exit pressures of the tooth respectively. In order to understand the overall effect of one tooth, these pressures are evaluated from the axial mid-point of the upstream and downstream cavities and radial mid-point of the main jet. These points are illustrated in the figure 7.1 with pressure contours. As can be seen, the pressure decreases from one cavity to the next, reducing the leakage flow which in turn increases the effectiveness.

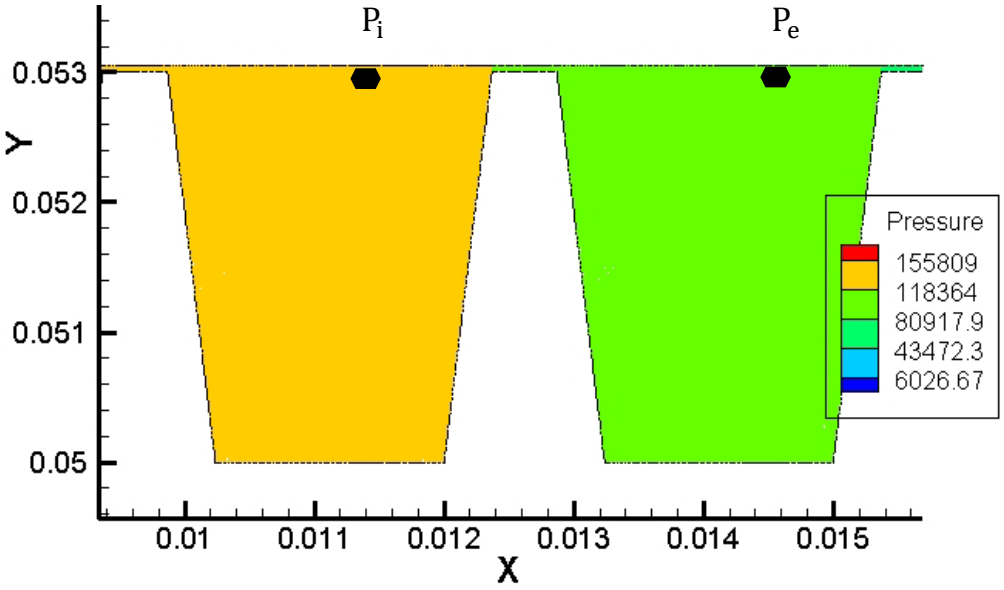

Figure 7.1 Discharge coefficient calculation

As can be seen from equation 7.1, for a given mass flow rate, a higher pressure difference, which is desired, is represented by a lower discharge coefficient. In another point of view, for a given pressure difference, a lower mass flow rate results in a lower discharge coefficient, which means that the leakage flow is reduced. Thus, the lower the discharge coefficient, the better the sealing effectiveness will be.

Figure 7.2 shows the discharge coefficient distribution for G17, G20 and G27 which are randomly chosen. As can be seen, the discharge coefficient of the first tooth is significantly different than that of consecutive teeth which have very similar values. Thus, it is decided to present the results for first tooth and consecutive teeth in separate sections. Similar to carryover coefficient analysis, the results of only incompressible flow will be presented. The effect of compressibility will be discussed in section 8.

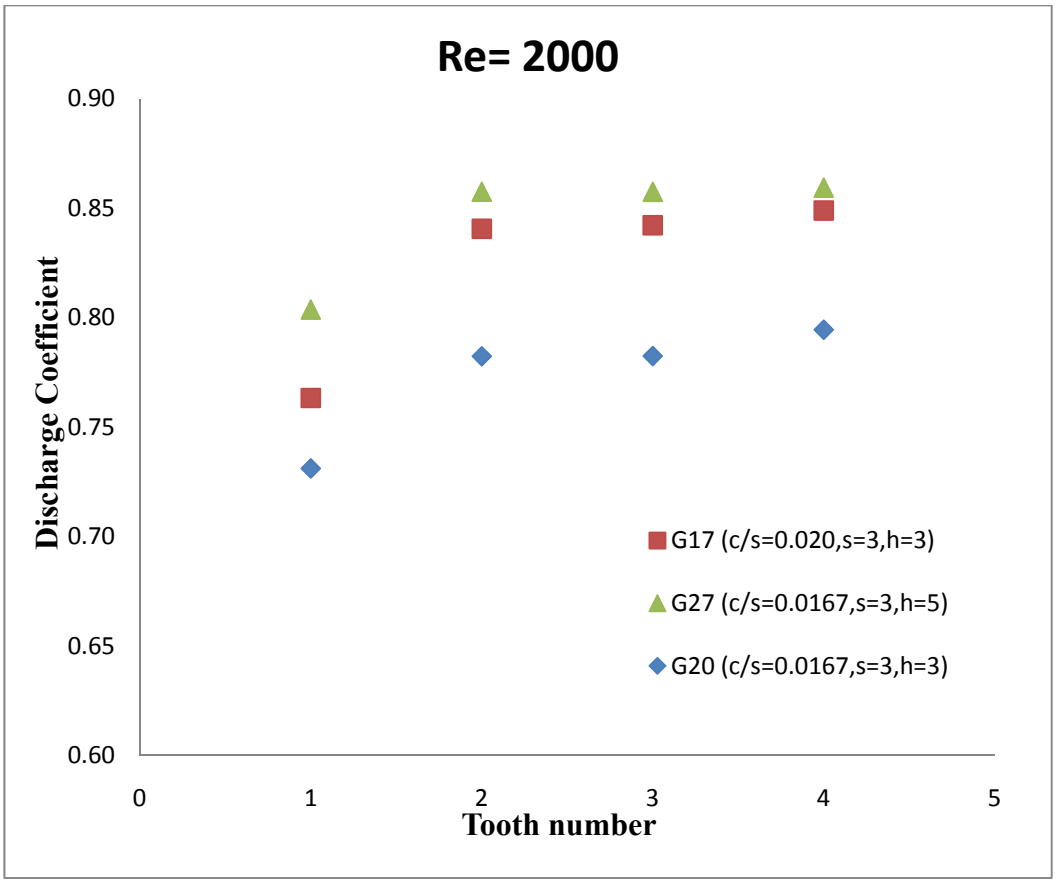

Figure 7.2 Variation of discharge coefficient with tooth position (incompressible flow, W_{sh}=0)

7.2 First Tooth

7.2.1 Effect of Reynolds Number

It was shown that the Reynolds number has a strong effect on carryover coefficient. Therefore, it is expected that it also has an effect on discharge coefficient. G10, G15 and G21 have different tooth width, clearance and upstream angle values. However, the effect of Reynolds number on discharge coefficients of first teeth is similar as shown in figure 7.3.

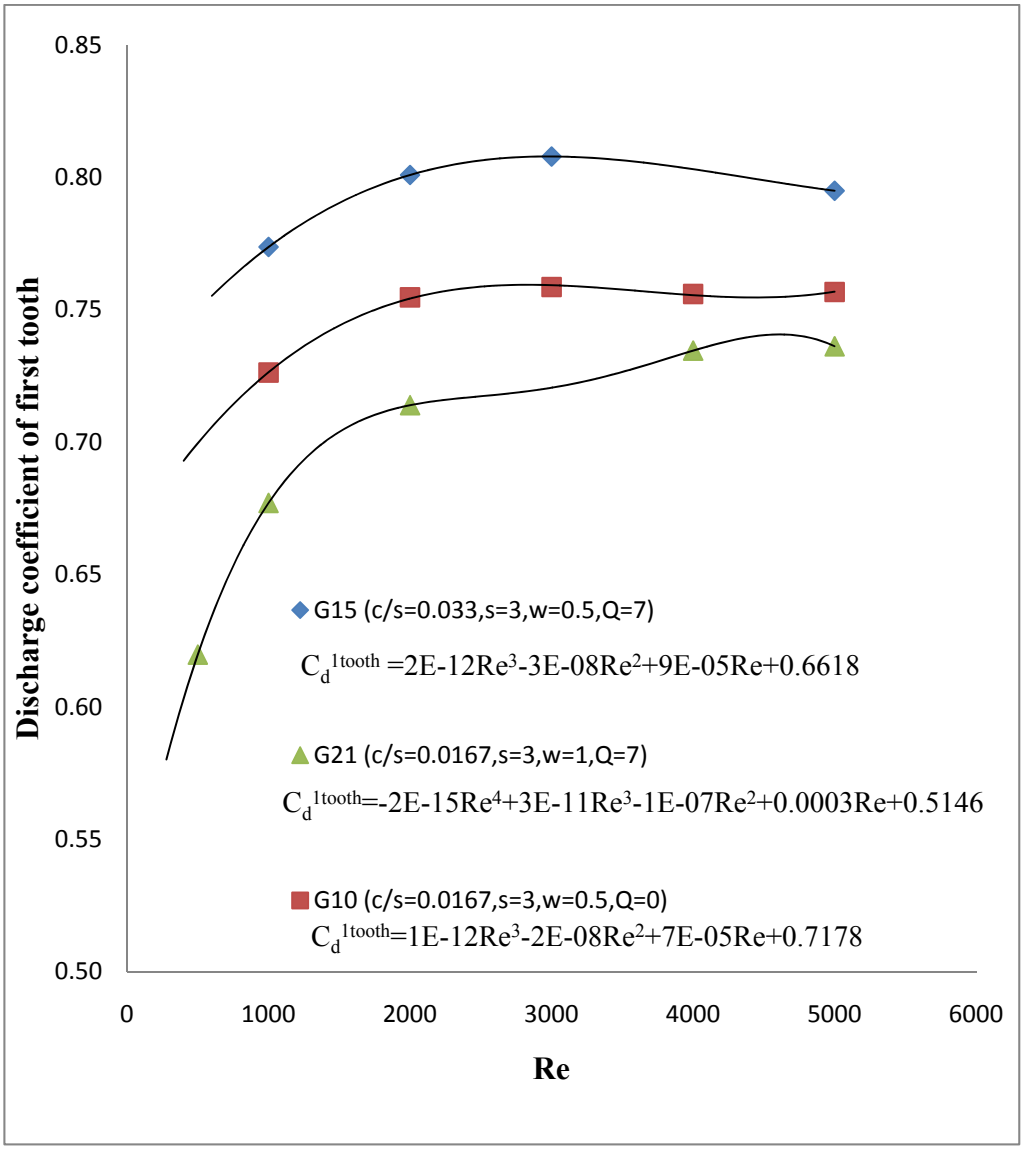

Figure 7.3 Effect of Reynolds number on C_d^{1tooth} (incompressible flow, W_{sh}=0)

As the Reynolds number increases, all cases show an increase in first tooth discharge coefficient. This pattern is more prominent when the Reynolds number is low. This can be attributed to the same affects as was attributed to the carryover coefficient

behavior. As the Reynolds number and accordingly the mass flow rate increases, the axial velocity of the fluid increases and a larger portion of the fluid directly goes to the next cavity without dissipating its kinetic energy in the cavity. As a result, the total loss of this portion is only due to viscous interaction which is less compared to that of the vortex. Thus, the discharge coefficient increases implying that the pressure reduction relative to the mass flow rate is decreased, reducing the seal effectiveness.

7.2.2 Effect of Clearance

In order to present the effect of clearance, G1, G2, G15 and G16 are chosen. They have different clearance values but the rest of the parameters are the same. As can be seen from figure 7.4, the discharge coefficient increases as the clearance is increased, reducing the effectiveness of the labyrinth seal. The same pattern was also observed for carryover coefficient in section 6.3. As the clearance is increased, a larger portion of the fluid flows above the tooth without dissipating kinetic energy in the cavity.

As Reynolds number is increased from 2000 to the Reynolds number where maximum pressure difference is obtained, G1, G2, G15 and G16 have overall increase in discharge coefficient of 2.5%, 2.6%, 4% and 8.5% respectively.

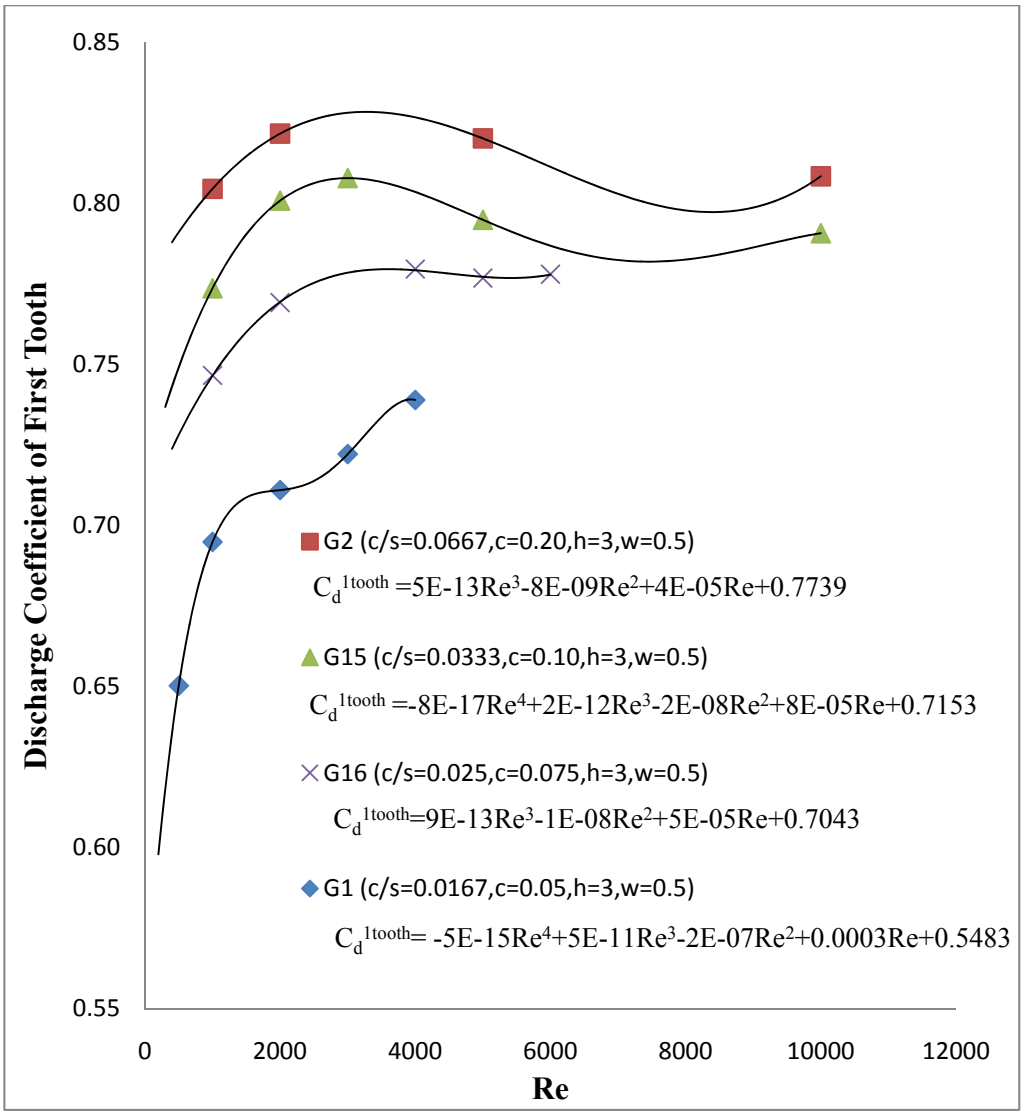

Figure 7.4 Effect of clearance on C_d^{1tooth} (incompressible flow, W_{sh}=0)

7.2.3 Effect of Tooth Width

Figure 7.5 shows the discharge coefficient distribution for G1, G18 and G21 for different Reynolds numbers. G1, G18 and G21 have different tooth width values but the rest of the dimensions are kept the same. It can be seen that the lowest tooth width has

higher discharge coefficient which slightly increases as Reynolds number increases. However, the two larger tooth widths have lower discharge coefficients which significantly increase as the Reynolds number increases. This can be attributed to the fact that the pressure drop along a longer channel is higher than that of a shorter channel. Similarly, the pressure drop along a wider tooth would be higher than that of shorter tooth. Comparing G21 and G1, It appears that once the tooth width is sufficiently large, further increasing it has only minimal effect upon discharge coefficient.

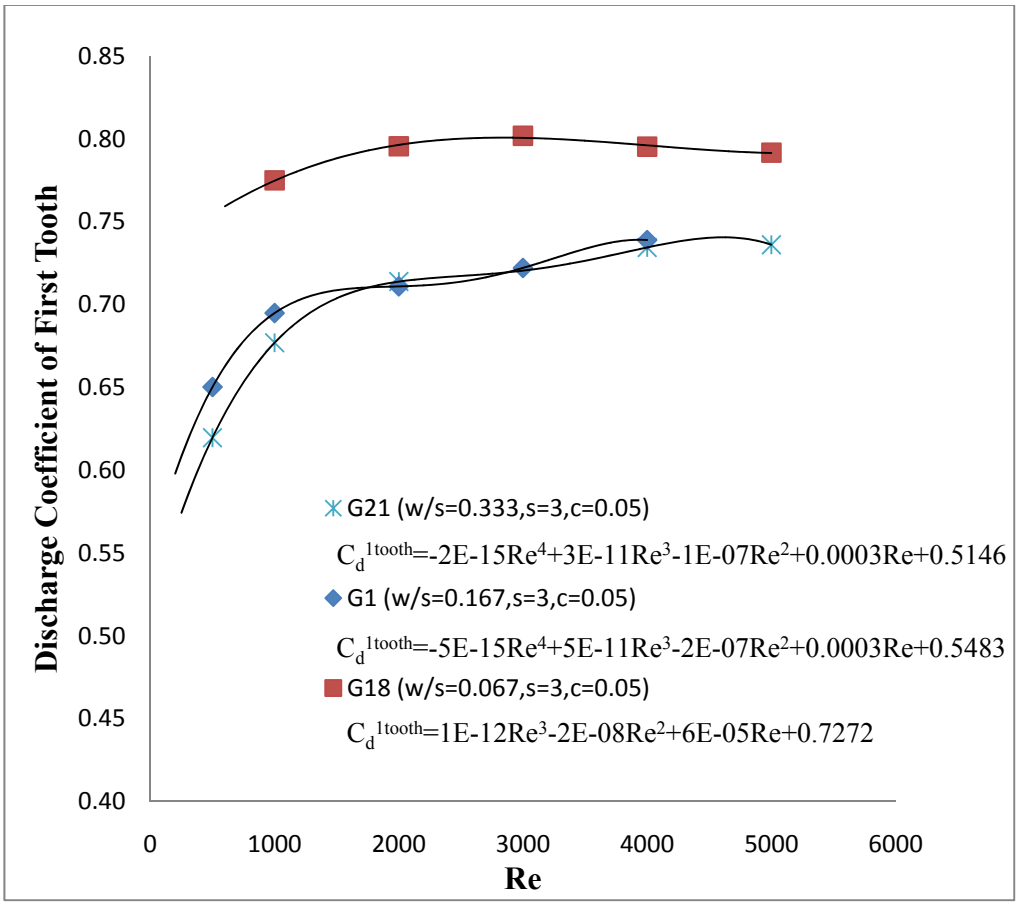

Figure 7.5 Effect of tooth width on C_d^{1tooth} (incompressible flow, W_{sh}=0)

7.2.4 Effect of Tooth Pitch

In section 7.2.2, the clearance was varied while the pitch was kept constant. In this section, the pitch will be varied while the clearance is kept constant. G2 and G4 have different pitch values and the rest of the parameters are same. Figure 7.6 shows the first tooth discharge coefficients for those cases.

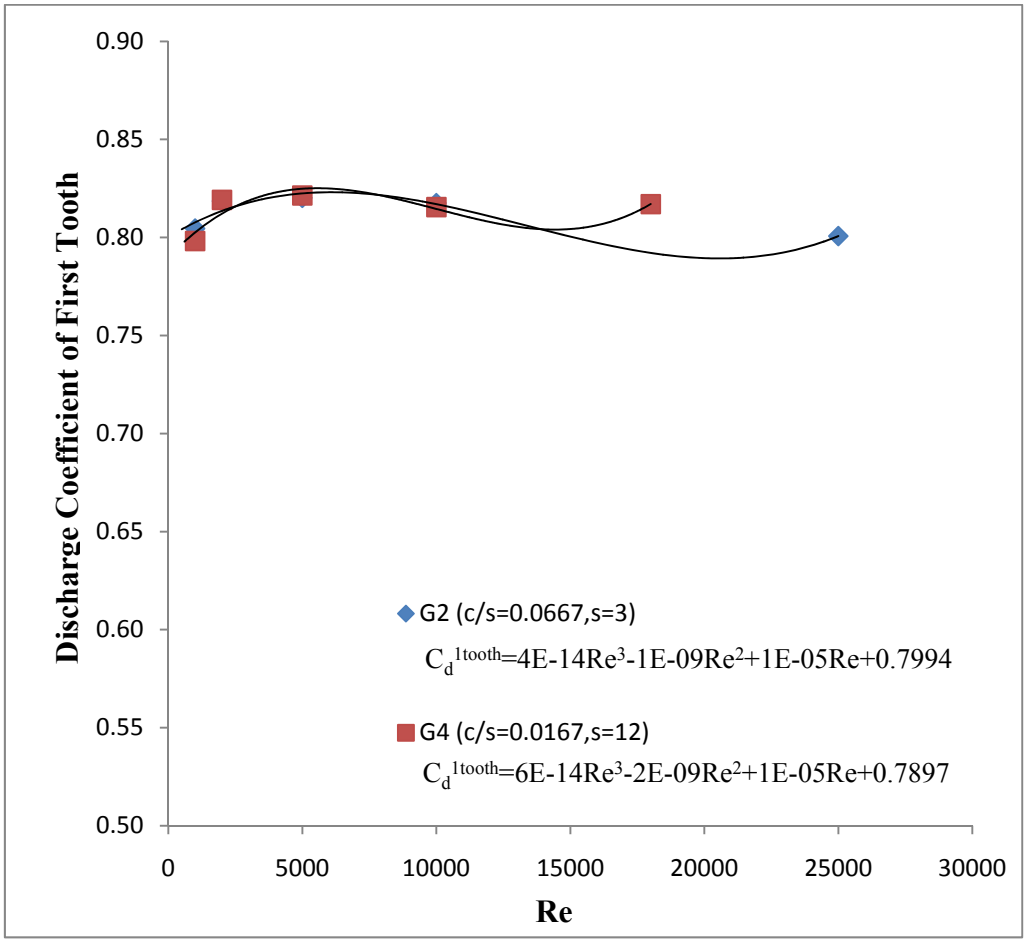

Figure 7.6 Effect of tooth pitch on C_d^{1tooth} (Incompressible flow, W_{sh}=0)

It is observed that the discharge coefficients for G2 and G4 are almost the same even though the c/s ratios greatly differ with similar clearance values. The difference is around %0.6 when the Reynolds number is below 10000. For higher Reynolds numbers, longer pitch apparently results in slightly higher discharge coefficients. Comparing figures 7.4 and 7.6, it is apparent that the same c/s ratios with different h/s ratios do not result in same discharge coefficients. Thus, it can be concluded that c/s ratio cannot be used alone for first tooth discharge coefficient without considering the clearance and tooth height. Additionally, considering the comparison of G2 and G4, it can also be concluded that the clearance is the major parameter affecting first tooth discharge coefficient.

In order to better understand the effect of c/s ratio, G2 and G6 are compared in figure 7.7. G6 has four times higher pitch, clearance and height value compared to G2. The differences in discharge coefficients are between 1-2.5% for same Reynolds numbers. Thus, it can be concluded that as long as tooth height is also proportionally varied, the geometries with the same c/s ratio will produce similar first tooth discharge coefficients.

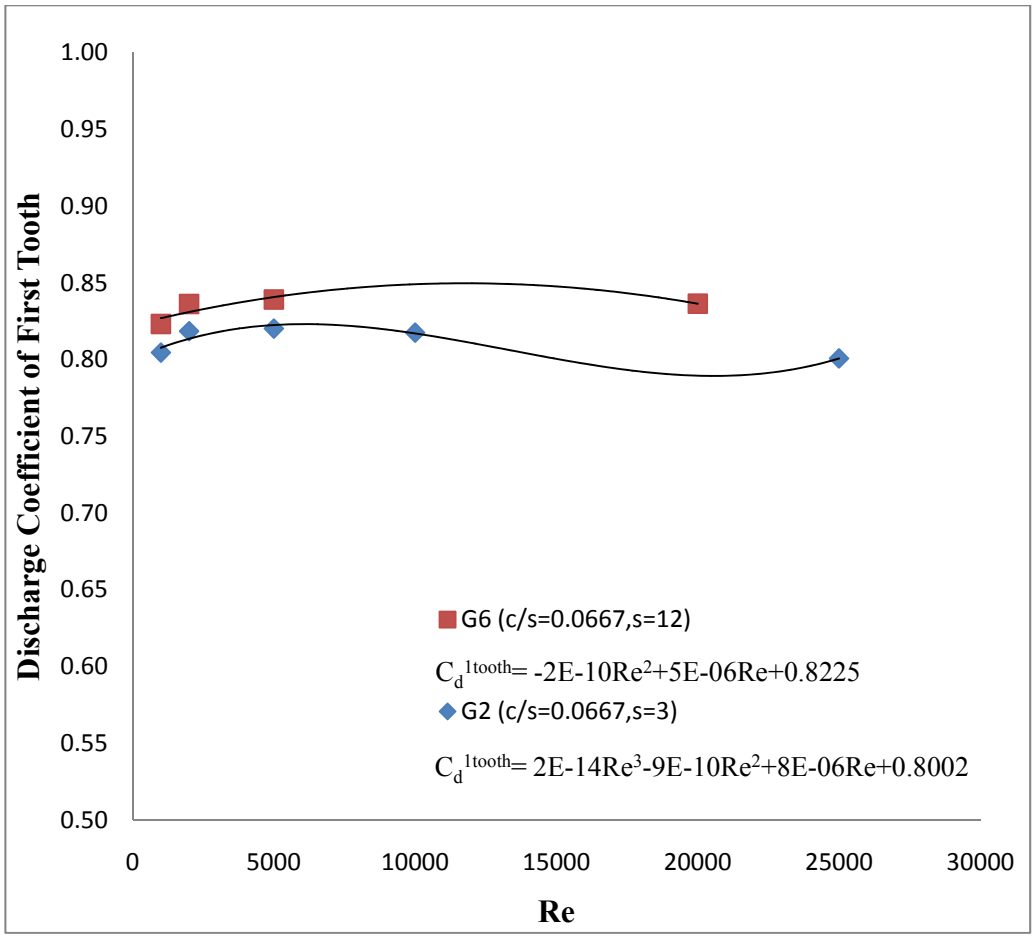

Figure 7.7 Effect of tooth pitch on C_d^{1tooth} (Incompressible flow, W_{sh}=0)

7.2.5 Effect of Tooth Height

Figure 7.8 presents the first tooth discharge coefficients for G1, G24, G25 and G27. Apart from tooth height, all cases have the same dimensions. The lowest first tooth discharge coefficient is obtained when h/s ratio is unity. As the height increases or decreases, the discharge coefficient increases and this pattern is more prominent when the Reynolds number is high.

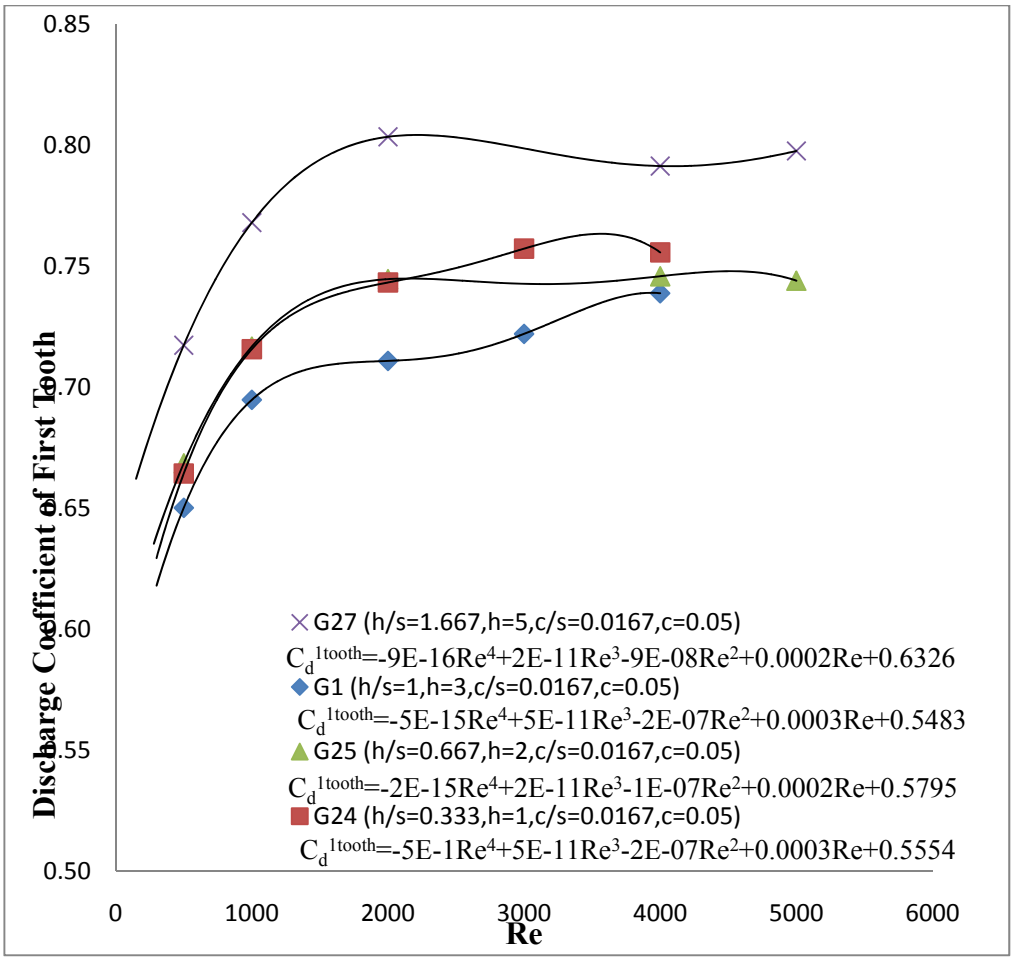

Figure 7.8 Effect of tooth height on C_d^{1tooth} (Incompressible flow, W_{sh}=0)

7.2.6 Effect of Upstream Side Angle

Figure 7.9 shows the first tooth discharge coefficient for G3, G13, G4 and G9. G3 and G13 have same dimensions rather than upstream side angle which is 7° for G3 and 0° for G13. Similarly, G4 and G9 have same dimensions rather than upstream side angle which is 7° for G4 and 0° for G9. It was observed that the carryover coefficient increases as the upstream angle is varied from 7° to 0°. However, for the first tooth

discharge coefficient, this pattern is not observed. The first tooth discharge coefficient shows a negligible amount of change (around 1%) as the upstream angle varies.

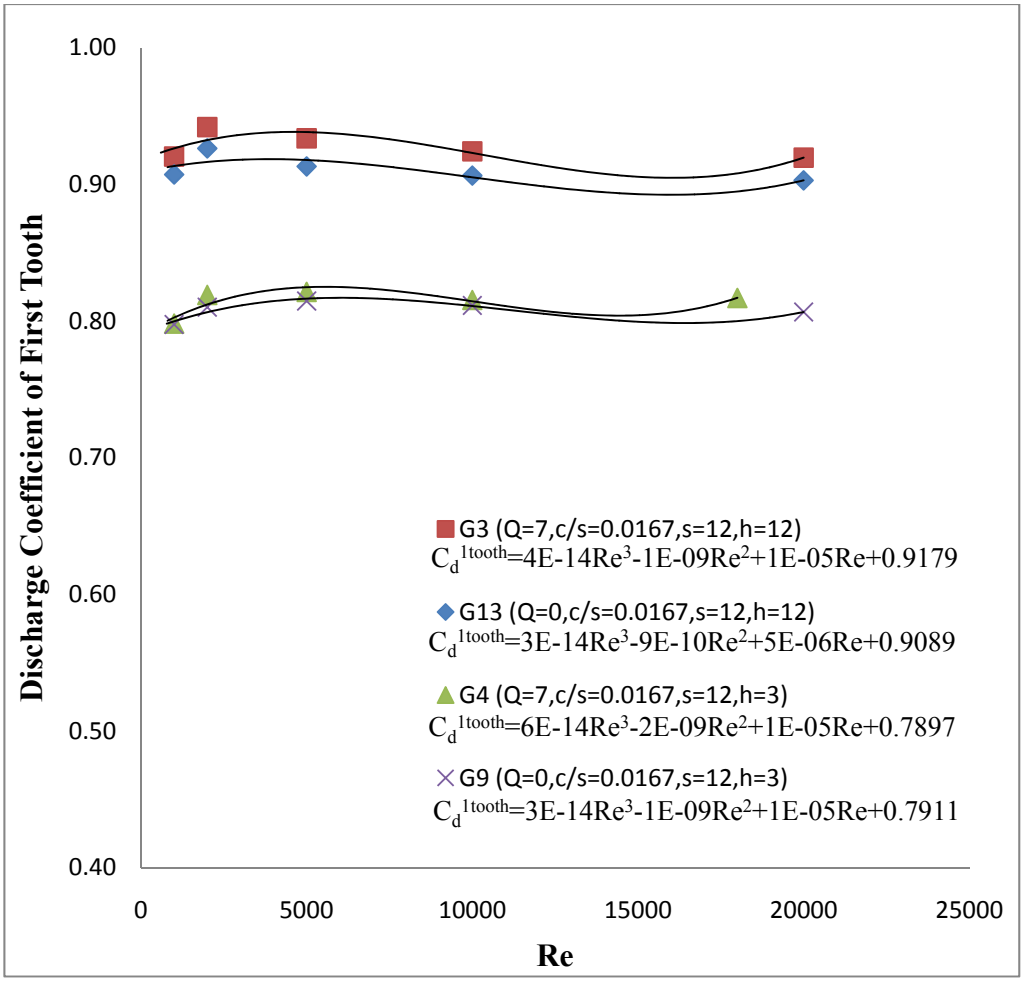

Figure 7.9 Effect of upstream side angle on C_d^{1tooth} (Incompressible flow, W_{sh}=0)

Moreover, from figure 7.9, it was also observed that the smaller value of h/s (G4 and G4) for a fixed c/s produces significantly lower (around 10%) discharge coefficients than the h/s=1 case (G3 and G13).

The effect of geometrical parameters and Reynolds number were studied so far without considering the effect of shaft speed. These effects are summarized in table 7.1.

Table 7.1 Effects of geometrical parameters and Re on C_d^{1tooth}

Increasing	C_d
c	increases
s	decreases
w	decreases
h	increases
Q	increases
Re	increases

It should be noted that tooth height and upstream angle have a very small effect on discharge coefficient compared to other parameters given in table 7.1 Remaining parameters have relatively stronger effects on discharge coefficients. Amongst them, tooth clearance (c/s) is the strongest parameter followed by Reynolds number.

7.2.7 Effect of Shaft Speed

Flow through the labyrinth seal is strongly affected by the shaft speed. As shaft speed increases, the vortices upstream and downstream of the tooth are enhanced. In this section, the effect of rotation on discharge coefficient is studied on G1, G4 and G21.

As illustrated in figure 7.12, the discharge coefficient initially slightly decreases then drastically increases for low Reynolds numbers as the shaft speed increases. This

can be attributed to the fact that for the low Reynolds number flow there is less axial inertia and the centrifugal force pushes the fluid to the stator wall, causing higher pressure in the near-wall region as shown in figure 7.10. As a result, the pressure difference in the axial direction reduces. The pressure distribution of this case would be uniform in the radial direction if the shaft speed was zero.

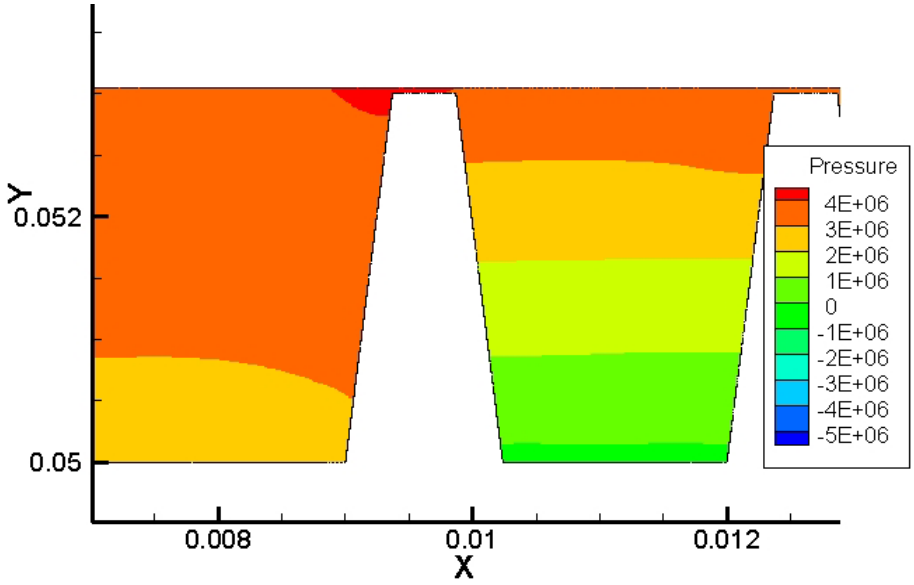

Figure 7.10 Pressure distribution near first tooth (G1, Re=500, W_{sh}=350, incompressible flow)

However, for higher Reynolds numbers, the flow has higher axial inertia which dominates the centrifugal force causing a more uniform pressure distribution in the radial direction as shown in figure 7.11. As a result, the pressure difference in the axial direction is still high even though the shaft speed is increased and the corresponding discharge coefficient is still similar to that of low shaft speed. Additionally, as can be

seen from figure 7.12, the discharge coefficient distribution for higher Reynolds numbers (i.e. 2000-4000) does not follow a certain pattern but it shows an overall decrease of 2-3%.

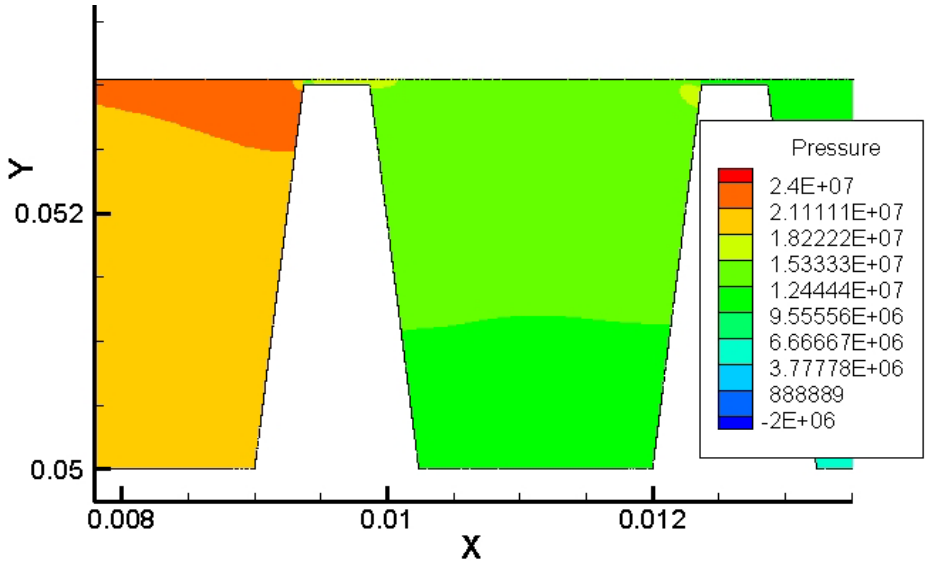

Figure 7.11 Pressure distribution near first tooth (G1, Re=4000, W_{sh}=350, incompressible flow)

It is also apparent that when the Reynolds number is between 3000 and 4000, the discharge coefficients are the same. The reason is that the axial pressure difference is near the maximum when the Reynolds number is higher than 3000 so the axial pressure difference is very large compared to the radial variance.

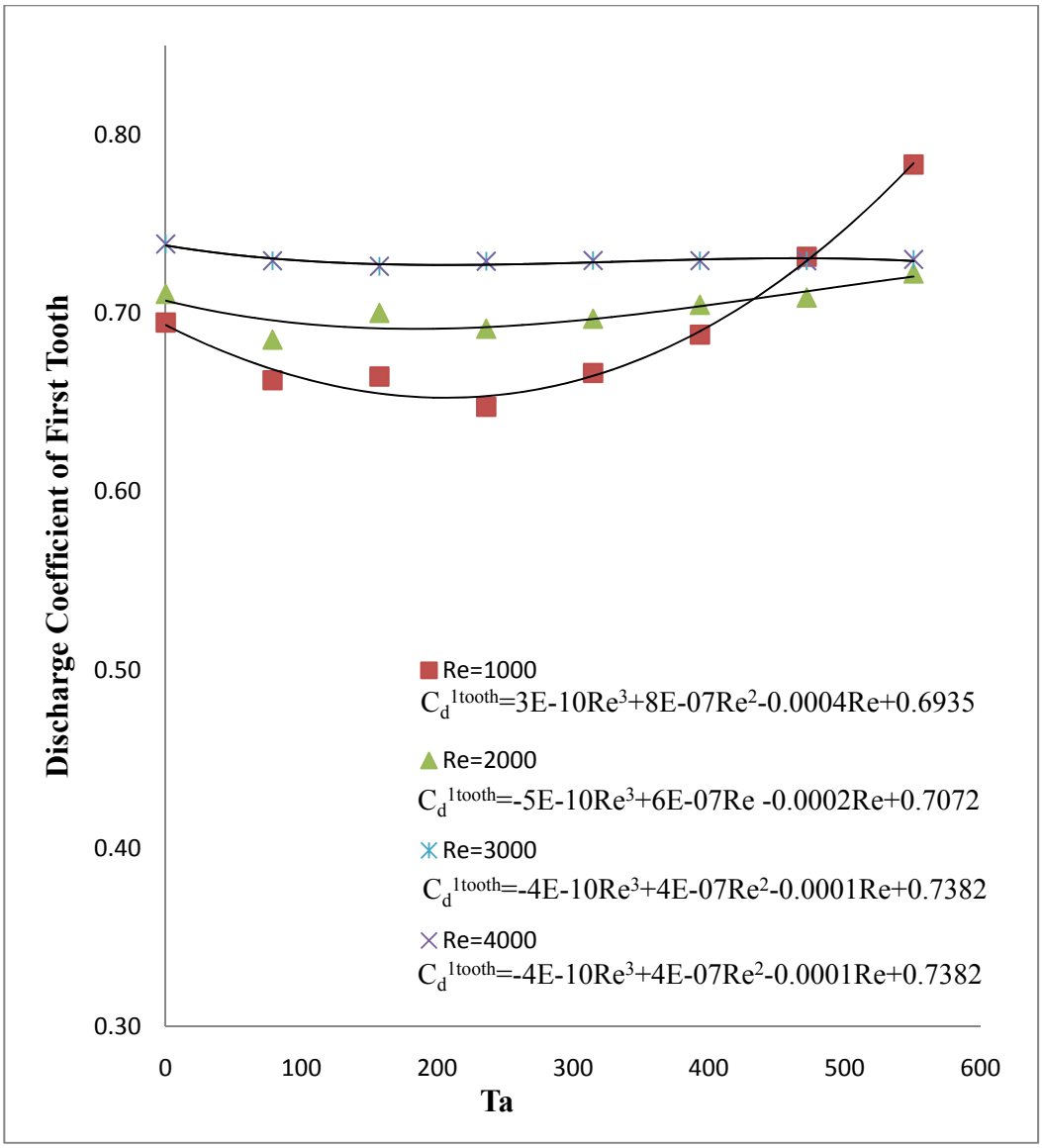

Figure 7.12 Effect of shaft speed on C_d^{1tooth} (G1, c/s=0.0167, s=3, h=3, w=0.5, incompressible flow)

Figure 7.15 shows the discharge coefficient distribution of G4 for different Reynolds numbers. For the lowest Reynolds number, a pattern similar to that explained for G1 is observed. The discharge coefficient initially decreases then it begins to increase as the centrifugal force dominates the flow. Compared to G1, the effect of

rotation is more prominent in G4. The main reason is that G4 has longer pitch which allows the flow to diverge downwards, increasing the energy dissipated in the cavity which reduces the pressure. Figures 7.13 and 7.14 show the streamlines along with pressure contours of G4 for different shaft speeds.

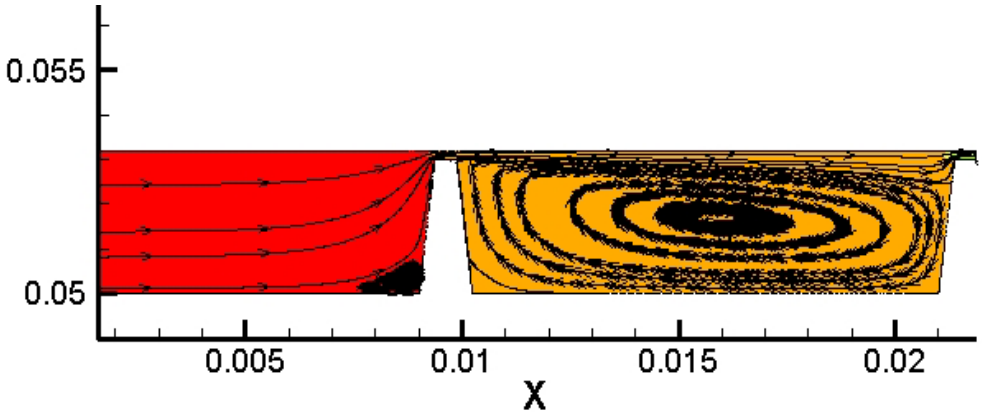

Figure 7.13 Streamlines and pressure distribution around first tooth (G4, Re=5000, W_{sh} =0, incompressible flow)

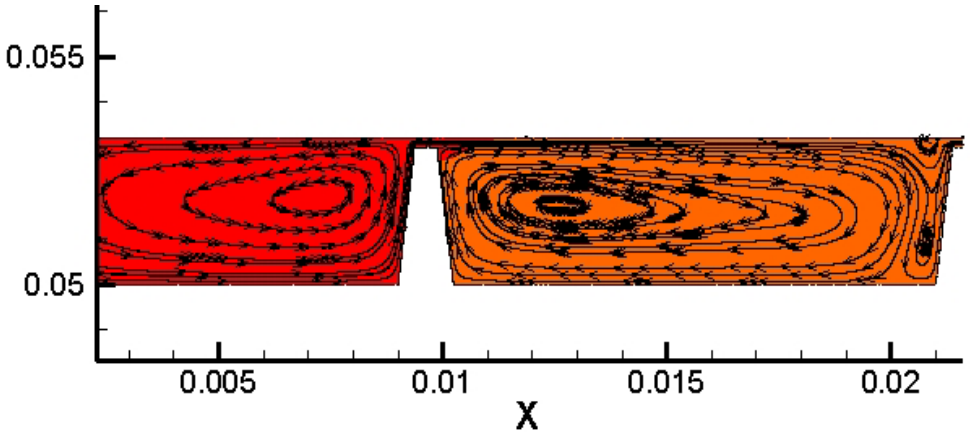

Figure 7.14 Streamlines and pressure distribution around first tooth (G4, Re=5000, W_{sh} =350, incompressible flow)

As can be seen from figure 7.14, the rotation causes a large vortex upstream of the first tooth. Moreover, it also causes a secondary circulation zone far downstream of the first tooth (shallow cavity) which also reduces the pressure at the mid-region of the cavity at which the discharge coefficient is evaluated. Additionally, the shear stress losses are also increased due to higher velocity in the boundary layer. As a result, the discharge coefficient decreases up to 45% for low Reynolds numbers (i.e. 1000-2000). For higher Reynolds numbers (i.e. 5000-10000), the discharge coefficient decreases around 10-20%.

Comparing figures 7.12 and 7.15, it is clear that for low Taylor numbers G1 has lower discharge coefficients indicating better sealing. The only difference between G1 and G4 is the tooth pitch which is four times higher in G4 compared to that of G1. However, as Taylor number increases, wider tooth pitch (G4) results in lower discharge coefficients compared to shorter tooth pitch (G1).

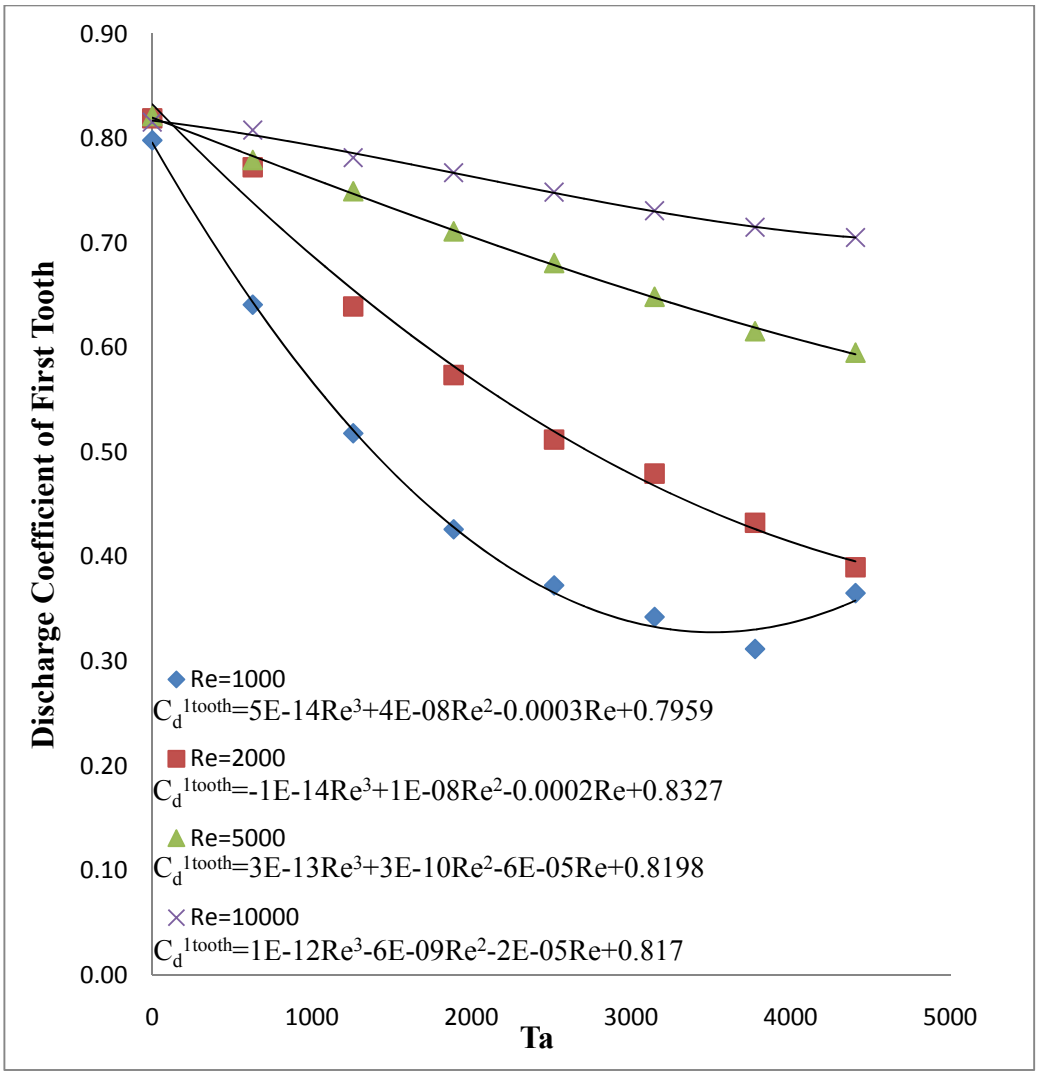

Figure 7.15 Effect of shaft speed on C_d^{1tooth} (G4, c/s=0.0167, s=12, h=3, w=0.5, incompressible flow)

Figure 7.16 shows the discharge coefficient distribution of G21 for different Reynolds numbers. This seal is the same as seal G1 but has a wider tooth. Similar to what was observed for G1 and G4, for low Reynolds numbers, the discharge coefficient

gradually decreases and then increases. For higher Reynolds numbers, the discharge coefficient gradually decreases as the Taylor number increases.

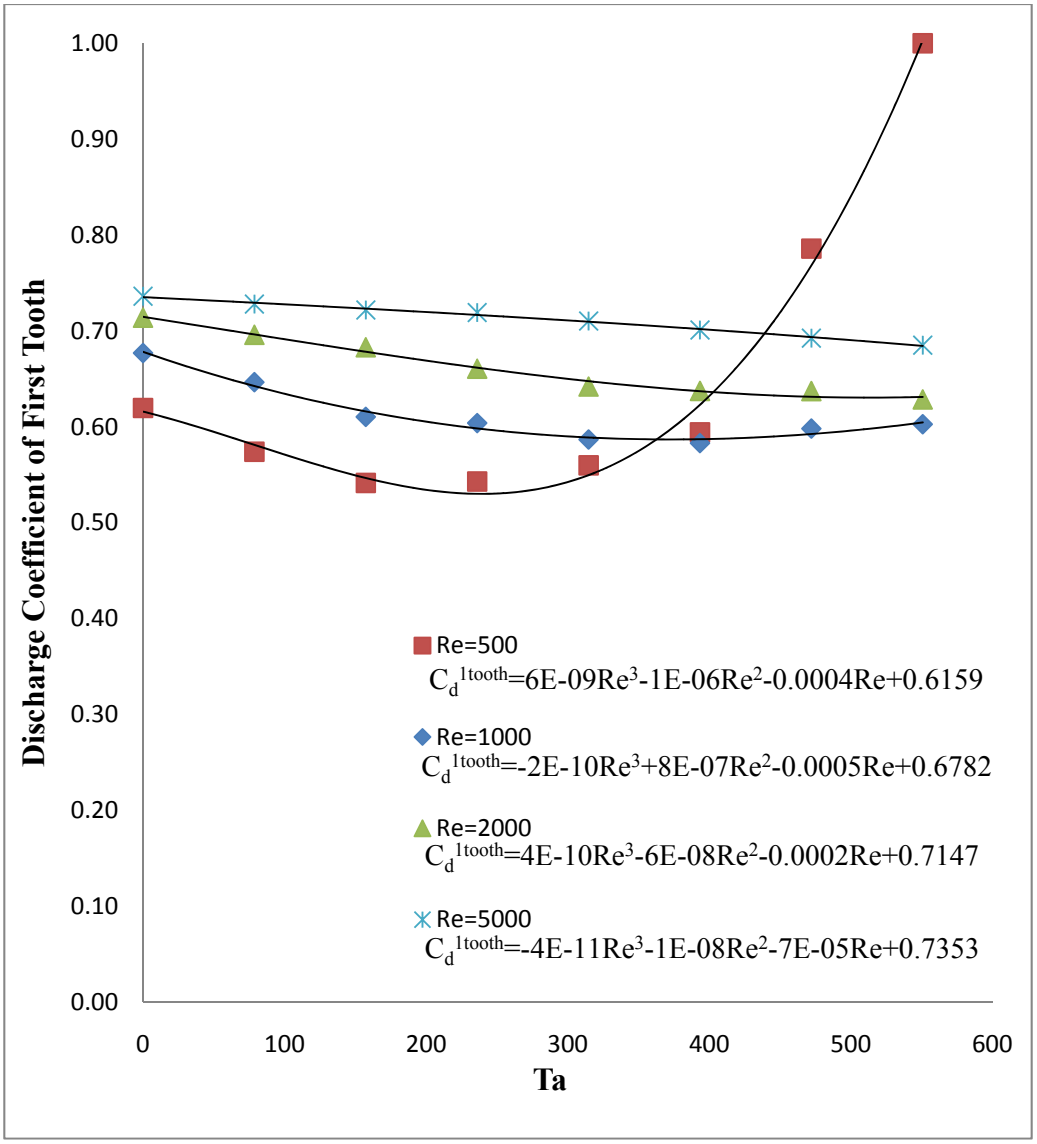

Figure 7.16 Effect of shaft speed on C_d^{1tooth} (G21, c/s=0.0167, s=3, h=3, w=1, incompressible flow)

When the Taylor number is 550, the streamlines and pressure contours are pictured below for Reynolds numbers of 500 and 5000 respectively. As can be seen from figure 7.17, the high Taylor number causes a secondary recirculation zone which diverts the flow into the cavity far downstream of the first tooth preventing the main streamline to impinge on the downstream tooth wall.

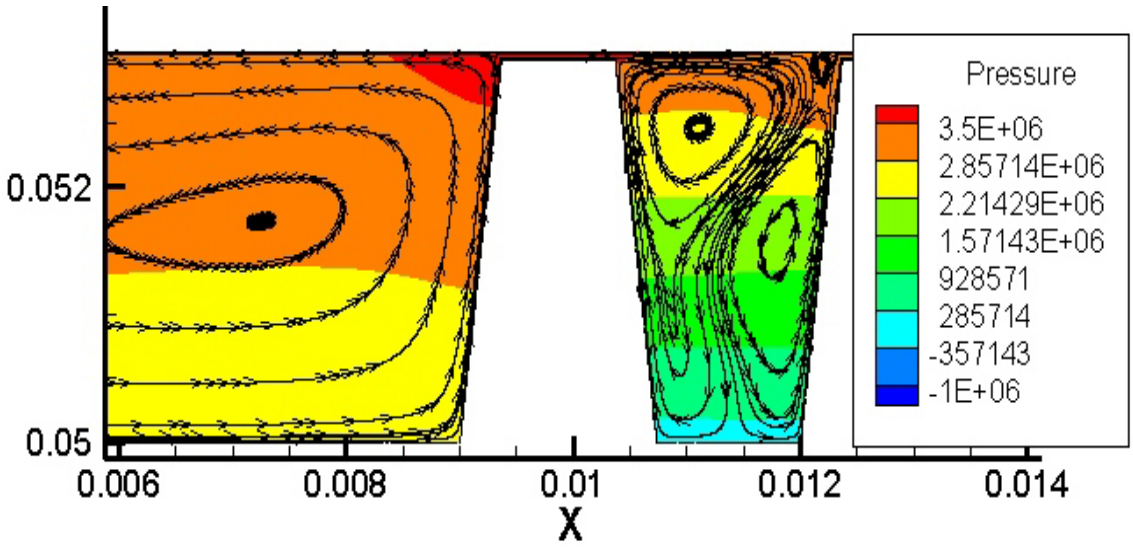

Figure 7.17 Streamlines and pressure distribution around first tooth (G21, Re=500, W_{sh} =350, incompressible flow)

Figure 7.18 illustrates the streamlines and pressure contours for G21 when Reynolds number is 5000 and Taylor number is 550. The pressure distribution in the redial direction appears uniform since the pressure change in the axial direction from cavity to cavity is very large. As a result, the pressure difference in the axial direction is high compared to that of a low Reynolds number case. This increases the axial

momentum which alters the flow pattern inside the seal. The secondary circulation zone is forced to the lower half of the seal cavity while a single large circulation zone occupies the top half. The flow moves through the seal similar to the zero shaft speed case. This increases the discharge coefficient compared to the low Reynolds number case due to less restriction to the through flow.

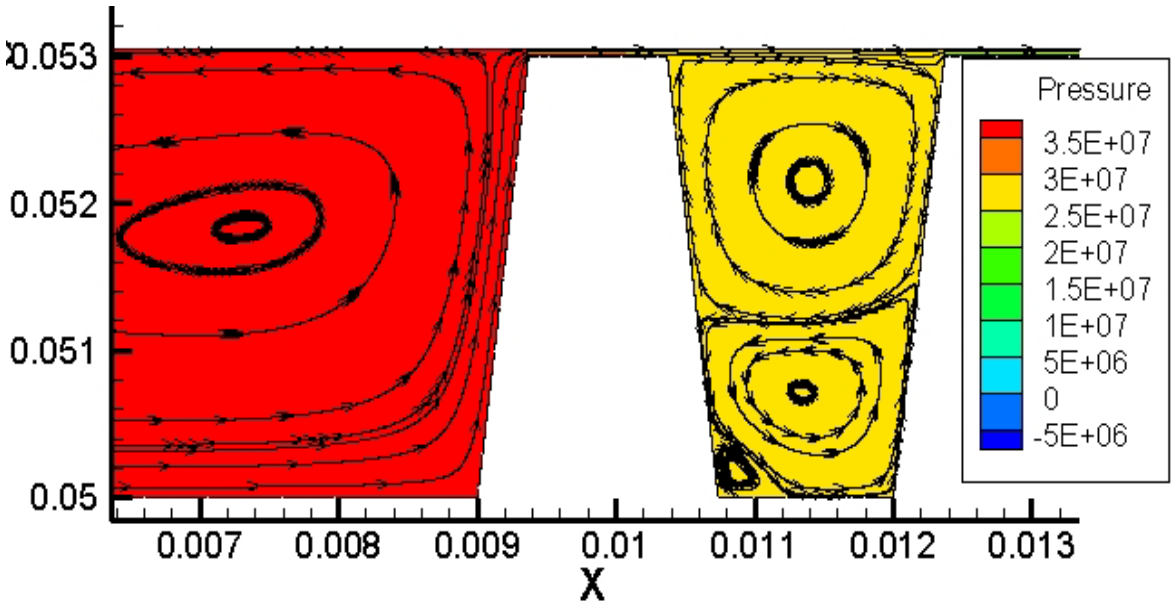

Figure 7.18 Streamlines and pressure distribution around first tooth (G21, Re=5000, W_{sh} =350, incompressible flow)

7.2.8 Combined Effects

The individual effect of geometrical features and flow parameters on the first tooth discharge coefficient was investigated so far. It was seen that, amongst geometrical

features, clearance has a stronger effect on the first tooth discharge coefficient compared to other parameters. The effect of these parameters can change as the rest of the parameters are also varied rather than being kept constant. This section aims to understand the combined effects of geometrical and flow parameters.

Figure 7.19 shows the first tooth discharge coefficient of G1 and G21 for different Reynolds and Taylor numbers. It is observed that for low Reynolds and Taylor numbers, both seals have almost the same discharge coefficients. However, as the Taylor number increases when the Reynolds number is between 500 and 2000, G21 has significantly lower discharge coefficient. Similarly, the same pattern with less prominence is also observed for higher Reynolds numbers. As the Reynolds number is increased when Taylor number is between 0 and 200, the discharge coefficients are almost same. Thus, it can be concluded that G21 is a better seal than G1 for high Taylor numbers.

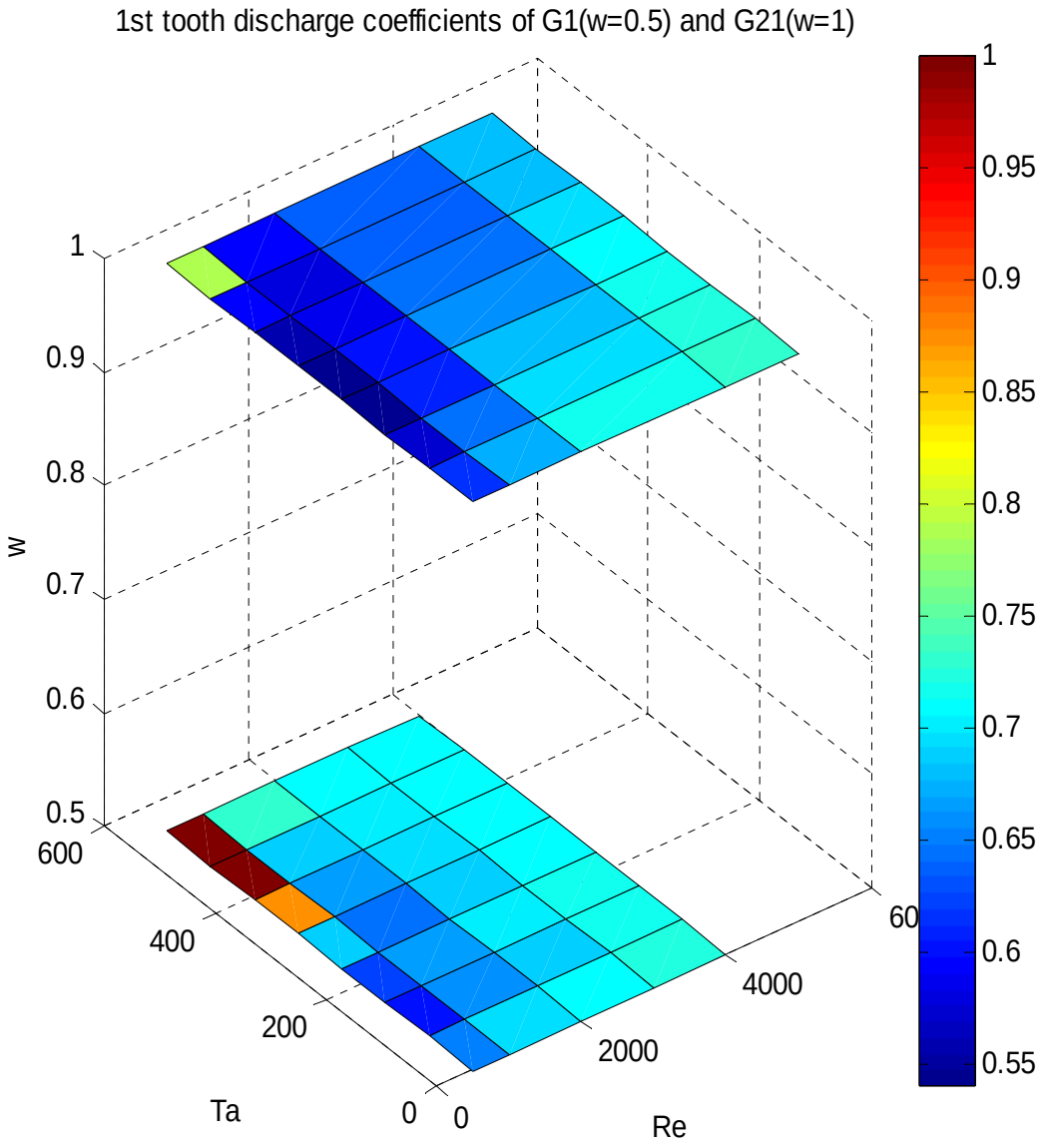

Figure 7.19 C_d^{1tooth} comparison of G1(c/s=0.0167, h/s=1, incompressible flow) and G21(c/s=0.0167, h/s=1, incompressible flow)

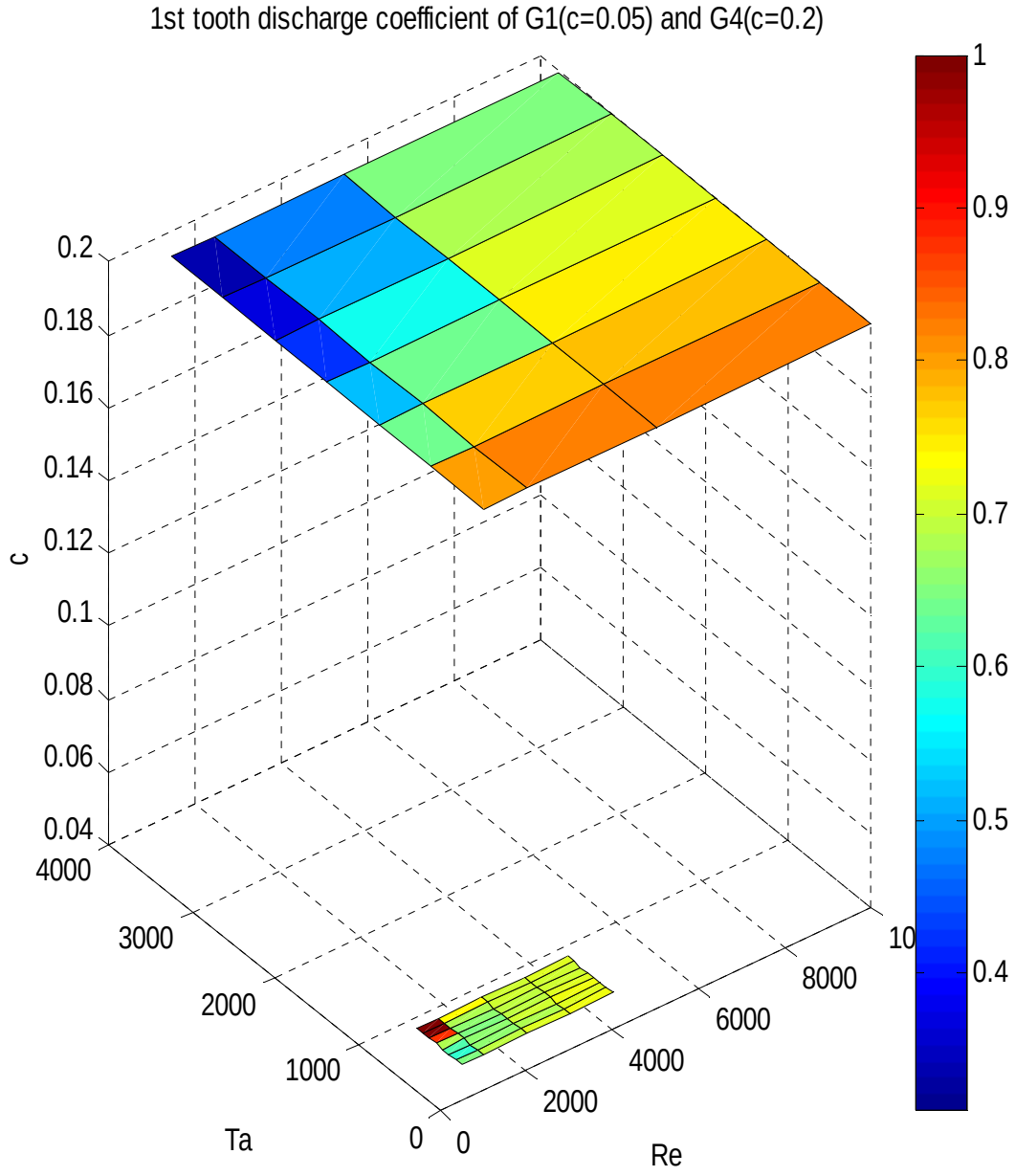

Figure 7.20 C_d^{1tooth} comparison of G1(c/s=0.0167, h/s=1, incompressible flow) and G4(c/s=0.0167, h/s=0.25, incompressible flow)

Figure 7.20 shows the discharge coefficient of G1 and G4 for different Reynolds and Taylor numbers. It is observed that when the shaft speed is less than 250 m/s, G1 has significantly lower discharge coefficients for all Reynolds numbers. However, when the shaft speed is further increased, G4 has better discharge coefficients for Reynolds numbers less than 2000. If the Reynolds number is further increased for the same range of shaft speed, G1 possesses lower discharge coefficients. Thus, smaller clearance is always better than large clearance for high Reynolds numbers. For low Reynolds numbers, a smaller clearance is still better for low Taylor numbers but a larger clearance is better when the Taylor number is high.

7.3 Intermediate Tooth

7.3.1 Effect of Reynolds Number

The same seal geometries that were used to analyze the Reynolds number effect on first tooth discharge coefficients are also used here to analyze intermediate tooth discharge coefficients. All results presented here are for incompressible flow. The effects of compressibility will be discussed in section 8. The discharge coefficients of the second tooth of G15, G21 and G10 are presented in figure 7.21.

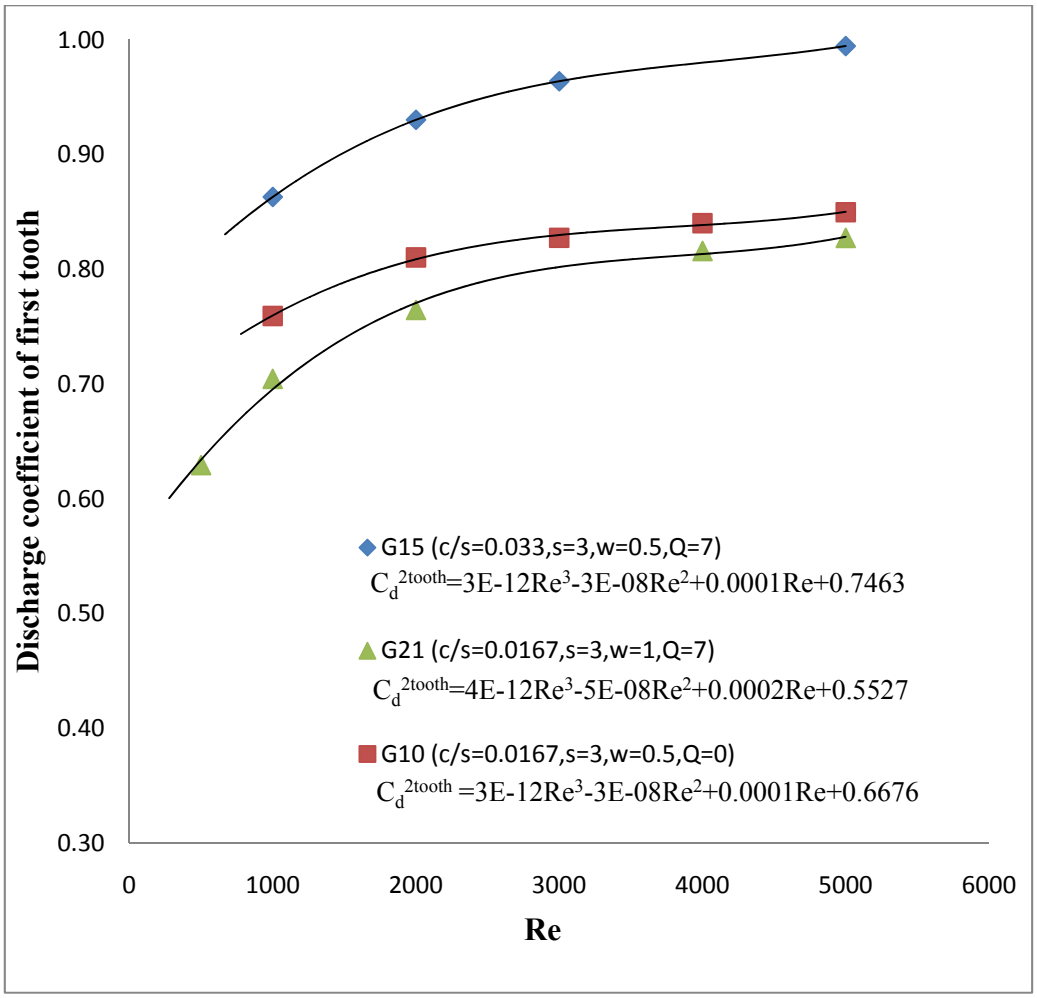

Figure 7.21 Effects of Reynolds Number on C_d (Incompressible flow, W_{sh}=0)

It is apparent that the discharge coefficient increases as the Reynolds number increases. It can be attributed to the same reason as was discussed for the first tooth. It should be noted that the variation of discharge coefficient with respect to the Reynolds number is similar to that of first tooth but the value of discharge coefficient is higher. This difference is more pronounced when the Reynolds number is high (i.e. 3000-5000).

Thus, it can be concluded that the effect of first tooth increases the discharge coefficient for the next tooth.

7.3.2 Effect of Clearance

G2, G15, G16 and G1 are studied in order to understand the effect of clearance on intermediate tooth discharge coefficient. These geometries have different clearance values and rest of the parameters are the same. Figure 7.22 shows the discharge coefficients of second teeth of these cases for different Reynolds numbers.

It is observed that the discharge coefficients of G2 are 1 for all Reynolds numbers, which means that the seal is not working effectively. This agrees with the findings in section 6.3 in which it was presented that increasing the c/s ratio significantly increases the carryover coefficient, reducing the effectiveness. If the clearance of G2 is reduced to half (G15), the seal works effectively for low Reynolds numbers. However, when the Reynolds number is more than 5000, the discharge coefficient again reaches 1.

G16 and G1, which have lower clearance compared to G2 and G15, have lower discharge coefficients for all of the Reynolds numbers. Thus, it can be concluded that the c/s ratio should not be higher than approximately 0.025 for effective sealing.

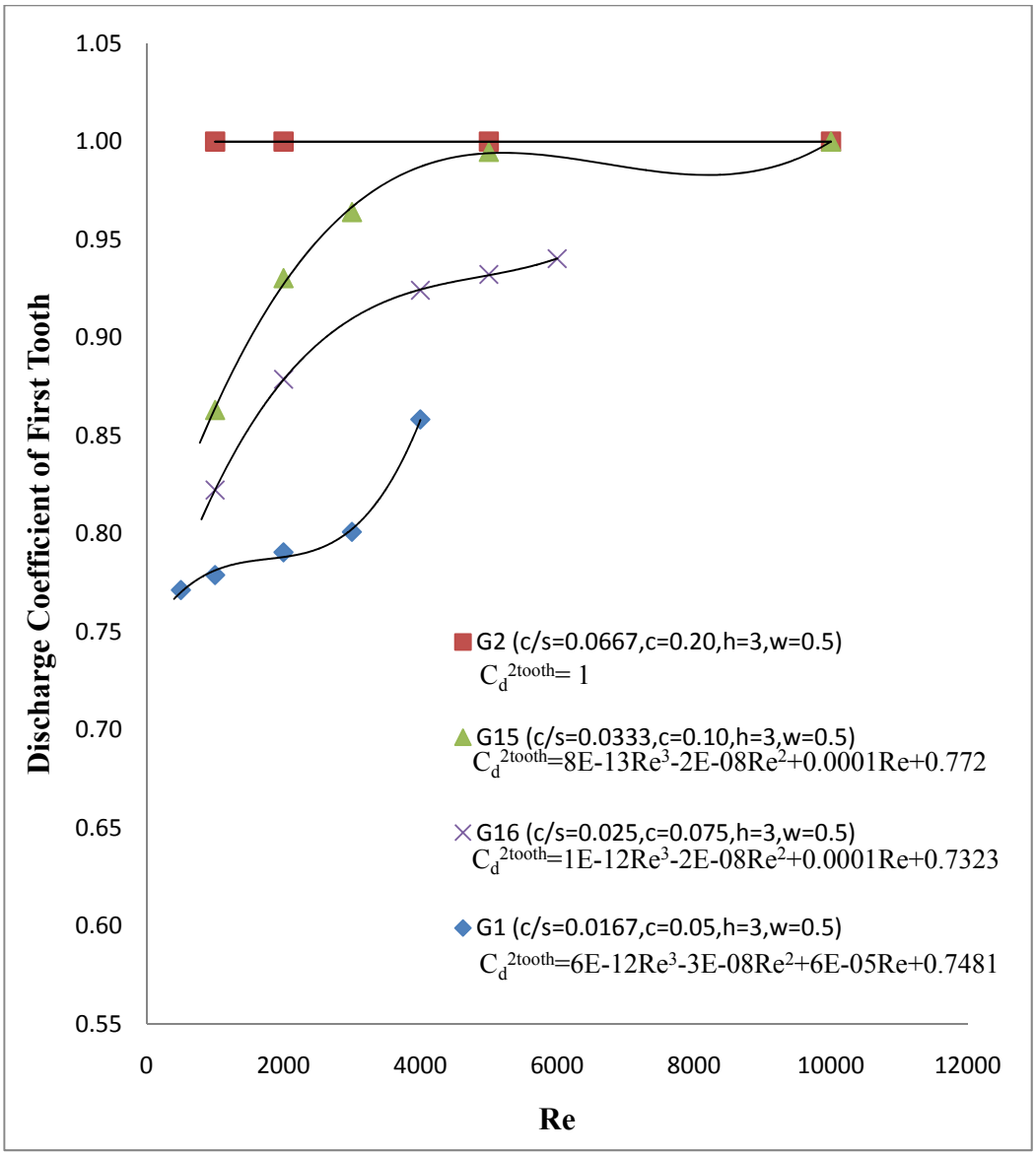

Figure 7.22 Effect of Clearance on C_d (Incompressible flow, W_{sh}=0)

7.3.3 Effect of Tooth Width

Figure 7.23 shows the discharge coefficient distribution of intermediate teeth for G21, G1 and G18 for a set of Reynolds numbers. In the carryover coefficient analysis, it was found that the lower tooth width gives lower carryover coefficient which means that

the energy dissipation inside the cavity is higher compared to that of higher tooth width. However, similar to discharge coefficient of first tooth, the highest discharge coefficient value is obtained for the lowest tooth width contradicting with the findings of carryover coefficient analysis. Thus, it can be concluded that even though less energy is dissipated inside the cavity for higher tooth width, the total pressure loss is higher for higher tooth width.

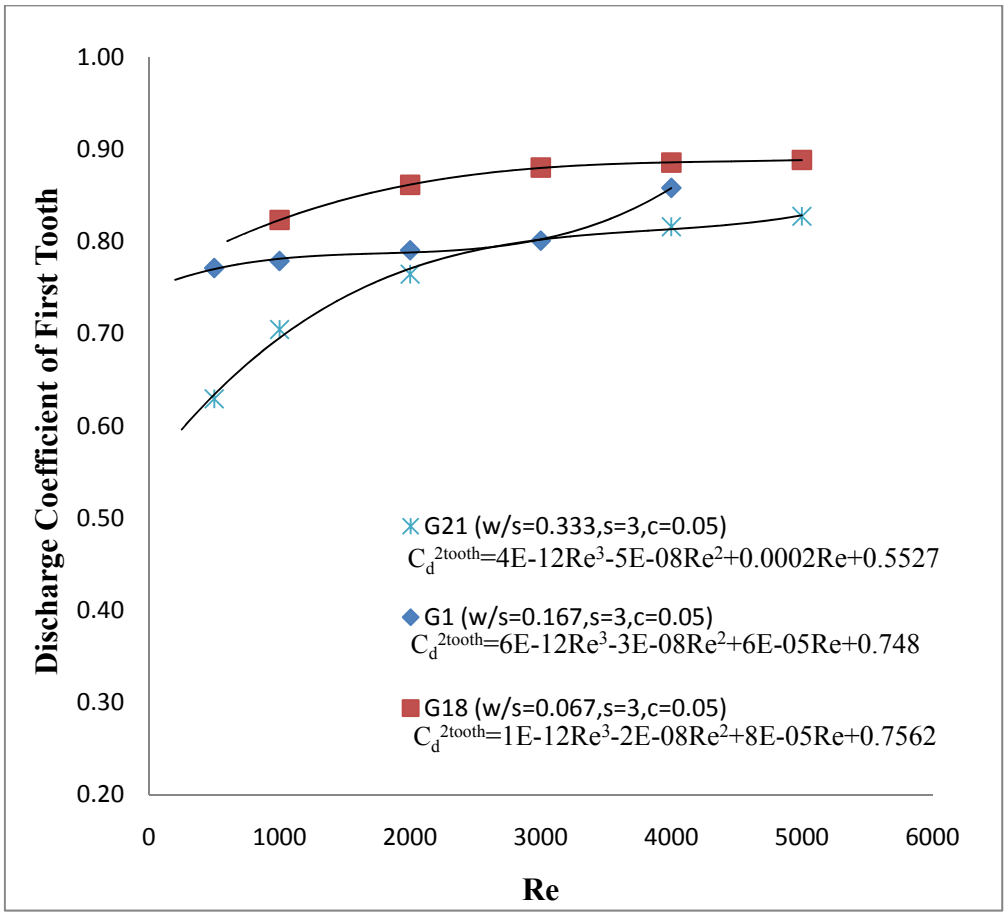

Figure 7.23 Effect of tooth width on C_d (Incompressible flow, W_{sh}=0)

7.3.4 Effect of Tooth Pitch

In this section, the clearance and other dimensions will be kept constant while the tooth pitch is varied. Figure 7.24 shows intermediate tooth discharge coefficient of G7 and G4. As can be seen from the above figure, the discharge coefficient is higher for lower tooth pitch. This agrees with the results of carryover coefficient and first tooth discharge coefficient analysis. Longer pitch allows the flow to diverge more compared to smaller pitch. As a result, the energy dissipation through the vortex increases as well as the friction losses due to longer flow path.

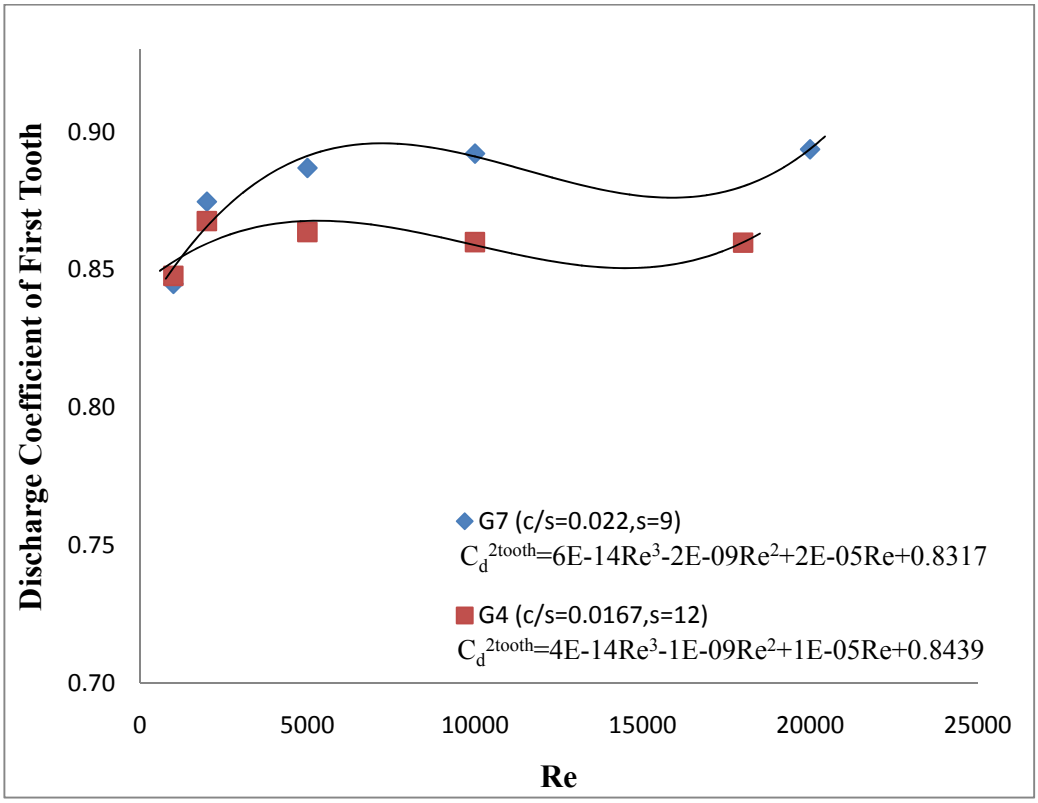

Figure 7.24 Effect of tooth pitch on C_d (Incompressible flow, W_{sh}=0)

7.3.5 Effect of Tooth Height

The effect of tooth height on intermediate tooth discharge coefficient is illustrated in figure 7.25. G27, G25 and G24 have the same tooth width, clearance and pitch but their tooth heights are different. It can be seen that the lower tooth height has lower discharge coefficient and this pattern is more prominent for higher Reynolds numbers.

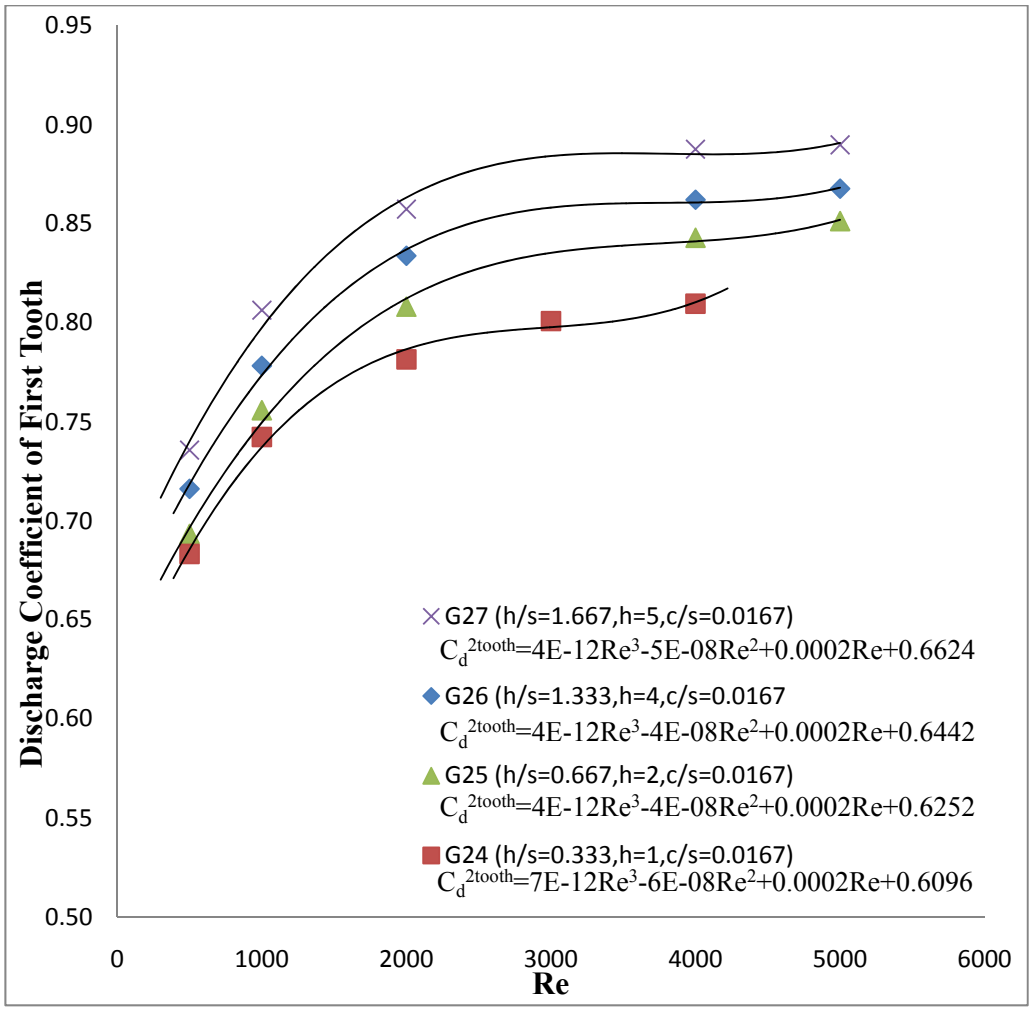

Figure 7.25 Effect of tooth height on C_d (Incompressible flow, W_{sh}=0)

7.3.6 Effect of Upstream Side Angle

G4 and G9 are compared to understand the effect of upstream side angle on intermediate tooth discharge coefficient. Their dimensions are same apart from the upstream angle which is 7^o and 0^o for G4 and G9 respectively. As can be seen from figure 7.26, It is observed that 7^o gives slightly (approximately %1.3) higher discharge coefficient compared to 0^o.

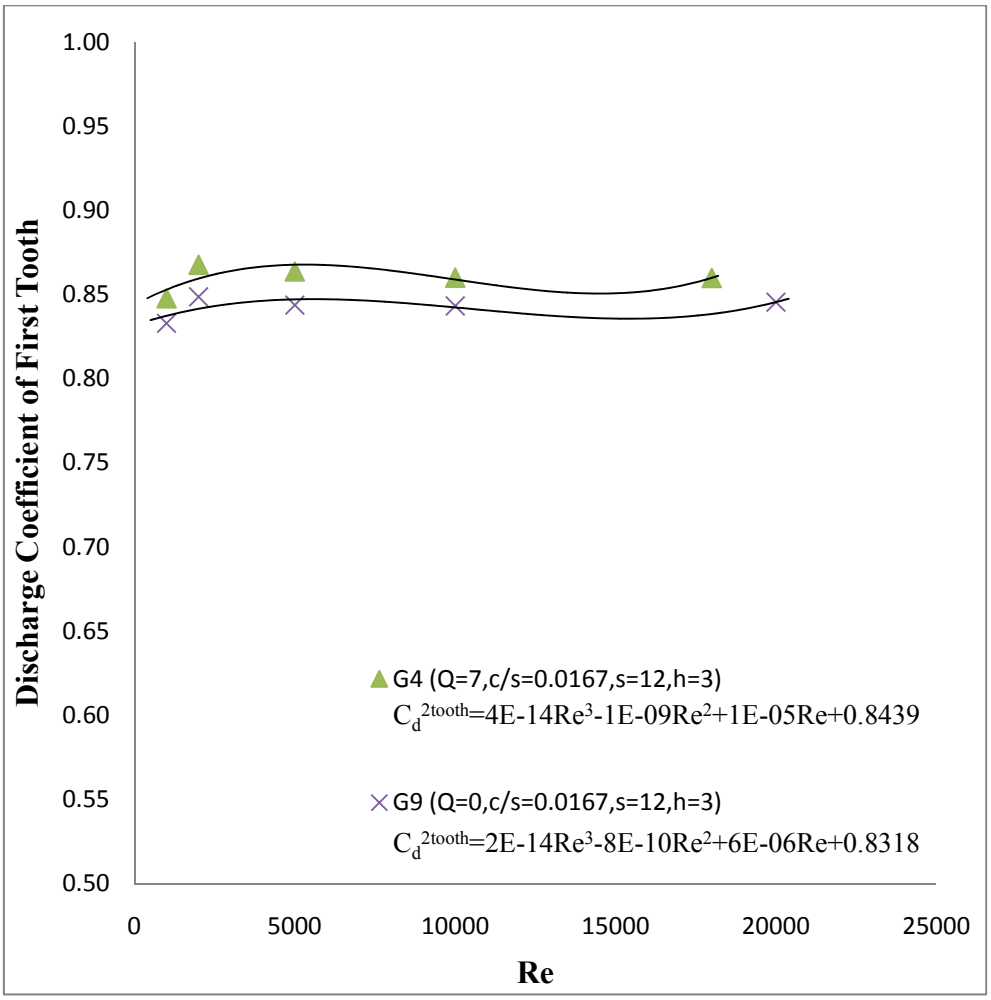

Figure 7.26 Effect of upstream side angle on C_d (Incompressible flow, W_{sh}=0)

The effect of geometrical parameters and Reynolds number were studied so far without considering the effect of shaft speed. These effects are summarized in table 7.2.

Table 7.2 Effects of geometrical parameters and Re on C_d

Increasing	C_d
c	increases
s	decreases
w	decreases
h	increases
Q	increases
Re	increases

It should be noted that tooth height and upstream angle have a very small effect on discharge coefficient compared to other parameters given in table 7.2. However, the effect of tooth height is slightly higher for intermediate tooth discharge coefficient compared to that of first tooth. Remaining parameters have relatively stronger effects on discharge coefficients. Amongst them, tooth clearance (c/s) is the strongest parameter followed by Reynolds number.

7.3.7 Effect of Shaft Speed

It was observed that the shaft speed gradually reduces the first tooth discharge coefficient. A similar pattern is also observed for intermediate tooth discharge coefficient. Figure 7.27 shows the intermediate tooth discharge coefficients for G1. As the Taylor number increases, the discharge coefficient gradually decreases. This is more

prominent when the Reynolds number is low (i.e.1000). When the Reynolds number is 1000, the overall decrease in intermediate tooth discharge coefficient is 33% as the Taylor number increases from 0 to 550. When the Reynolds number is 4000, this decrease is 4%. This can be attributed to the same reason as discussed in section 7.2.7.

Figures 7.28 and 7.29 show the intermediate tooth discharge coefficients for G4 and G21 respectively. It is seen from figure 7.28 that the intermediate tooth discharge coefficient drastically decreases when the Reynolds number 1000 and 2000 while this decrease is more gradual for higher Reynolds numbers. Similar pattern is also observed for G21 which is shown in figure 7.29. As the Taylor number increases, the discharge coefficient gradually decreases.

Consequently, it is clear that as shaft speed increases the discharge coefficient decreases. However, if the Reynolds number is low as discussed in section 7.2.7, the centrifugal effect can push the flow to the stator wall, reducing the effectiveness.

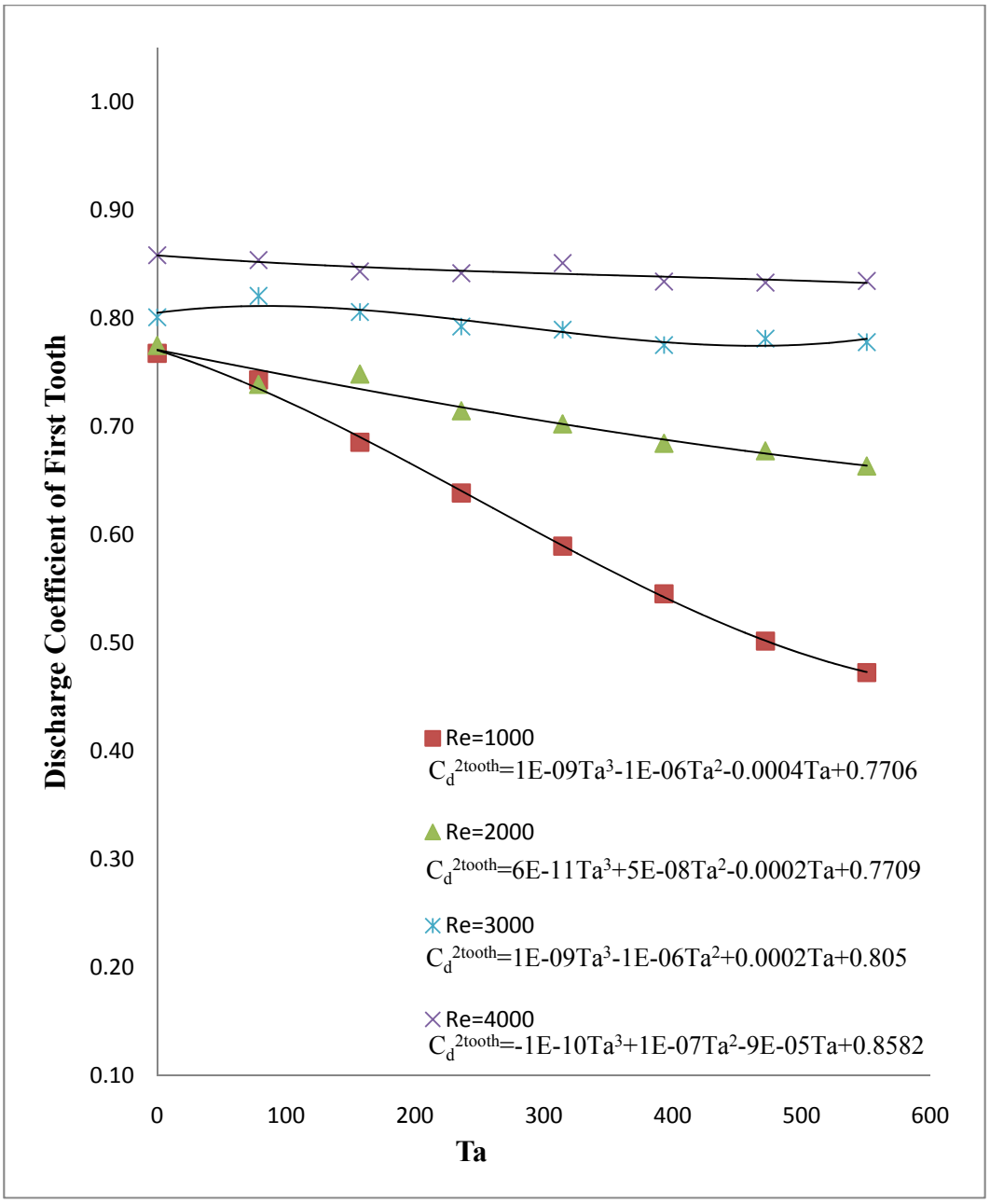

Figure 7.27 Effect of shaft speed on C_d (G1, c/s=0.0167, s=3, h=3, w=0.5, incompressible flow)

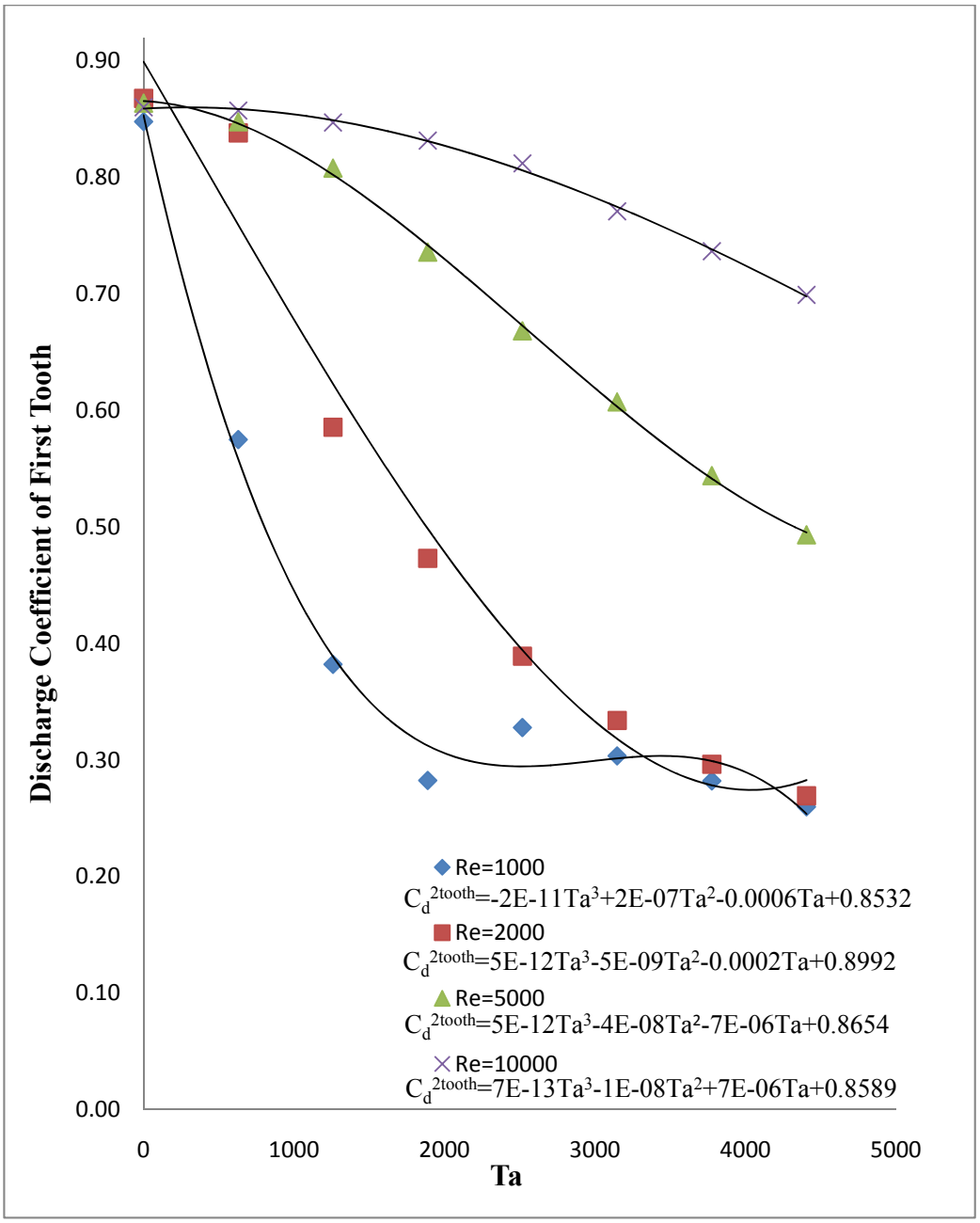

Figure 7.28 Effect of shaft speed on C_d (G4, c/s=0.0167, s=12, h=3, w=0.5, incompressible flow)

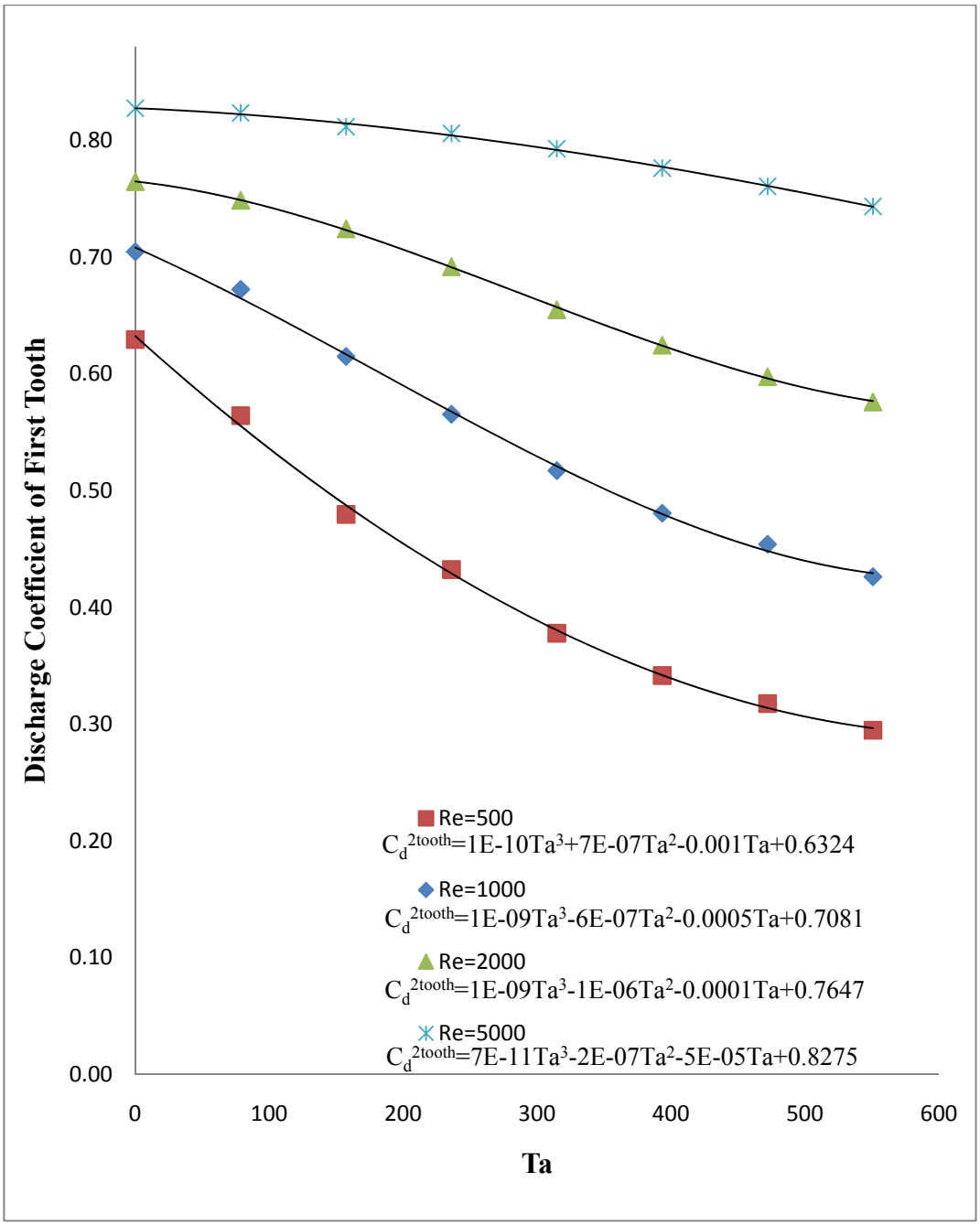

Figure 7.29 Effect of shaft speed on C_d (G21, c/s=0.0167, s=3, h=3, w=1, incompressible flow)

7.3.8 Combined Effects

Individual effects of geometrical features and flow parameters were presented. This section deals with the combined effects of geometrical and flow parameters. G1, G4 and G21 are used to present the combined effects.

Figures 7.30, 7.31 and 7.32 show the discharge coefficients of G1 and G21 for second, third and fourth tooth respectively. It is seen that the distribution is similar to that of first tooth but the values are higher. It is observed that when the Taylor number is lower than 100, both seals have almost same discharge coefficients for second, third and fourth teeth. When the Reynolds number is lower than 2000, wider tooth (G21) gives slightly lower (approximately 3%) discharge coefficients. However, when the Reynolds number is more than 2000 and the Taylor number is more than 100, a wider tooth produces significantly lower discharge coefficients. As the Taylor number is increased from 100 to 550, this difference increases from 5% to 15%. Thus, it can be concluded that a wider tooth profile is better for high Taylor numbers. It is especially more prominent when the Taylor number is higher than 200 (W_{sh}=150 m/s).

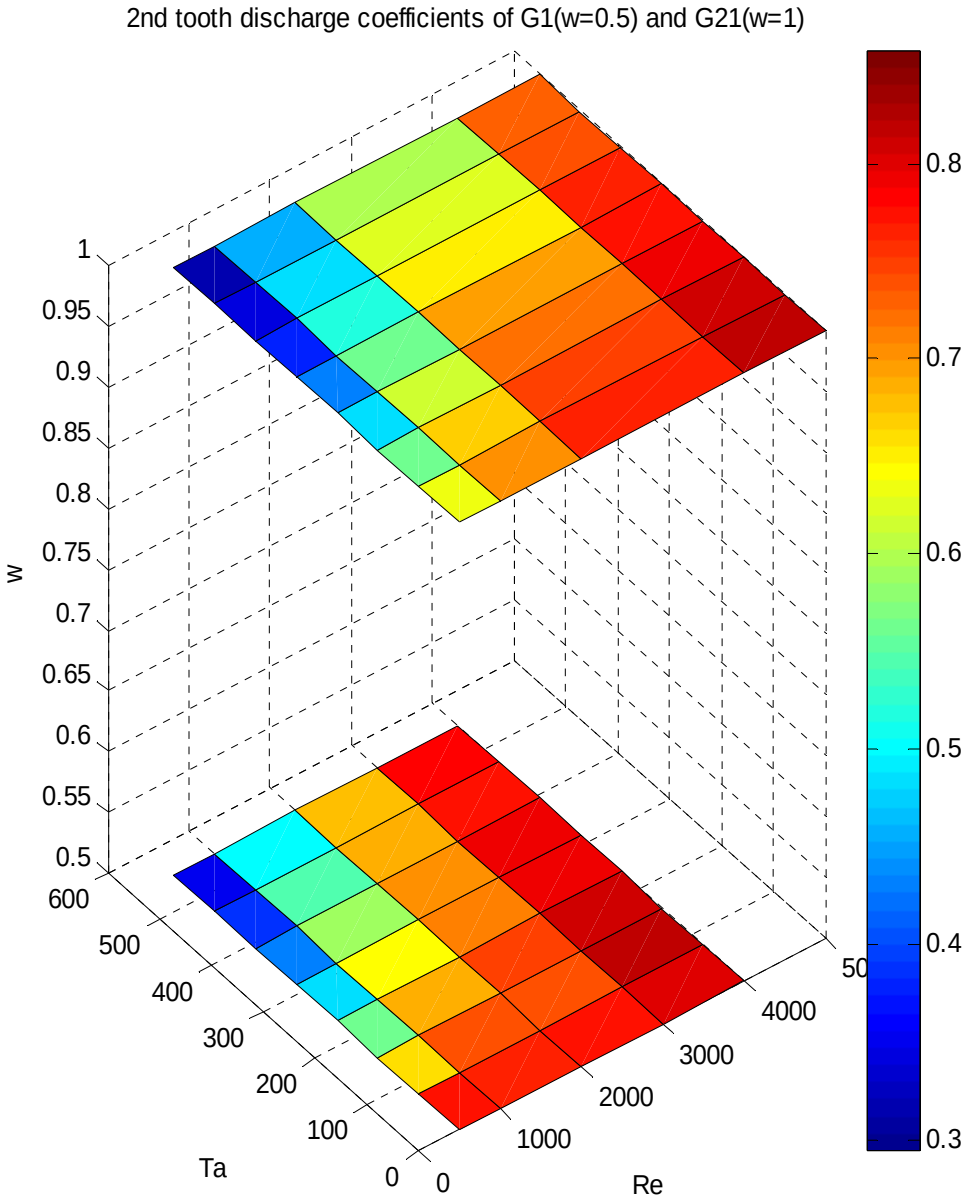

Figure 7.30 Second tooth discharge coefficient comparison of G1(c/s=0.0167, h/s=1, s=3, incompressible flow) and G21(c/s=0.0167, h/s=1, s=3, incompressible flow)

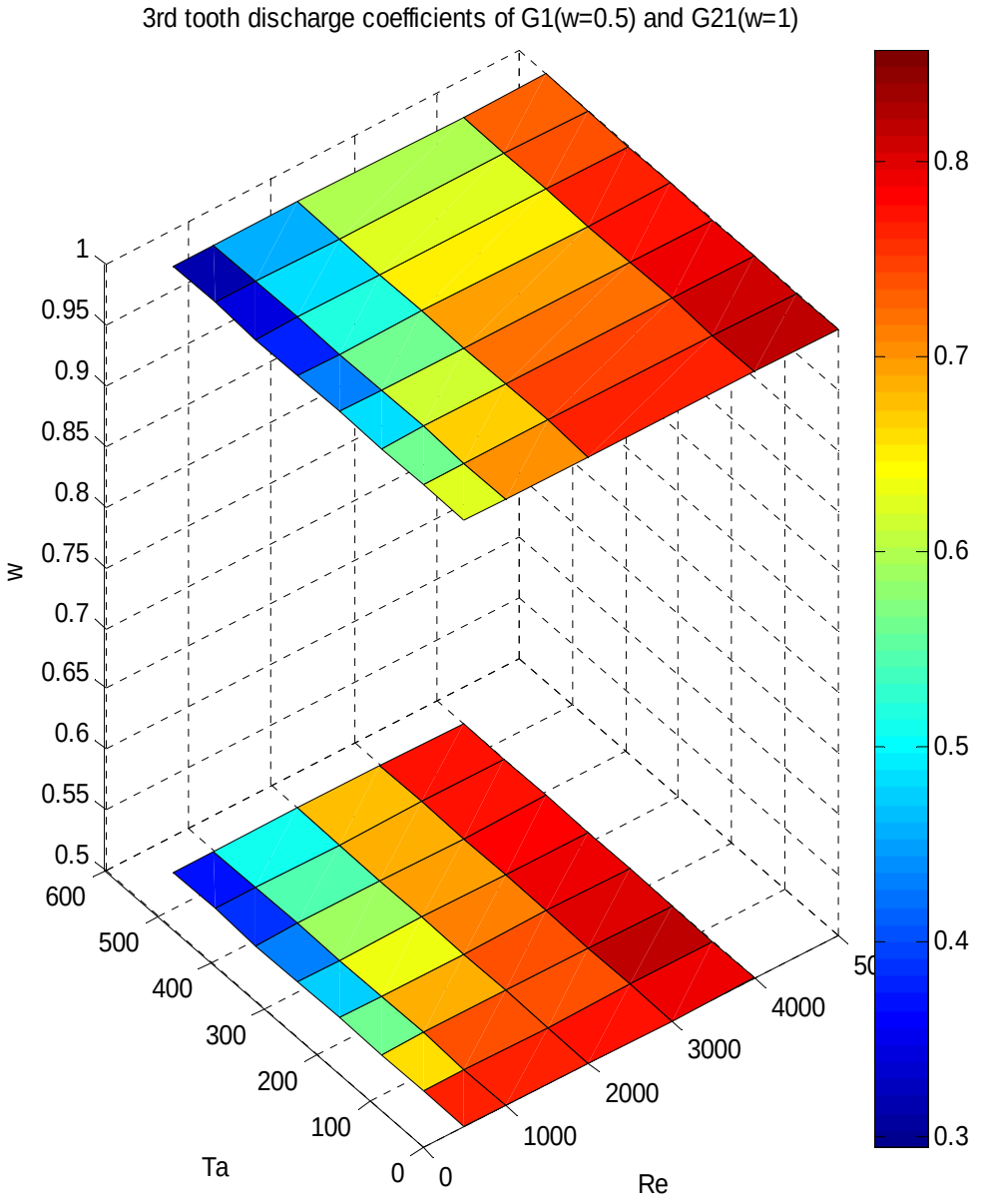

Figure 7.31 Third tooth discharge coefficient comparison of G1(c/s=0.0167, h/s=1, s=3, incompressible flow) and G21(c/s=0.0167, h/s=1, s=3, incompressible flow)

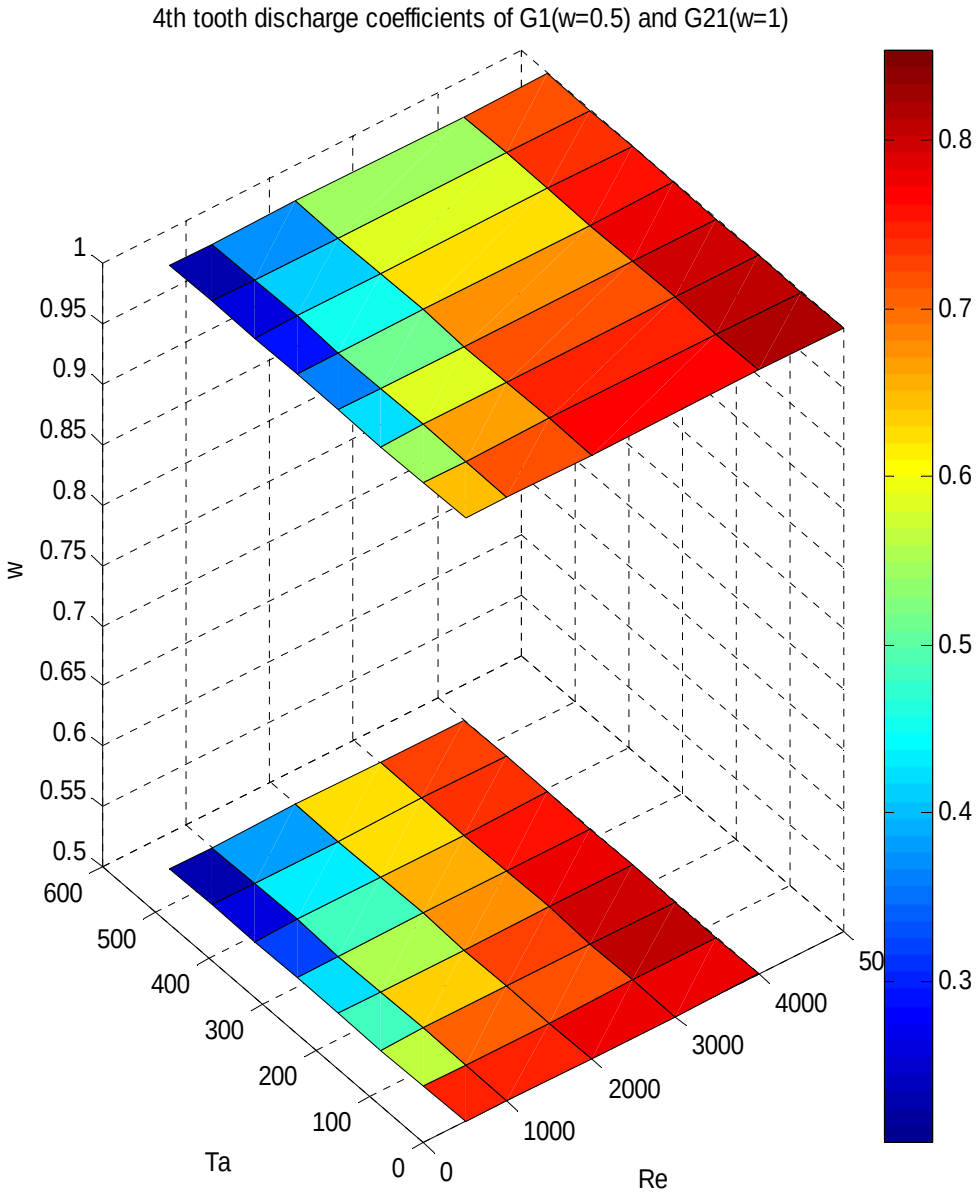

Figure 7.32 Fourth tooth discharge coefficient comparison of G1(c/s=0.0167, h/s=1, s=3, incompressible flow) and G21(c/s=0.0167, h/s=1, s=3, incompressible flow)

Figures 7.33, 7.34 and 7.35 present the discharge coefficient comparison of G1 and G4 for second, third and fourth teeth respectively. G1 and G4 have the same c/s ratio but theirs h/s ratio are different. So the effect of h/s combined with the shaft speed effect will be investigated here. It is clear from the figures that the discharge coefficients of second, third and fourth teeth are same as validated in the previous sections.

It is observed that wider cavity profile (G4) gives significantly higher discharge coefficients than G1 when the shaft speed is less than 150 for all Reynolds numbers. However, when shaft speed is further increased, G4 gives significantly less discharge coefficient at 5000 Reynolds number. For, smaller Reynolds numbers, both profiles give almost same discharge coefficients. Thus, it can be concluded that for low shaft speed (less than 150), narrower cavity gives significantly better discharge coefficient compared to wider cavity. For higher shaft speeds (more than 150) and higher Reynolds numbers (5000), wider cavity gives significantly better discharge coefficients.

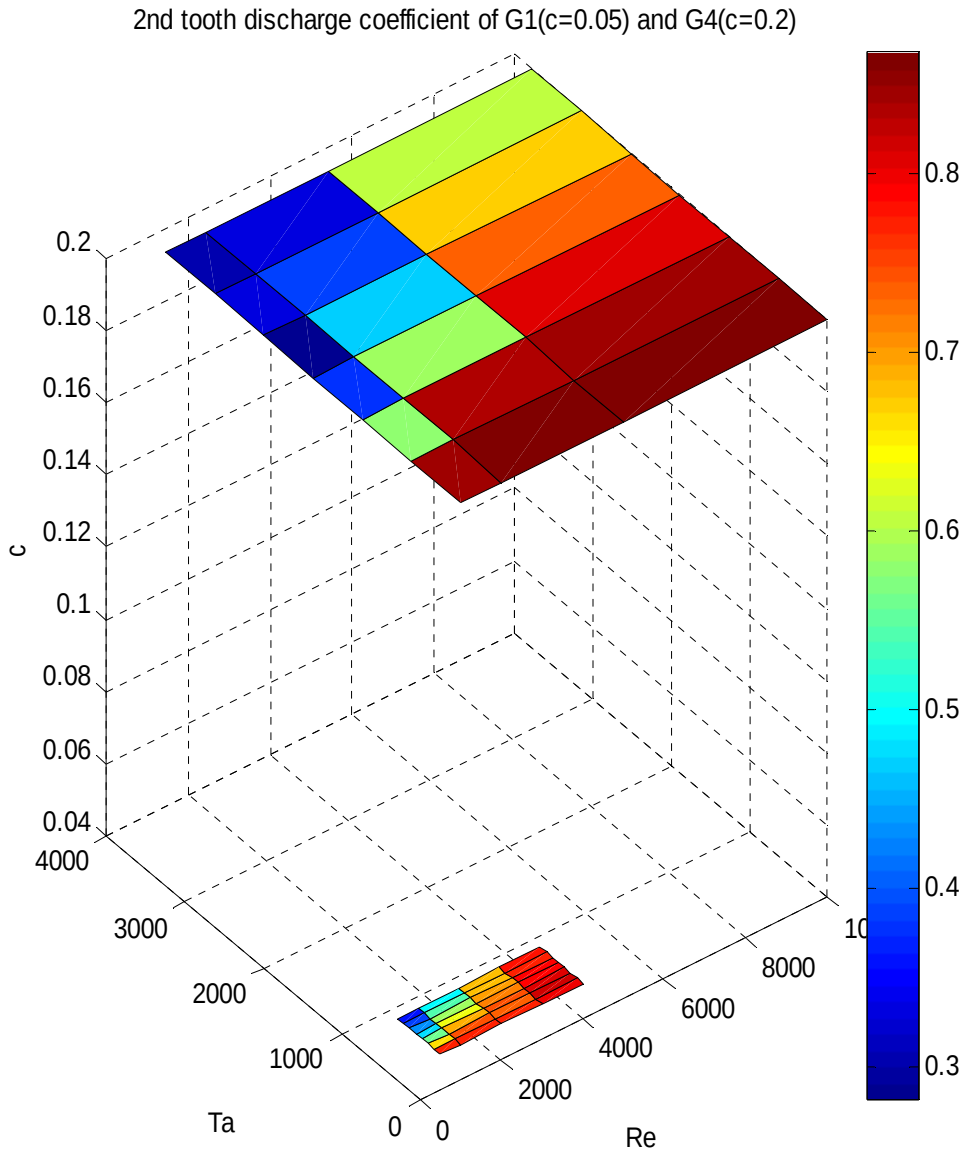

Figure 7.33 Second tooth discharge coefficient comparison of G1(c/s=0.0167, h/s=1, s=3, incompressible flow) and G4(c/s=0.0167, h/s=0.25, s=12, incompressible flow)

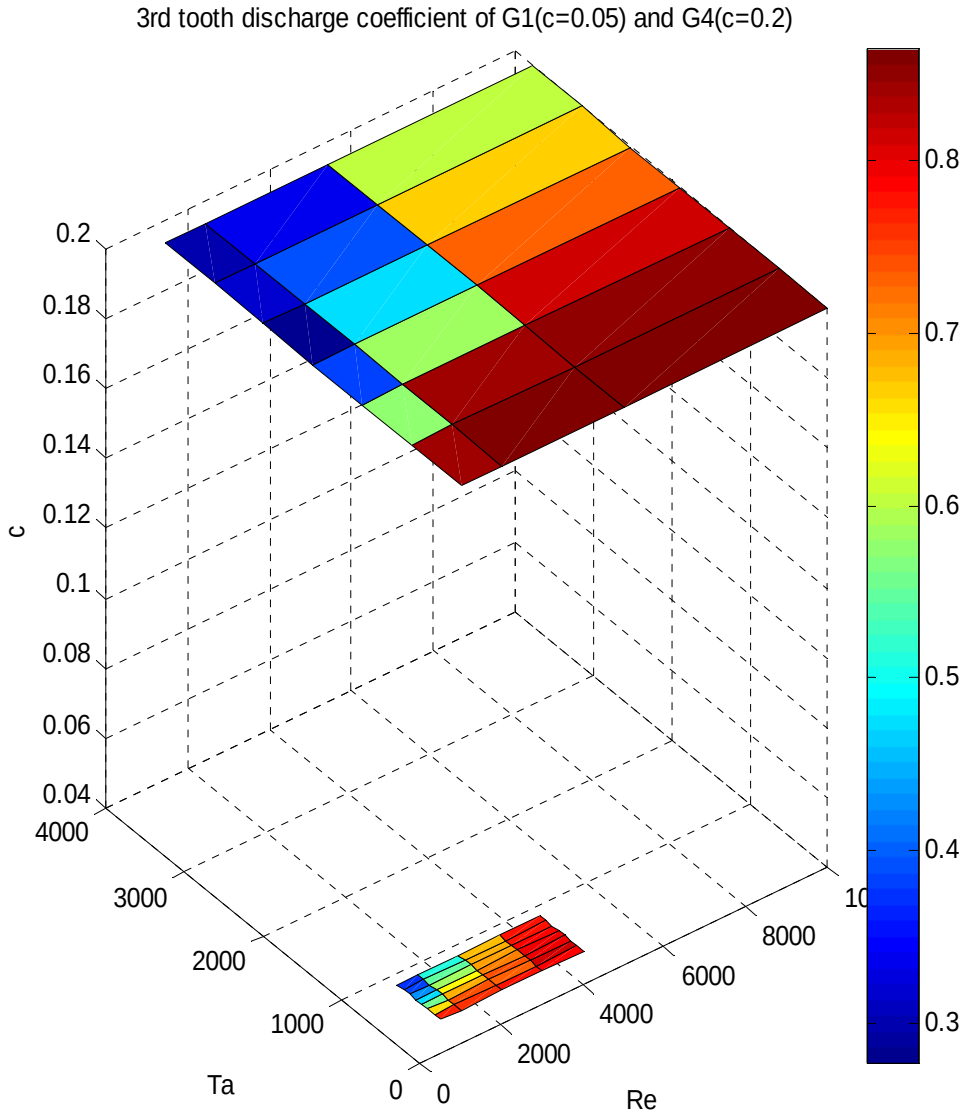

Figure 7.34 Third tooth discharge coefficient comparison of G1(c/s=0.0167, h/s=1, s=3, incompressible flow) and G4(c/s=0.0167, h/s=0.25, s=12, incompressible flow)

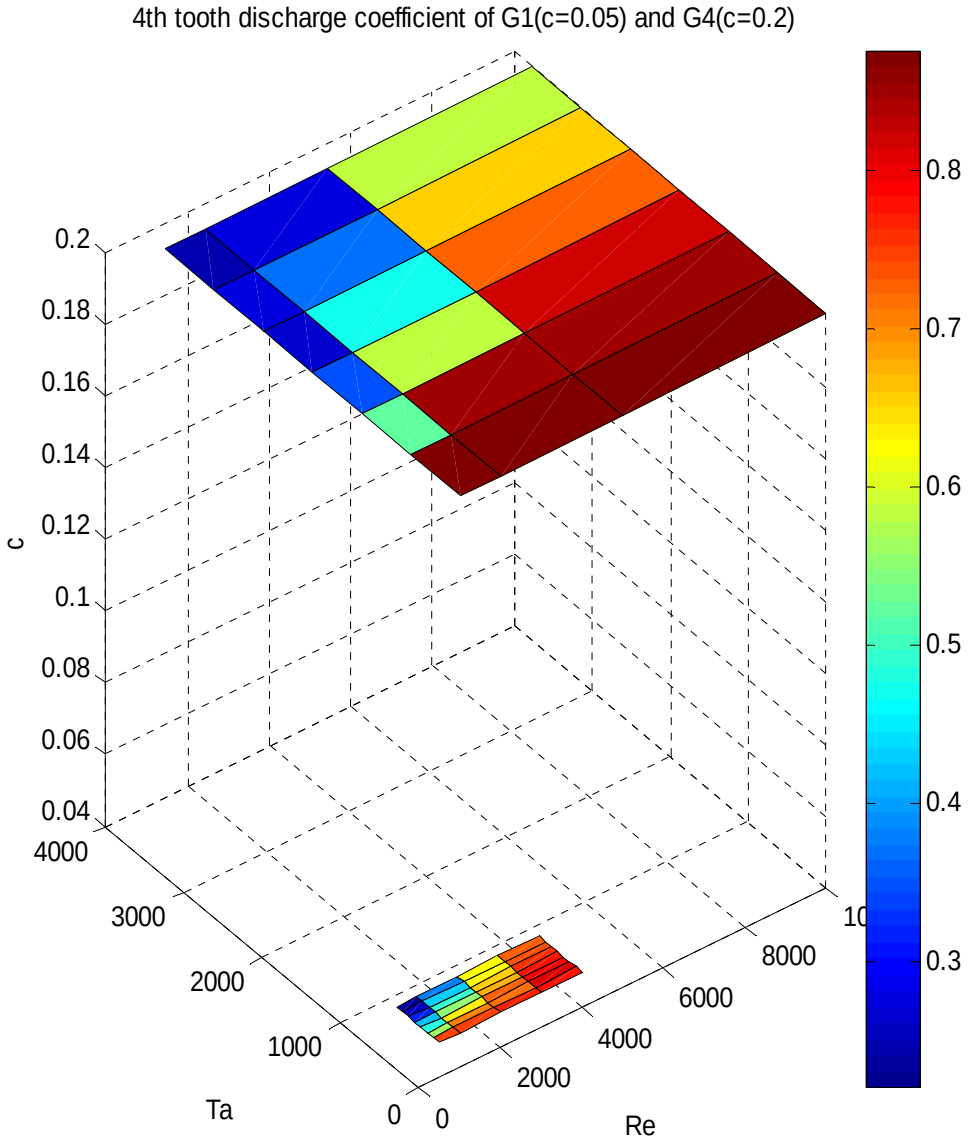

Figure 7.35 Fourth tooth discharge coefficient comparison of G1(c/s=0.0167, h/s=1, s=3, incompressible flow) and G4(c/s=0.0167, h/s=0.25, s=12, incompressible flow)

8. EFFECTS OF COMPRESSIBILITY

8.1 Introduction

The analysis so far considered incompressible flow in which water was used as the working medium. However, labyrinth seals are used in many kinds of turbomachinery which also use compressible fluids as working medium. Hence, the effects of compressibility should also be taken into account.

First of all, the previous models, which were developed for incompressible flow, should be compared with the discharge coefficients of compressible flow in order to understand the need for taking compressibility into account. This will be done by introducing the pressure ratio and expansion factor.

$$Pr = \frac{P_e}{P_i} \quad \text{..... (8.1)}$$

$$\psi = \frac{C_{d_{air}}}{C_{d_{water}}} \quad \text{..... (8.2)}$$

The pressure ratio, as given in equation 8.1, is the ratio of downstream absolute pressure to the upstream absolute pressure of a tooth. Since flow across the tooth reduces the pressure of the fluid, the maximum pressure ratio should always be smaller than 1. The expansion factor, as given in equation 8.2, is the ratio of the discharge coefficient of air to that of water for the same tooth at a given Reynolds number. The highest value of the expansion factor can be 1 indicating that the discharge coefficients

of air and water are the same. This means that there is no effect of compressibility. On the other hand, smaller expansion factor indicates that there is a difference between air and water discharge coefficients due to the compressibility of the air.

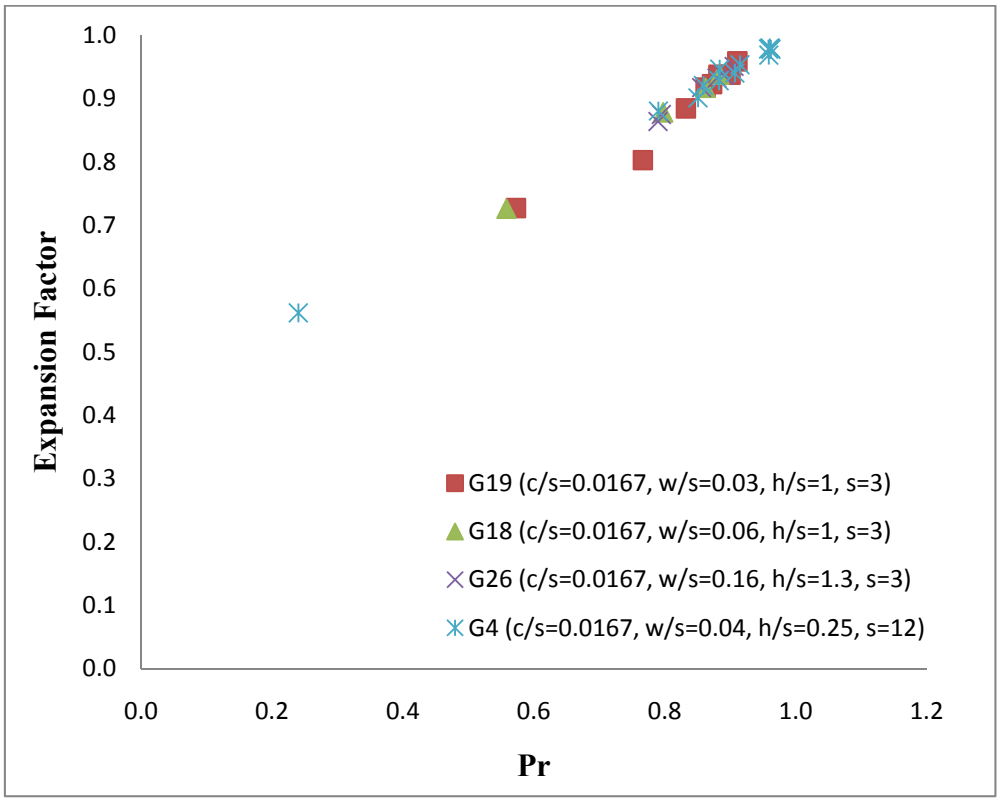

Figure 8.1 Variation of ψ with different pressure ratios (Re=500-5000, W_{sh} =0)

It can be seen from figure 8.1 that the expansion factor increases as the pressure ratio is increased. For lower pressure ratios, the effects of compressibility should be taken into consideration due to the higher difference between air and water discharge coefficients. For higher pressure ratios, air and water possess almost the same discharge

coefficient, resulting in an expansion factor value very close to 1. When the expansion factor is close to 1, the effects of compressibility can be neglected. However, if it is further reduced, the effects of compressibility should be taken in to account.

The expansion factor is also affected by the geometry of the seal. As can be seen in figure 8.1, different geometries have slightly different expansion factors even though the pressure ratio is the same. Moreover, pressure ratio is also a function of flow parameters and tooth position. Thus, it is required to study the effect of geometrical features and flow parameters on expansion factor.

8.2 Effect of Tooth Position

The pressure ratio can greatly differ from one tooth to another. Accordingly, the expansion factor is also expected to change. Moreover, for a given pressure ratio, the expansion factor might also change from one tooth to another. Thus, the effect of tooth position should be investigated.

Figure 8.2 shows the expansion factor distribution of G4 for all of the teeth. The linear trend line is added to the last tooth which has the widest expansion factor range. It is apparent that the expansion factor values of the other teeth follow this trend line. Therefore, it can be concluded that the expansion factor is not a function of tooth position. So there is no need to study all teeth separately. The results presented in the following sections will include both the first tooth and the other teeth.

It should be noted that the pressure ratio can change for the last tooth and accordingly the expansion factor also changes. However, for a given pressure ratio, all

teeth have the same expansion factor. Thus, expansion factor is not a function of tooth position.

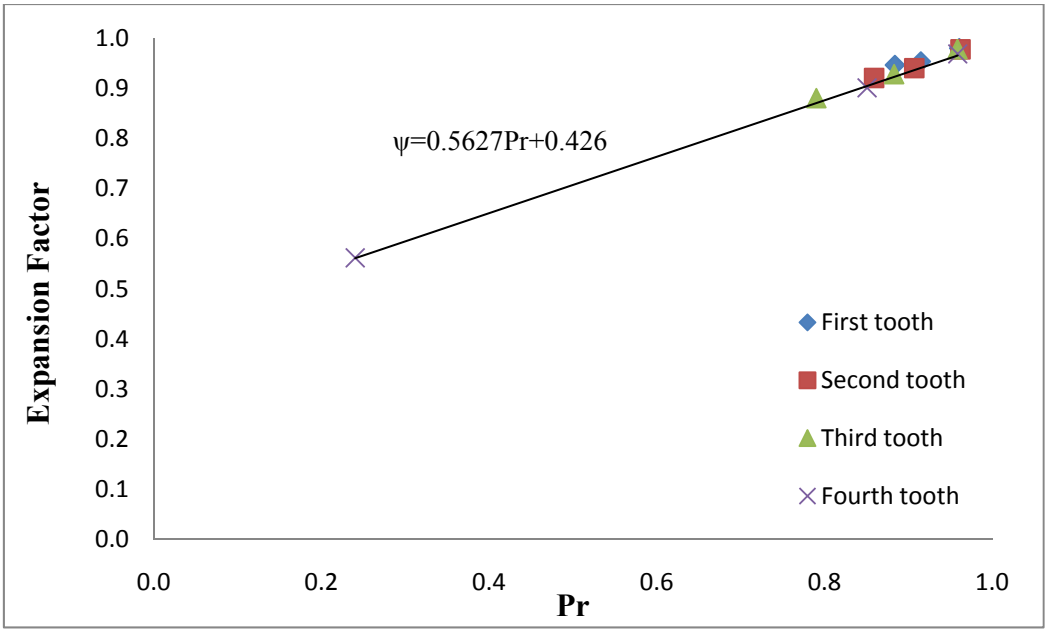

Figure 8.2 Variation of ψ with tooth position (G4, c/s=0.0167, w/s=0.0417, h/s=0.25, s=12, W_{sh} =0, Re=1000, 2000, 10000)

8.3 Effect of Reynolds Number

The effect of Reynolds number will be investigated by using pressure ratio. An increase in Reynolds number causes a decrease in the pressure ratio indicating that the ratio of downstream absolute pressure to that of upstream decreases.

Figure 8.3 shows the variation of expansion factor with increasing Reynolds numbers. G26 and G4 are randomly chosen to present the effect of Reynolds numbers.

The highest pressure ratio represents the lowest Reynolds number and lowest pressure ratio represents the highest Reynolds number.

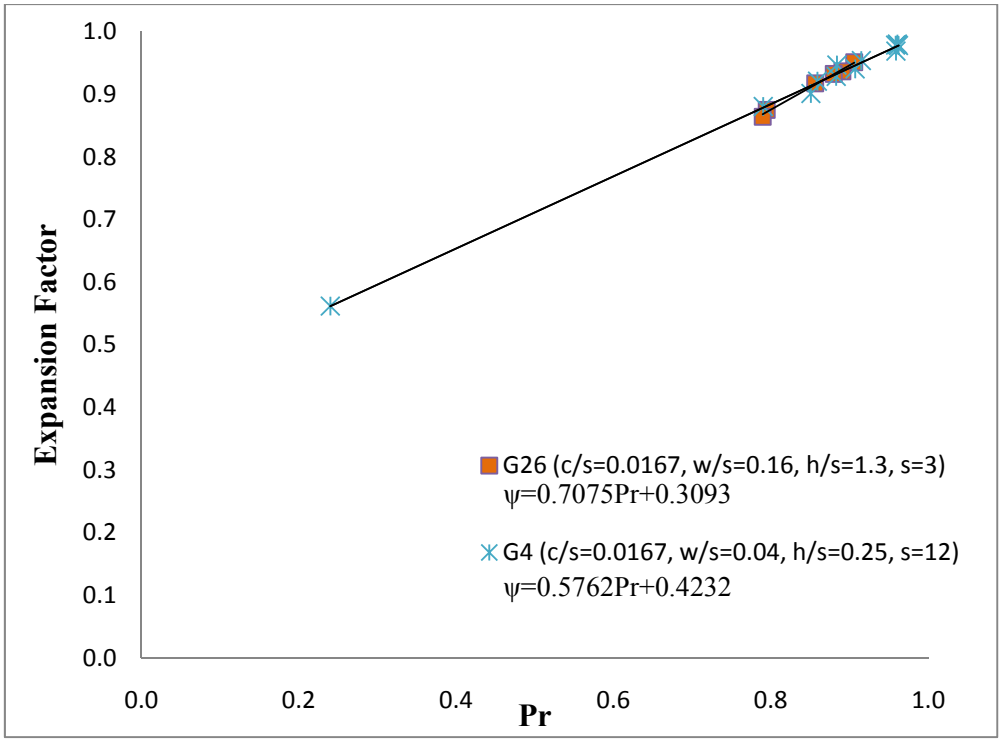

Figure 8.3 Effect of Reynolds number on ψ of (W_{sh} =0)

As can be seen from the figure, as Reynolds number increases from 500 to 1000, the pressure ratio and expansion factor decreases. The lowest Reynolds number (500) has the highest pressure ratio and the highest Reynolds number (5000) has the lowest pressure ratio. However, the relationship between the expansion factor and the pressure ratio remains the same for all Reynolds numbers. For low Reynolds numbers, compressibility has negligible effect on discharge coefficient. However, for higher Reynolds numbers, the discharge coefficient of air can reduce to as much as 50% of that

of water. The expansion factor distribution of both G4 and G26 show a linear variation as given in the figure.

8.4 Effect of Clearance

It was discussed that clearance to pitch ratio is the major geometrical parameter that affects the discharge and carryover coefficients. It can also have an effect on expansion factor which is discussed in this section. For this purpose, the expansion factors of G15, G16 and G1 will be investigated. All of the dimensions of those geometries are same but the clearance is different.

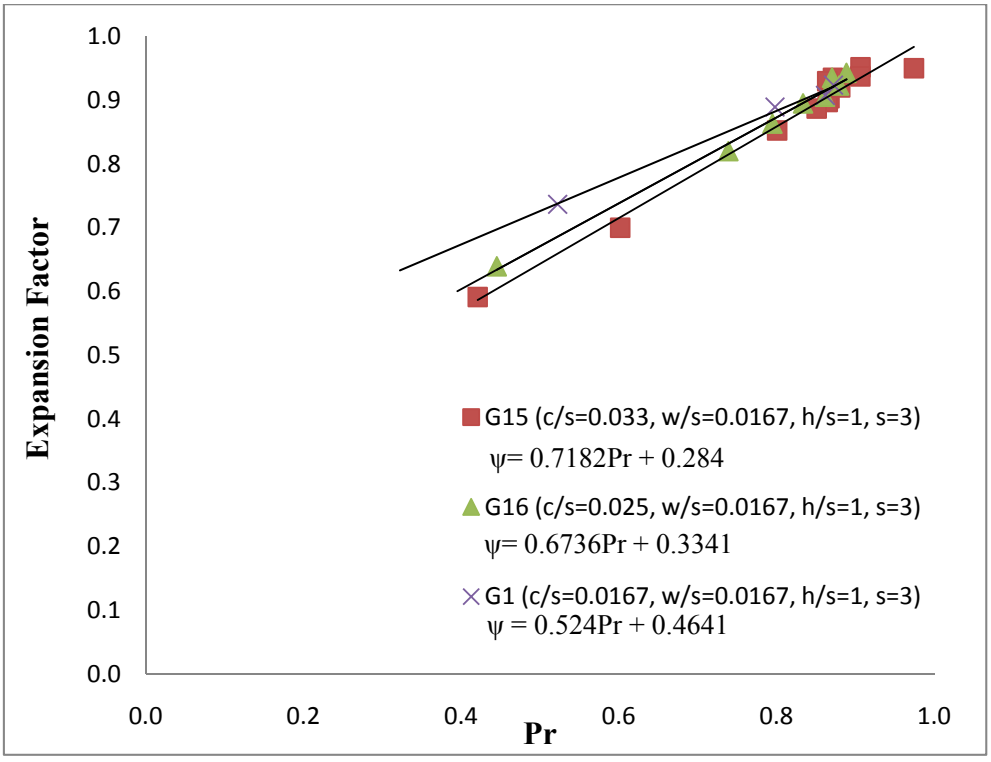

Figure 8.4 Effect of clearance on ψ (W_{sh}=0)

From figure 8.4, it is apparent that clearance has a much smaller effect on expansion factor than it has on the discharge coefficient. The expansion factor decreases slightly as the clearance is increased. G15 is derived from G1 by doubling its clearance. However, as can be seen from the figure, the expansion factor decreased around only 6% even though the clearance is increased by 100%. Thus, clearance has some effect on expansion factor but it is not a primary parameter.

8.5 Effect of Tooth Width

Figure 8.5 shows the variation of the expansion factor with pressure ratio for different geometries. It is apparent that the tooth width varying from w/s=0.0167 to w/s=0.33 does not have a significant effect unless it is zero. G21, G1, G18 and G22 have almost same expansion factors as seen in the figure. Only one linear trend line is required to present those data. However, when the tooth width is zero, the expansion factor drastically increases which means that the difference between air and water discharge coefficients is reduced. It means that the sharp tooth profile has almost the same efficiency regardless of the working medium being compressible or incompressible. Considering the remaining tooth profiles, it can be concluded that the expansion factor is not a strong function of tooth width.

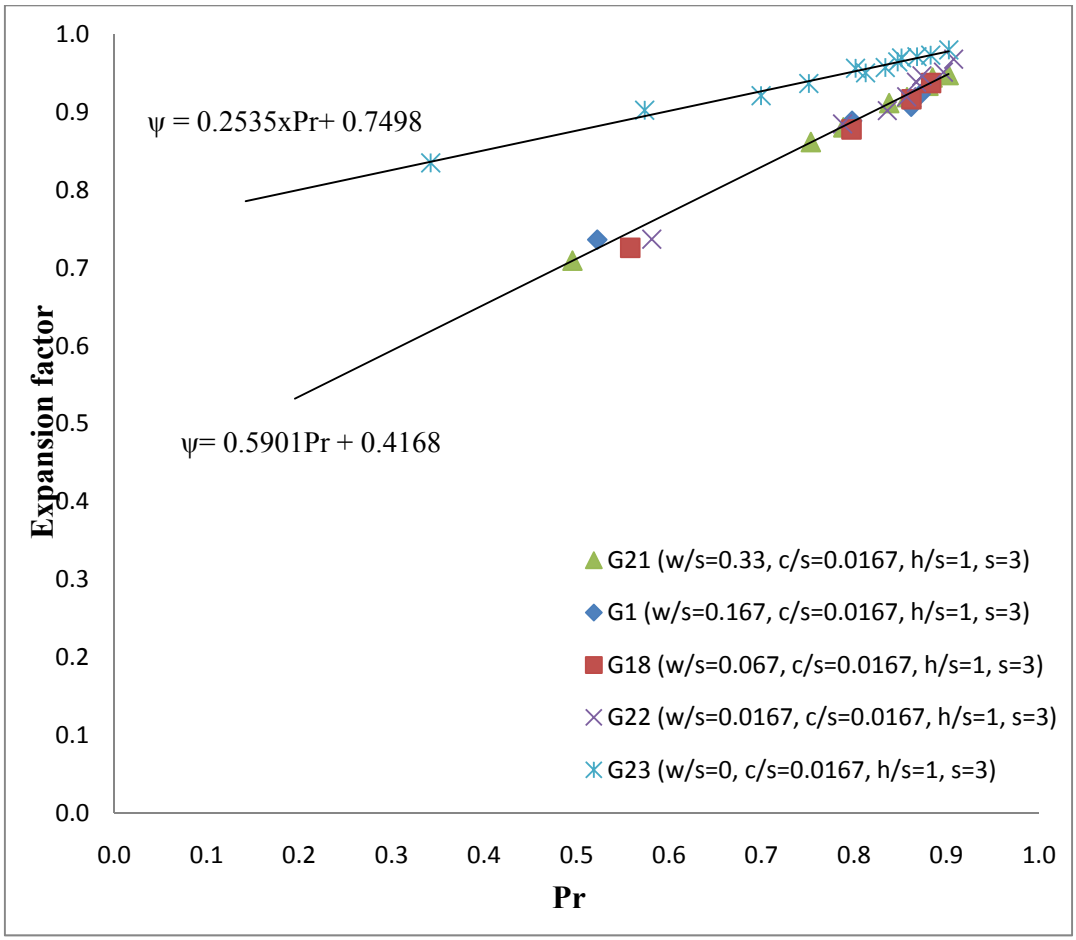

Figure 8.5 Effect of tooth width on ψ (W_{sh}=0)

8.6 Effect of Tooth Pitch

The effect of tooth pitch on expansion factor is investigated by comparing G4 and G7. Their pitch values are different and the remaining parameters are the same. Figure 8.6 shows the expansion factors for these two cases. As can be seen from the figure, tooth pitch does not have a significant effect on expansion factor. The expansion factors are almost the same for the whole set of pressure ratios. Thus, the expansion factor is not a function of tooth pitch.

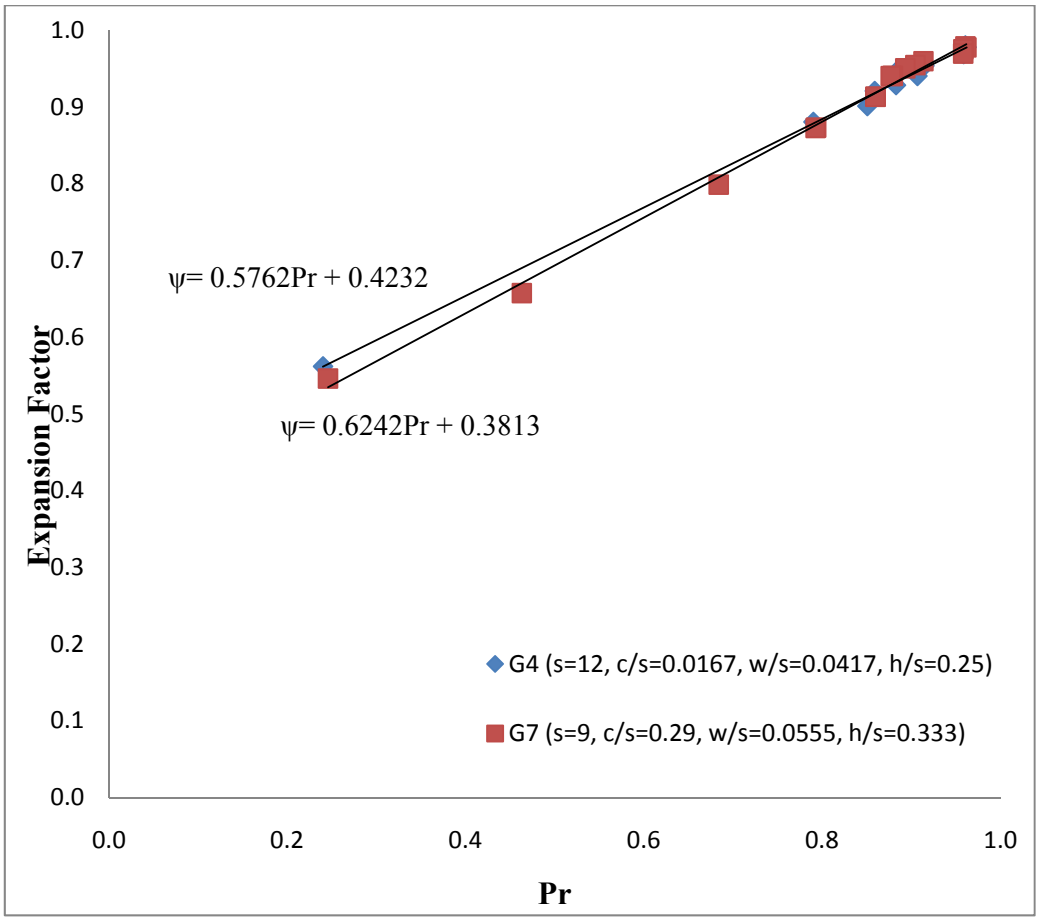

Figure 8.6 Effect of tooth pitch on ψ (W_{sh} =0)

8.7 Effect of Tooth Height

In order to present the effect of tooth height on expansion factor, five seal geometries with different tooth heights but the same values for the remaining geometrical features are chosen. As can be seen from figure 8.7, all geometries have similar expansion factors. Trend lines are plotted only for the smallest tooth height (G24) and highest tooth height (G27). It is apparent that the difference between

expansion factors of any two cases is not more than 5%. Mostly, it is around 2-3%. Thus, it can be concluded that the expansion factor is not a function of tooth height.

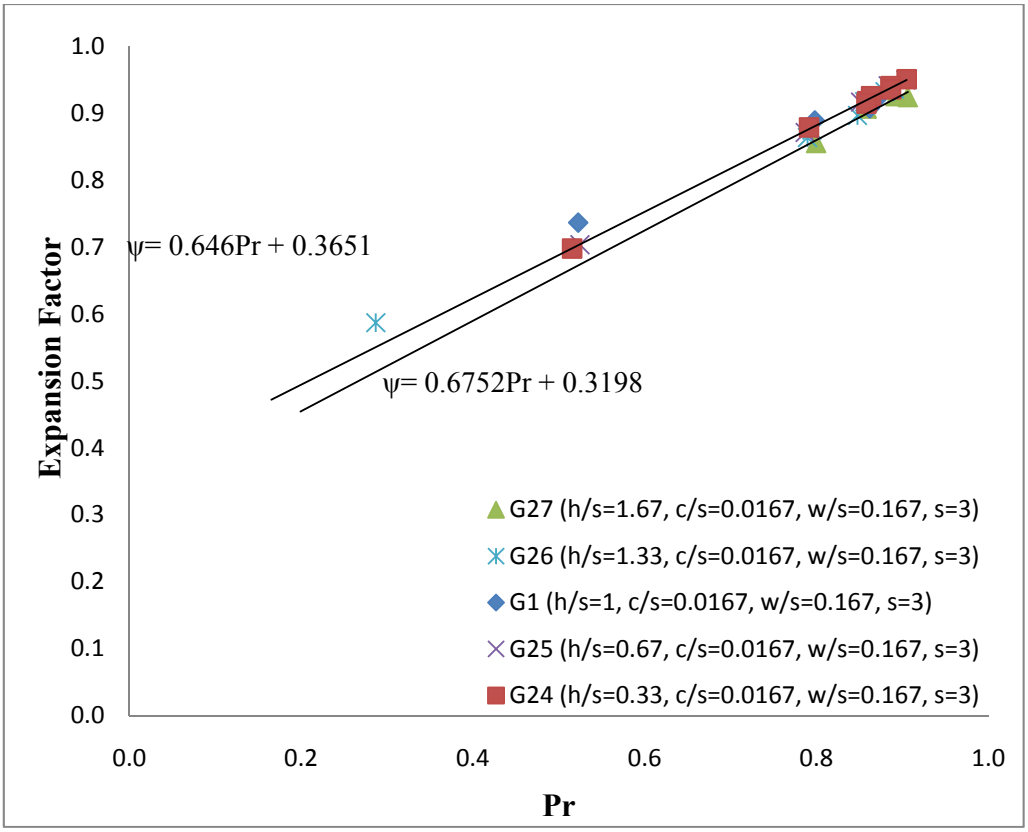

Figure 8.7 Effect of tooth height on ψ (W_{sh} =0)

8.8 Effect of Upstream Side Angle

It was shown that the upstream side angle of the tooth has an effect on discharge coefficient up to 7-8%. However, as can be seen from figure 8.8, it has no effect on expansion factor. In this figure, the expansion factors of G4 and G9 are plotted. G9 is derived from G4 by changing the upstream side angle from 7° to 0 ° and the remaining

parameters are the same. Only one trend line is required to present all of the data for both cases. Thus, the expansion factor is also not a function of upstream side angle.

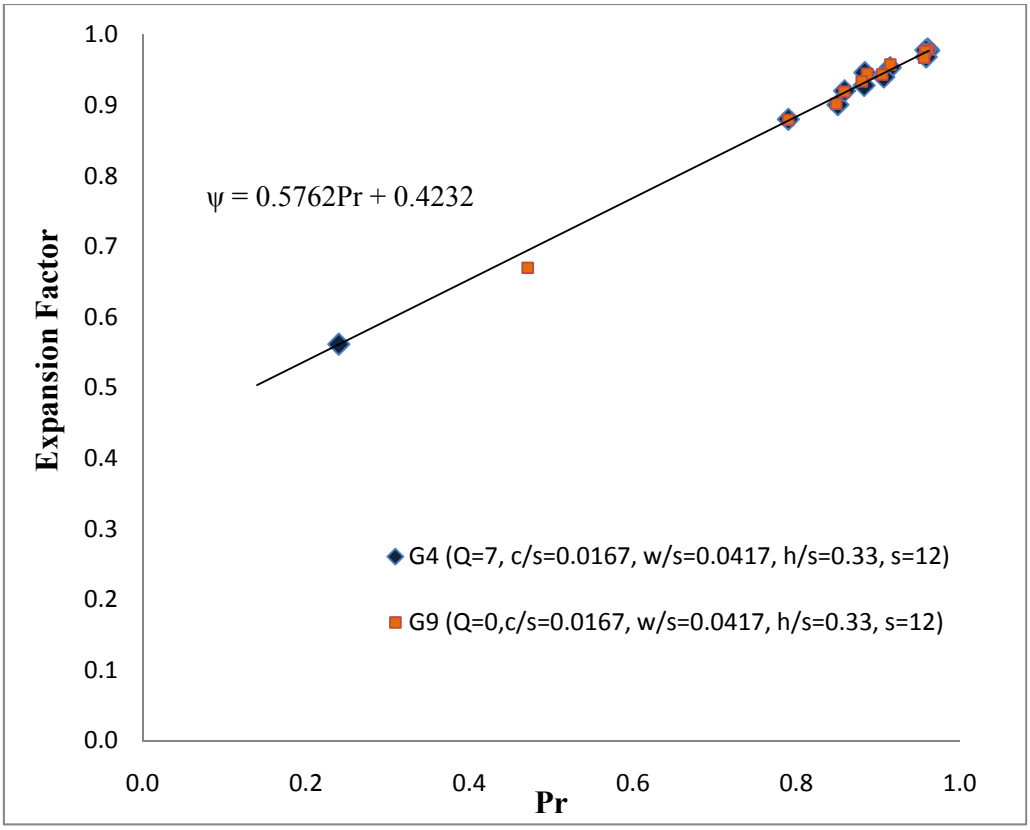

Figure 8.8 Effect of upstream side angle on ψ (W_{sh} =0)

8.9 Effect of Shaft Speed

It was shown that the discharge coefficient of water decreases as the shaft speed is increased. The same pattern can also be observed for air with less prominence. Compared to the compressible flow discharge coefficient, the incompressible flow

discharge coefficient is much less dependent on shaft speed. As a result, expansion factor increases as the shaft speed is increased.

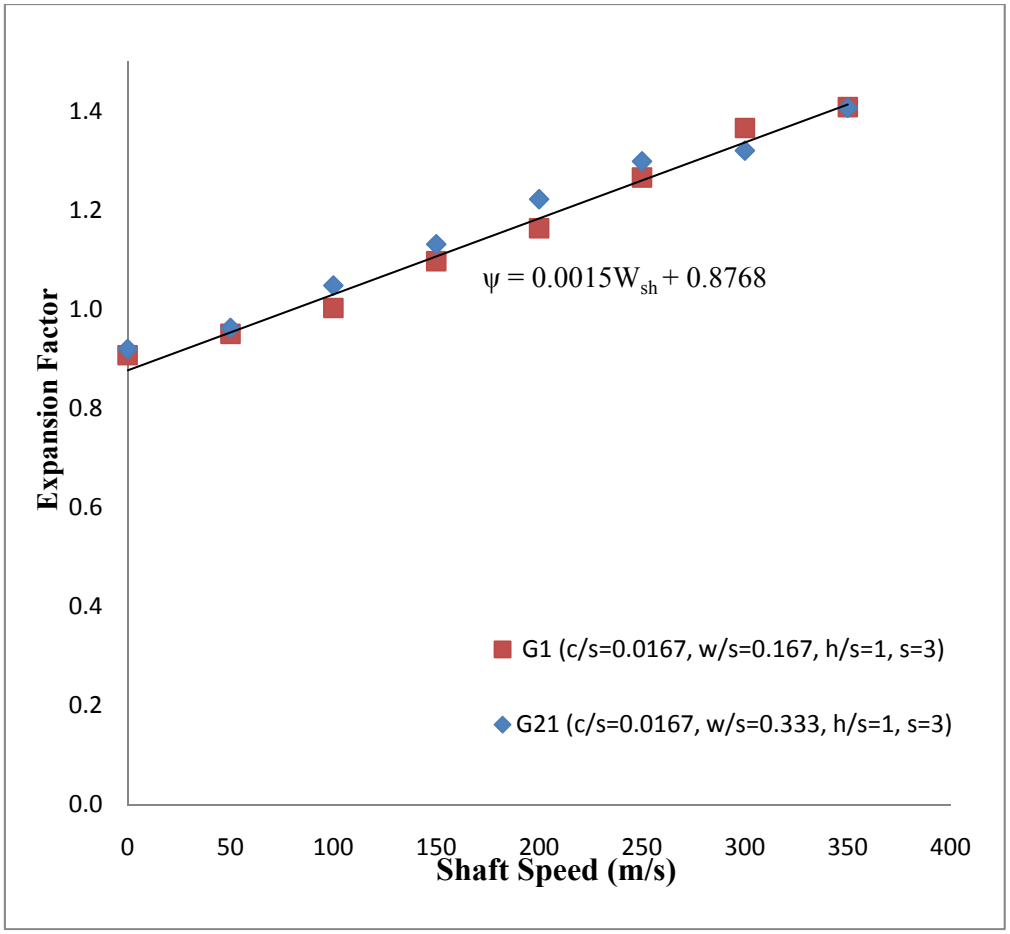

Figure 8.9 Effect of shaft speed on ψ (Re=1000)

It is clear that the expansion factor is a strong function of shaft speed as given in figure 8.9. The Reynolds number effects the expansion factor by changing the pressure ratio while the Taylor number directly changes the expansion factor even for a given pressure ratio. This effect is illustrated in the following figures.

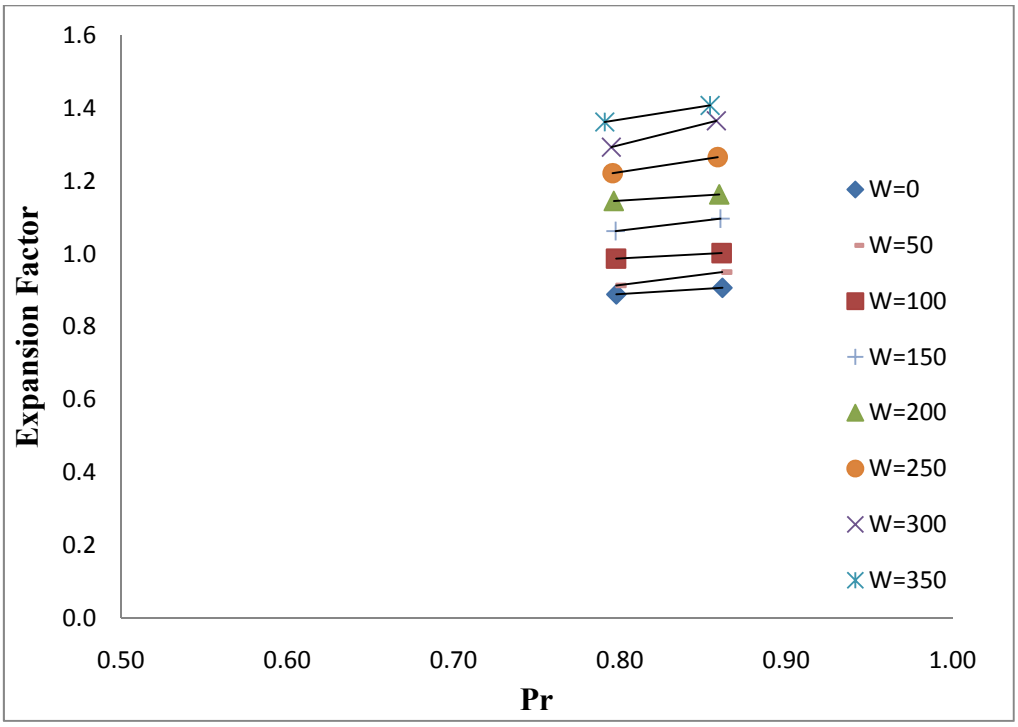

Figure 8.10 ψ variation with shaft speed (G1, c/s=0.0167, s=3, h/s=1, w/s=0.167, Re=1000)

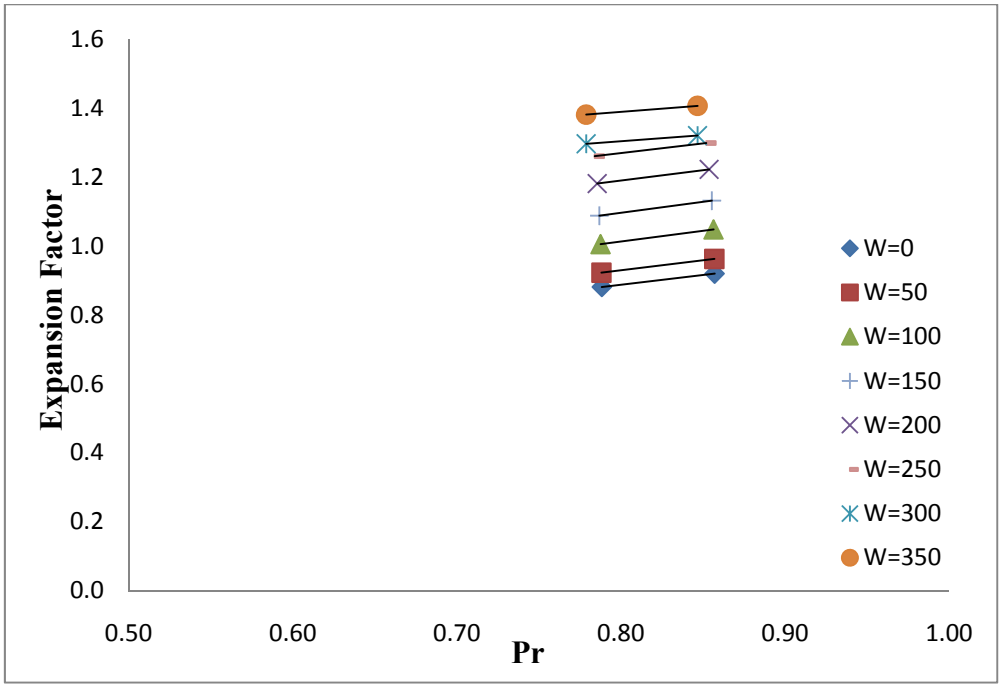

Figure 8.11 ψ variation with shaft speed (G21, c/s=0.0167, s=3, h/s=1, w/s=0.33, Re=1000)

Figures 8.10 and 8.11 clearly show that the Taylor number has negligible effect on pressure ratio but a very significance effect on expansion factor. The 2nd and 3rd tooth expansion factors for several Taylor numbers are plotted. As can be seen, the expansion factor increases as the pressure ratio is increased. It is also observed that the point at which the expansion factor is nearly one is also the point at which the secondary recirculation zone is formed for water. The secondary recirculation zone is observed for both G1 and G21 when the shaft speed is 100 m/s with a corresponding Taylor number of 157. The secondary recirculation zone is also checked for compressible flow simulations where air is used as working fluid. However, it is not observed for compressible flow even though the shaft speed is increased up to 350 m/s with a corresponding Taylor number of 37.8. Assuming that Taylor number is a major parameter that affects the formation of the secondary circulation zone, the same Taylor numbers should be compared for compressible and incompressible flow to understand whether or not the secondary recirculation occurs at similar Taylor numbers for both compressible and incompressible flow. However, it is clear from equation 6.3 that the Taylor number of air is significantly lower than that of water due to its density. As a result, to obtain the same Taylor number for both compressible and incompressible flow, the shaft speed of compressible flow should be approximately 15 times higher than that of incompressible flow. Considering the secondary recirculation zone is observed for these seal geometries (G1 and G21) at a shaft speed of 100 m/s for water, the shaft speed of compressible flow should be 1500 m/s for exact comparison. This requires further simulations for compressible flow with very high shaft speeds and it can be a possible

future study. It should be again noted here that an additional recirculation zone may occupy the lower half of the cavity even when the shaft speed is very small or zero. This circulation zone is not what is presented in figure 6.31 or what is meant here. The secondary recirculation zone meant here is the one which prevents the main streamline to impinge on the downstream tooth wall similar to that of given in figure 6.24.

The effects of flow parameters and geometrical features on expansion factor have been discussed so far. It was shown that geometrical features do not have significance effect on expansion factor. Thus, all of them along with tooth position are considered as secondary parameters effecting expansion factor. It should be noted that, amongst them, clearance has the highest effect. The tooth width effect is negligible unless it is a sharp tooth (w=0) profile. On the other hand, Reynolds number and Taylor number (due to shaft speed) have significant effect on expansion factor. As Reynolds number increases, the pressure ratio decreases and corresponding expansion factor decreases. As Taylor number increases, the expansion factor increases even for the same pressure ratio as shown in figures 8.10 and 8.11.

9. SUMMARY AND CONCLUSIONS

9.1 Carryover Coefficient

Carryover coefficients for different cases were calculated by using equation 6.1 and 6.2 which are based on Hodkinson's [2] definition. It was found that the carryover coefficient does not change with tooth position but both flow parameters and the geometry of the seal can significantly change the carryover coefficient.

Amongst geometrical features, c/s ratio was found to be the main parameter. It was validated that different geometries with the same c/s ratios have similar carryover coefficients even though both clearance and pitch values are different. Smaller values of c/s have lower carryover coefficient indicating better energy dissipation inside the cavity. Tooth width effect on carryover coefficient is negligible for small Reynolds numbers but it should be taken into account for higher Reynolds numbers. As the tooth width increases, the carryover coefficient slightly increases. Tooth height has even less effect on carryover coefficient compared to tooth width. Higher tooth height results in a slightly lower carryover coefficient. It was observed that upstream side angle also has an effect on carryover coefficient. When the upstream side angle is 0^o, the carryover coefficient increases compared to the 7^o upstream side angle case.

Flow parameters have significant effects on the carryover coefficient. When the Reynolds number is increased, the carryover coefficient significantly increases. As the maximum pressure difference is about to be obtained, the carryover coefficient increment with Reynolds number is only marginal. The effect of shaft speed is much

more complex than the effect of other parameters. In general, it was observed that the shaft speed decreases the carryover coefficient. Moreover, if the shaft speed is sufficiently increased, a secondary circulation zone can occupy the downstream region of the cavity preventing the main streamline from impinging on the downstream tooth. These cases are represented by a carryover coefficient of 1.

9.2 Discharge Coefficient

The discharge coefficient reveals the overall efficiency of the seal while carryover coefficient only presents the efficiency of a cavity. It was found that the discharge coefficient can significantly vary from the first tooth to the rest of the teeth. Thus, the analysis of discharge coefficient for first tooth and intermediate teeth were conducted separately.

Similar to carryover coefficient analysis, c/s ratio was found to be the major parameter that affects the discharge coefficient. Lower c/s ratios result in lower discharge coefficient for both first tooth and intermediate teeth indicating higher pressure loss across the tooth and cavity which in turn increases the sealing effectiveness. Tooth width has a small effect on discharge coefficient compared to the effect of c/s ratio. As tooth width increases, the discharge coefficient increases which is opposite to the effect of tooth width on carryover coefficient. However, once the tooth width is sufficiently increased, the discharge coefficient does not change anymore even though the tooth width is further increased. This effect has the same prominence for both the first tooth and the intermediate teeth. It was found that as tooth height decreases, the

discharge coefficient also decreases. This effect is more prominent for high Reynolds numbers and the intermediate teeth. Upstream side angle has negligible effect on both the first tooth and the intermediate teeth discharge coefficients. The discharge coefficient slightly increases as the upstream side angle is increased.

It was observed that the flow parameters have significant effect on both first tooth and intermediate teeth discharge coefficients. As the Reynolds number increases, the discharge coefficient increases. Similar to the effect of Reynolds number on carryover coefficient, as the maximum pressure difference is about to be obtained, the carryover coefficient increment with Reynolds number is only marginal. As shaft speed increases, the discharge coefficient decreases. This effect is more prominent for low Reynolds numbers. However, if the Reynolds number is sufficiently decreased, the shaft speed can increase the discharge coefficient.

9.3 Expansion Factor

Expansion factor is the ratio of the compressible flow discharge coefficient to the incompressible flow discharge coefficient. It was calculated for a given Reynolds number, shaft speed and tooth position. It was observed that the expansion factor does not change with tooth position. However, as Reynolds number is increased, the pressure ratio, which the ratio of downstream pressure to upstream pressure, decreases. This will result in a significant decrease in expansion factor. The relationship between pressure ratio and expansion factor is found to be linear.

The relationship between the expansion factor and geometrical parameters were investigated. It was found that clearance and tooth width have small effects on the expansion factor. As clearance increases, the expansion factor slightly increases. Several different tooth widths were examined and it was found that the sharp tooth profile (w=0) has significantly higher expansion factor compared to those of the remaining tooth widths (w/s>0.0167). The effect of tooth height and upstream side angle on expansion factor is marginal.

It was observed that shaft speed has a significant effect on expansion factor. As shaft speed increases, the expansion factor linearly increases regardless of the seal geometry. What is of importance is that it was found that this increment in expansion factor is not due to the increasing pressure ratio. Even though the shaft speed is drastically increased, the pressure ratio is almost same for the lowest and highest shaft speeds. However, the expansion factor increases as the shaft speed is increased.

9.4 Ideal Seal Geometry

In sections 6, 7 and 8, the effects of geometrical and flow parameters on carryover coefficient, discharge coefficient and expansion factor were studied. In order to optimize the seal geometry, the effects of those parameters on carryover coefficient, discharge coefficient and expansion factor should be studied together. The responses of carryover coefficient, discharge coefficient and expansion factor to an increase in the flow or geometrical parameter on the left column are presented in table 9.1 below.

Table 9.1 Effect of flow parameters and seal geometry on γ, C_d and ψ

Increases	γ	C_d	ψ
c	increases	increases	decreases
s	decreases	decreases	increases
w	increases	decreases	constant
h	decreases	increases	constant
Q	decreases	increases	constant
Re	increases	increases	decreases
W_{sh}	decreases	decreases	increases

It should be noted that, amongst the geometrical features, tooth height has the smallest effect followed by upstream side angle and tooth width. Moreover, the effect of clearance and pitch on expansion factor is only marginal. The primary geometrical parameters are tooth clearance and pitch. Both flow parameters (Re, W_{sh}) have significant effects on the carryover coefficient, discharge coefficient and expansion factor.

First of all, it is should be noted again that the discharge coefficient presents the overall efficiency of a tooth and a cavity while carryover coefficient only tells about the cavity performance. Thus, the major parameter while optimizing the seal geometry is the discharge coefficient. It is clear from the table that c/s ratio should be kept as small as possible for better sealing. This can be done either by decreasing clearance or increasing pitch. However, as discussed in section 7.2.4, smaller tooth clearance has slightly lower discharge coefficient even though the c/s ratios are same (figure 7.7). Thus, decreasing the clearance is a slightly better option compared to increasing tooth pitch. Increasing tooth pitch will ease the formation of secondary recirculation zone which even increases

the kinetic energy dissipation in the cavity. However, the overall efficiency of the smaller clearance and pitch (same c/s ratio) is still better. It should be noted that as the shaft speed increases, the discharge coefficient of both small clearance and large clearance reduces but small clearance has slightly lower discharge coefficient. Thus, smaller c/s is always better than higher c/s in any flow condition. For the same c/s ratios, smaller clearance has slightly better performance than that of larger clearance. Moreover, in terms of actual fluid leakage, a larger clearance increases the flow area and hence leakage for the same discharge coefficient value.

It was shown that the smaller tooth width has lower carryover coefficient compared to the larger tooth width due to vena-contracta effect. However, due to higher pressure loss through the wider tooth, the discharge coefficient for the wider tooth is lower than that of a sharper tooth. It should be noted that the wider tooth is especially better than the sharper tooth for high shaft speeds. Tooth height and upstream side angle have smaller effect on discharge coefficient compared to clearance, pitch and tooth width. It was shown that shorter teeth have slightly lower discharge coefficients than that of a longer tooth. The discharge coefficient slightly reduces when the upstream side angle is reduced from 7^{o} to 0^{o}.

Considering the effects of geometrical features, it can be concluded that the c/s ratio should be kept a small as possible by keeping the clearance at a possible smallest value. The h/s ratio should be kept small and w/s ratio should be kept large. Consequently, G21 is found to be the best geometry that studied. The sealing performances of G1, G10, G20, G24 and G25 are also close to that of G21.

10. RECOMMENDED FUTURE WORK

The effects of seal geometry and flow parameters were investigated in this study. However, there are still plenty of possible seal geometries that remain to be studied in order to better understand the flow behavior through the labyrinth seal. The effects of geometrical parameters can change under different shaft speed conditions. Thus, there is still a need of further study to reach a better design. The following issues can be addressed in a possible future study.

1- It was shown that the formation of the secondary recirculation zone strongly depends on the seal geometry, especially on pitch. The secondary recirculation zone has an effect on seal performance. The critical Re/Ta ratio that secondary recirculation zone expected was estimated in this study (figure 6.31). In a future study, a more detailed analysis of critical Re/Ta ratio can be investigated.

2- The effect of shaft speed on expansion factor was studied. It was observed that the expansion factor increases as the shaft speed is increased even though the pressure ratio is almost constant (figures 8.10 and 8.11). Thus, the shaft speed has a sole effect on expansion factor. In a future study, this effect can be explored more in detail.

3- It was proven that the seal geometry strongly affects the discharge coefficient for compressible flow. However, it was observed that the expansion factor does not change (or slightly changes) as the seal geometry changes. This means that the effect of seal geometry on compressible and incompressible flow is same. This observation should

further be validated. It can be done by using different models for air. In this study, air was modeled as an ideal gas.

REFERENCES

[1] Parsons C.A., 1938, "The Labyrinth Packing", Engineer, **165**, No. 4280, pp.23-84

[2] Hodkinson, B., 1939, "Estimation of the Leakage Through a Labyrinth Gland", Proc.Inst.Mech.Engrs. , **141**, pp.283-288

[3] Becker, E., 1907, "Stromungsvergange in Ringformigen Spalten", V.D.I., **51**, pp.1133-1141

[4] Martin, H.M., 1908, 'Labyrinth Packings', Engineer, **85**, pp. 35-36

[5] Stodola, A., 1927, Steam and Gas Turbines, sixth ed., McGraw-Hill, **1**, pp. 189-194, New York

[6] Gercke, M.J., 1934, 'Berechnung der Ausflussmengen von Labyrinth Dichtungen", Die Warme, **57**, pp.413-417

[7] Egli, A., 1935, "The Leakage of Steam Through Labyrinth Seals", Trans. ASME, **57**, pp. 115-122

[8] Dollin, F., and Brown, W.S., 1937, "Flow of Fluids Through Openings in Series", Engineer, **164**, No. 4259, pp.223-224

[9] Jeri, J., 1948, "Flow Through Straight-Through Labyrinth Seals", Proc. Seventh Int. Cong. Appl. Mech., **2**, pp. 70-82

[10] Kearton, W. J., 1955, "Flow of Air Through Radial Labyrinth Glands", Proc. Inst. Mech. Engrs., **169**, No. 30, pp. 539-550

[11] Bell, K. J. and Bergelin, O. P., 1957, "Flow Through Annular Orifices," Trans. ASME, **79**, No. 3, pp 593-601

[12] Zabriskie, W., and Sternlicht, B., 1959, "Labyrinth Seal Analysis", Journal of Basic Engineering, Trans. ASME, Series D, **81**, No. 3, pp. 332-340

[13] Vermes, G., 1961, "A Fluid Mechanics Approach to the Labyrinth Seal Leakage Problem", Journal of Basic Engineering, Trans. ASME, Series D, **83**, No. 1, pp. 161-169

[14] Zimmerman, H. and Wolff, K. H., 1987, "Comparison between Empirical and Numerical Labyrinth Flow Correlations", ASME 87-GT-86

[15] Wittig S., Schelling, U., Kim, S., and Jacobsen, K., 1987, "Numerical Predictions and Measurements of Discharge Coefficients in Labyrinth Seals," ASME 87-GT-188

[16] Suryanarayanan Saikishan, 2008, "Labyrinth Seal Leakage Equation", M.S. thesis, Texas A&M University, College Station, TX

[17] Morrison, G.L. and Al-Ghasem, A., 2007, "Experimental and Computational Analysis of a Gas Compressor Windback Seal," GT2007-27986, Proceedings of ASME Turbo Expo 2007, Montreal, Canada

[18] Demko J.A., 1986, "The Prediction and Measurement of Incompressible Flow in a Labyrinth Seal", PhD dissertation, Texas A&M University, College Station, TX

APPENDIX

STANDARD k – ε TURBULENCE MODEL

Reynolds Averaged Navier Stokes (RANS) equations are one of the ways to model turbulent reacting flows. It separates the velocity into 'mean' and 'fluctuating' parts. When the mean flow is steady, the RANS equation has the following form.

$$\overline{U_k}\frac{\partial\overline{\rho U_i}}{\partial x_k} = -\frac{\partial\overline{P}}{\partial x_i} + \mu\frac{\partial^2\overline{U_i}}{\partial x_k\,\partial x_k} - \frac{\partial\,(\overline{\rho u_i' u_k'})}{\partial x_k} \quad \text{..... (A1)}$$

The Reynolds stress tensor ($\overline{\rho u_i' u_k'}$) appears in the mean flow, which behaves similar to a laminar flow, equations due to the effect of fluctuations. This term can be modeled by using a 'turbulent viscosity (μ_t)' to arrive equation A2.

$$\overline{U_k}\frac{\partial\overline{\rho U_i}}{\partial x_k} = -\frac{\partial\overline{P}}{\partial x_i} + (\mu + \mu_t)\frac{\partial^2\overline{U_i}}{\partial x_k\,\partial x_k} \quad \text{..... (A2)}$$

The k-ε model is now can be implemented on A2. It express the turbulent viscosity as a function of turbulent kinetic energy (κ) and dissipation (ε) as given in equation A3.

$$\mu_t = \rho C_\mu \frac{\kappa^2}{\varepsilon} \quad \text{..... (A3)}$$

Where C_μ is a constant with a value of 0.09. The turbulent kinetic energy and dissipation in equation A3 are defined as

$$\kappa = \frac{1}{2}\,\overline{u_i' u_i'} \quad \text{..... (A4)}$$

$$\varepsilon = \frac{\mu}{\rho}\overline{\left(\frac{\partial u_i'}{\partial x_k}\frac{\partial u_i'}{\partial x_k}\right)} \quad \text{..... (A5)}$$

However, equations A4 and A5 cannot be directly used since the exact closure equations for κ and ε are not known. Instead, equation A6, which is based on equation A4, and equation A7, which is empirical, are used to calculate these terms.

$$\frac{\partial(\rho\kappa)}{\partial t} + \frac{\partial(\rho\kappa u_j)}{\partial x_j} = \frac{\partial}{\partial x_j}\left[\left(\mu + \frac{\mu_t}{\sigma_k}\right)\frac{\partial \kappa}{\partial x_j}\right] + G_k + G_b - \rho\varepsilon - Y_M + S_k \quad \text{.....(A6)}$$

$$\frac{\partial(\rho\varepsilon)}{\partial t} + \frac{\partial(\rho\varepsilon u_j)}{\partial x_j} = \frac{\partial}{\partial x_j}\left[\left(\mu + \frac{\mu_t}{\sigma_\varepsilon}\right)\frac{\partial \varepsilon}{\partial x_j}\right] + C_{1\varepsilon}\frac{\varepsilon}{k}(G_k + C_{3\varepsilon}G_b) - C_{2\varepsilon}\,\rho\frac{\varepsilon^2}{k} + S_\varepsilon \quad \text{...(A7)}$$

where

G_k is the production of κ and is modeled as $2\mu_t \frac{\partial \overline{U_i}}{\partial x_j}\frac{\partial \overline{U_i}}{\partial x_j}$.

G_b represents generation of κ due to buoyancy.

Y_M represents compressibility effects on turbulence and is modeled as $2\rho\varepsilon\frac{\kappa}{kRT}$.

S_k and S_ε are user defined source terms.

σ_k and σ_ε are the turbulent Prandtl numbers for κ and ε, and have default values of 1.0 and 1.3 respectively.

$C_{1\varepsilon}$ and $C_{2\varepsilon}$ are constants with default values of 1.44 and 1.92.

FINITE VOLUME METHOD

Finite volume method (FVM) is a discretization technique, similar to the finite element method and finite difference method, to reduce the partial differential equations into a system of algebraic equations that can be solved by a computer. FVM divides the computational domain into a number of finite control volumes and solves the conservation equations for each control volume. FVM discretization can be illustrated by the following 2-D transport equation.

$$\int_V \frac{\partial \rho\phi}{\partial t}\, dV + \oint \rho\phi\, \vec{v} \cdot d\vec{A} = \oint \Gamma_\phi \nabla\phi \cdot d\vec{A} + \int_V S_\phi\, dV \quad \text{……. (A8)}$$

where

ρ = density

$\vec{v}$ = velocity vector

$\vec{A}$ = surface area vector

Γ_ϕ = diffusion coefficient for ϕ

$\nabla\phi$ = gradient of ϕ

S_ϕ = source of per unit volume of ϕ

$$\frac{\partial \rho \phi}{\partial t} V + \sum_{f}^{N_{\text{faces}}} \rho_f \vec{v}_f \phi_f \cdot \vec{A}_f = \sum_{f}^{N_{\text{faces}}} \Gamma_\phi \nabla \phi_f \cdot \vec{A}_f + S_\phi V \quad \text{..... (A9)}$$

where

N_{faces} = number of faces enclosing cell

ϕ_f = value of ϕ convected through face f

$\rho_f \vec{v}_f \cdot \vec{A}_f$ = mass flux through the face f

$\vec{A}_f$ = area of face f

$\nabla \phi_f$ = gradient of ϕ at face f

V = cell volume

VITA

Orcun Inam was born in Adana, Turkey. After completing his education in MTSO Anatolian High School, Mersin, Turkey, he attended Gazi University, Ankara, Turkey for his undergraduate education with a major of mechanical engineering. He received his bachelor of engineering degree in 2008. He came to United States in 2009 to pursue graduate studies in mechanical engineering at Texas A&M University, College Station, TX. He received Master of Science degree in mechanical engineering in August 2011.

Orcun Inam may be contacted through Texas A&M University, Department of Mechanical Engineering, College Station, TX 77843-3123. His email address is orcuninam@hotmail.com